

# G protein coupled receptors require active Gαq to mobilize Gi-Gβγ-dependent calcium

Dissertation  
zur  
Erlangung des Doktorgrades (Dr. rer. nat.)  
der  
Mathematisch-Naturwissenschaftlichen Fakultät  
der  
Rheinischen Friedrich-Wilhelms-Universität Bonn

vorgelegt von  
**Eva Marie Pfeil**  
aus  
Köln

Bonn 2021



Angefertigt mit Genehmigung der Mathematisch-Naturwissenschaftlichen Fakultät der Rheinischen Friedrich-Wilhelms-Universität Bonn.

1. Gutachter: Prof. Dr. Evi Kostenis

2. Gutachter: Prof. Dr. Bernd K. Fleischmann

Tag der Promotion: 08.06.2021

Erscheinungsjahr: 2021



Die vorliegende Arbeit wurde in der Zeit von Januar 2017 bis März 2021 am Institut für Pharmazeutische Biologie der Rheinischen Friedrich-Wilhelms-Universität Bonn unter der Leitung von Frau Prof. Dr. Evi Kostenis angefertigt.



*Für meine Freunde*





# Abstract

The mechanisms by which GPCRs drive calcium mobilization in living cells have been a topic of intense research interest for many years. One such mechanism is the paradigmatic Gi-calcium pathway, which describes how G $\beta\gamma$  subunits released from heterotrimeric Gi proteins upon stimulation of a Gi-coupled GPCR can bind and activate PLC $\beta$ 2 and PLC $\beta$ 3. These enzymes of the PLC $\beta$  family then hydrolyze PIP $_2$  into DAG, which regulates a number of cellular effectors, and IP $_3$ , which triggers the release of calcium from the cellular stores via IP $_3$ -sensitive ion channels.

Despite the apparent clarity of this well-described Gi-G $\beta\gamma$ -PLC $\beta$ -calcium pathway, Gi-GPCR calcium is highly variable across cell types, and difficult to generate under most circumstances. Intriguingly, although Gi-G $\beta\gamma$ -PLC $\beta$ -calcium is widely accepted as a 'stand-alone' independent signaling module, a number of studies indicate that the canonical Gq-GPCR pathway, which also activates PLC $\beta$  to trigger calcium release, might affect or even control Gi-G $\beta\gamma$ -PLC $\beta$ -calcium.

Here we investigate a possible dependency of Gi-G $\beta\gamma$ -PLC $\beta$ -calcium on the Gq pathway, with the goal of determining why Gi-G $\beta\gamma$ -PLC $\beta$ -calcium is variable and difficult to generate. Using a set of recently discovered, cutting edge tools including CRISPR/Cas9-edited cell lines lacking G $\alpha_q$  expression and the Gq inhibitor FR, we show that Gi-G $\beta\gamma$ -PLC $\beta$ -calcium is fully dependent on, and only occurs in the presence of, active G $\alpha_q$ . We find that other, PLC $\beta$ -independent Gi signaling pathways do not share this requirement for active G $\alpha_q$ . While the downstream consequences of G $\alpha_q$ -activation do not suffice to restore Gi-G $\beta\gamma$ -PLC $\beta$ -calcium, removal of the auto-inhibitory domains of PLC $\beta$  enables activation by Gi-G $\beta\gamma$  that suffices to mobilize calcium without G $\alpha_q$ . Based on this, we argue that G $\alpha_q$  controls Gi-G $\beta\gamma$ -PLC $\beta$ -calcium by relieving the auto-inhibition of PLC $\beta$ . It thereby allows sufficient activation by Gi-G $\beta\gamma$  to achieve the acute production of IP $_3$  required for calcium mobilization. Finally, we demonstrate that the necessity of active G $\alpha_q$  for Gi-G $\beta\gamma$ -PLC $\beta$ -calcium is conserved across a wide variety of physiologically relevant cell types and influences calcium-dependent cellular functions, such as the aggregation of platelets. Our proposed molecular mechanism provides the missing link to explain the variability of Gi-G $\beta\gamma$ -PLC $\beta$ -calcium, and thereby fundamentally contributes to our understanding of how Gi-GPCRs signal.

# Kurzfassung

Mechanismen und Signalwege, die in eukaryotischen Zellen Calcium freisetzen, stellen seit Langem ein Forschungsgebiet von großem Interesse dar. Ein solcher Calcium-Freisetzungsmechanismus ist der Gi-Calcium Signalweg. Er beschreibt, dass bei der Aktivierung von Gi-gekoppelten GPCRs aus heterotrimeren Gi Proteinen freigesetzte G $\beta\gamma$  Untereinheiten an PLC $\beta$ 2 und PLC $\beta$ 3 Enzyme binden und diese aktivieren. Die Enzyme der PLC $\beta$  Familie hydrolysieren daraufhin PIP $_2$  aus der Zellmembran zu DAG und IP $_3$ . Durch diese Produktion von IP $_3$  werden IP $_3$ R auf der Membran des ER aktiviert, durch die daraufhin Calcium aus dem ER ins Zytosol strömt.

Obwohl dieser Mechanismus seit langem beschrieben ist und in der Theorie vergleichsweise unkompliziert wirkt, zeigt er sich in der Praxis oftmals unerklärlich variabel und ist in vielen Zellsystemen schwer zu generieren. Viele Studien deuten sogar darauf hin, dass dieser eigentlich als unabhängig akzeptierte Gi-G $\beta\gamma$ -PLC $\beta$ -Calcium Signalweg maßgeblich durch Gq-gekoppelte GPCRs reguliert wird, welche über die Freisetzung von G $\alpha_q$  auch die PLC $\beta$  aktivieren können.

Daher wird in dieser Studie der Gi-G $\beta\gamma$ -PLC $\beta$ -Calcium Signalweg erneut betrachtet, mit dem Ziel, den Grund für seine Variabilität zu identifizieren. Unter Verwendung der neusten Technologie, wie CRISPR/Cas9-editierten HEK Zelllinien und dem spezifischen Gq Protein Inhibitor FR, wird gezeigt, dass Gi-G $\beta\gamma$ -PLC $\beta$ -Calcium vollständig von aktivem G $\alpha_q$  abhängig ist und sich daher nur bei G $\alpha_q$  -Aktivierung generieren lässt. Diese Abhängigkeit zeigt sich allein für den Gi-G $\beta\gamma$ -PLC $\beta$ -Calcium Signalweg, während andere Gi-Signalwege ohne G $\alpha_q$  Aktivierung ablaufen können. Des Weiteren demonstrieren wir, dass die downstream Konsequenzen der Gq-Signalkaskade nicht ausschlaggebend sind, um Gi-G $\beta\gamma$ -PLC $\beta$ -Calcium wiederherzustellen. Dies ist darin begründet, dass G $\beta\gamma$  die PLC $\beta$  zwar ohne Gq-Aktivierung binden kann, allerdings kann G $\beta\gamma$  die starke Autoinhibition des PLC $\beta$  Enzyms nicht aufheben und somit allein nicht ausreichend PLC $\beta$  vermittelte IP $_3$  Produktion erreichen, um eine Calcium-Freisetzung auszulösen. Dies ändert sich, wenn die autoinhibitorischen Domänen der PLC $\beta$  durch Mutation entfernt oder gestört werden, oder wenn aktives G $\alpha_q$  die PLC $\beta$  bindet und dadurch in die aktive, nicht-autoinhibierte Konformation überführt. Dieser Mechanismus erklärt die G $\alpha_q$ -Abhängigkeit der Gi GPCR-vermittelten Calciumfreisetzung, welche wir in verschiedensten physiologischen Zellsystemen

darstellen. Die vorliegende Studie bietet damit nicht nur eine Erklärung für die Variabilität des paradigmatischen Gi-G $\beta$ -PLC $\beta$ -Calcium Signalwegs, sondern trägt auch maßgeblich zu unserem Grundverständnis der physiologischen Funktionen von Gi- und Gq GPCRs bei.

# Table of Contents

Abstract .....	1
Kurzfassung.....	2
Table of Contents .....	4
Introduction.....	8
The role of calcium signaling .....	8
Calcium mobilization in the cell.....	8
The phospholipase C.....	11
G protein-coupled receptors .....	12
G protein families and their signaling pathways.....	14
G $\beta\gamma$ signaling.....	15
PLC $\beta$ structure and activation.....	16
Variability of Gi-calcium .....	18
Approach of this study .....	19
Material.....	21
Chemicals and Reagents.....	21
Cell Culture Media .....	22
Base.....	22
Supplements .....	23
Antibodies .....	23
Plasmids .....	24
Bacterial strains .....	26
Experimental models .....	26
Cell lines.....	26
Organisms.....	26
Commercial Assay Kits .....	27
Methods.....	28
Cell culture.....	28
Culture conditions .....	28
Cell culture media.....	28
Transient Transfection .....	30
Generation of CRISPR/Cas9-edited HEK-PLC $\beta$ 1-4mut cell lines.....	31

CRISPR/Cas9 method .....	31
CRISPR/Cas9-edited genetic knockout strategy .....	31
Protocol to generate the HEK-PLC $\beta$ 1-4mut cell line.....	32
sgRNA selection.....	33
CRISPR/Cas9 transfection, FACS, and single clone culture.....	33
Clone screening by PCR and RE-digest .....	33
Genetic sequencing.....	34
Functional clone screening.....	35
What went wrong?.....	35
Isolation of primary cells .....	36
Murine brown preadipocytes (mBAT) .....	36
Murine pulmonary arterial smooth muscle cells (mPASMC) .....	37
Murine platelets.....	37
Cell-based assays.....	37
Population-based calcium mobilization .....	37
Calcium mobilization and aggregometry in platelets.....	38
Single cell calcium mobilization.....	38
IP <sub>1</sub> accumulation .....	39
cAMP accumulation.....	39
NanoBiT .....	39
IP <sub>3</sub> BRET .....	40
G $\alpha$ q-G $\beta$ $\gamma$ dissociation BRET.....	40
DMR .....	40
Thallium Flux.....	41
Western Blot.....	41
Data processing.....	41
Results.....	42
Chapter 1: Does Gi-calcium depend on Gq? .....	42
Gi-calcium is completely blocked by Gq inhibitor FR .....	42
FR-sensitive Gi-calcium is mobilized via PLC $\beta$ 2 and PLC $\beta$ 3.....	43
Gq is required and sufficient to restore Gi-calcium in HEK- $\Delta$ Gq/11 cells ...	44
Excursion 1.1: Gq overexpression shifts Gi/Gq balance of calcium signals towards Gq .....	46
All G $\alpha$ q family subunits restore Gi-calcium.....	48
Chapter 2: The Gq requirement for specifically Gi-coupled receptors .....	48

## Table of Contents

Specifically Gi-coupled DP2 requires additional Gq input to mobilize Gi-calcium .....	49
Gi-calcium via CXCR2 and CXCR4 requires Gq input .....	50
Excursion 2.1: Both basal and acute Gq activation restore Gi-calcium, but acute Gq stimulation does so more reliably .....	51
Chapter 3: Which Gi-pathways require Gq? .....	53
All model GPCRs are expressed and couple to Gi without Gq.....	54
Gai-mediated cAMP depression does not require Gq .....	55
Gi-Gβγ-PLCβ signaling, but not Gi-Gβγ-GIRK activation, fully depends on Gq. ....	56
Excursion 3.1: The effect of Gq-activation on Gi-Gβγ-GIRK activation. ....	58
Chapter 4: the canonical Gq pathway: which step allows Gi-calcium? .....	59
Gi-Gβγ-PLCβ-calcium does not require Gq-PKC-activation .....	59
An acute increase in intracellular calcium is not sufficient to allow Gi-calcium.....	61
Increased intracellular IP production does not restore Gi-Gβγ-PLCβ-calcium.....	62
Gαq-PLCβ interaction, rather than Gq-Gβγ-signaling, is required for Gi-Gβγ-PLCβ-calcium .....	64
Chapter 5: Identifying the molecular mechanism - what does Gαq do?.....	65
NanoBiT sensor displays Gβγ-PLCβ binding.....	66
Gq does not enhance Gβγ-PLCβ binding .....	67
Excursion 5.1: Why is there no binding of Gai2-Gβγ or Gaz-Gβγ to PLCβ3?.....	68
Excursion 5.2: Does Gq-Gβγ bind to PLCβ? .....	69
PLCβ3 constructs are not auto-inhibited and thus constitutively active. ....	70
Gi-Gβγ-PLCβ-calcium via crippled auto-inhibition PLCβ3 mutants does not require Gq. ....	71
Without Gq, Gβγ slightly increases basal cellular PLCβ activity, but does not mediate Gi-GPCR induced activation. ....	73
Gi-Gβγ-PLCβ activation does not trigger real-time IP <sub>3</sub> increase without Gq .....	74
Mechanistic model for Gi-Gβγ-PLCβ-calcium in living cells .....	75
Chapter 6: from HEK cells to physiological systems – is the Gq requirement conserved? .....	76

The Gq requirement for Gi-G $\beta\gamma$ -PLC $\beta$ -calcium is conserved across multiple cell types .....	77
Platelet calcium and aggregation by Gi-coupled receptors requires Gq input .....	78
Excursion 6.1: the role of G16 in the immune system.....	80
Discussion .....	82
Gi-calcium requires Gq .....	82
Literature discrepancy?.....	82
Gi-calcium might be more relevant than previously thought .....	84
G $\beta\gamma$ -calcium from other GPCRs? .....	84
Gi-calcium and G16 .....	86
Gq activation changes the signaling outcome of Gi-GPCRs.....	86
Gq inhibitors might appear to be unspecific. ....	87
Implications for drug development .....	88
Conclusion .....	88
Summary .....	89
References .....	91
Abbreviations.....	101
List of Figures .....	103
List of Tables .....	105
Publications .....	107
Publications in peer-reviewed journals.....	107
Talks and posters .....	109
Acknowledgements .....	111

# Introduction

## The role of calcium signaling

Calcium ions are ubiquitously important signaling messengers that govern eukaryotic life. The mobilization of calcium refers to a temporary increase in the cytosolic calcium concentration of a cell (Clapham, 2007; Berridge et al., 2003). This increase usually follows an extracellular or intracellular stimulus and is an important signal for acute or long-term cellular activation. Thus, it often triggers functions specific to the individual cell type. As such, calcium regulates the contraction of smooth muscle cells (Hill-Eubanks et al., 2011), the release of neurotransmitters from neurons (Burgoyne, 2007), insulin secretion from pancreatic beta-cells (Klec et al., 2019), and causes thrombocytes to aggregate (Nesbitt et al., 2003). In addition, calcium mobilization also controls gene transcription via the nuclear factor of activated T-cells (Feske, 2007) and plays a role in the maturation of cells (Clapham, 2007). Because of the importance of calcium mobilization, researchers have searched for, investigated, and characterized many pathways that trigger it. The insight gained through these efforts has advanced our understanding of the human body in both health and disease greatly and manipulating them has proved a useful approach for treating illnesses (Carafoli, 2004). To this day, there is still great interest for further insight into mechanisms of calcium mobilization.

## Calcium mobilization in the cell

To successfully orchestrate and balance the myriad of calcium-dependent physiological processes, the cytosolic calcium concentration of each cell is tightly regulated. At resting state, the calcium concentration in the cytosol is comparatively low at around 100 nM (Clapham, 2007; Berridge et al., 2003). The calcium concentration of the extracellular space is normally higher, around 2 mM, which enables an influx via calcium channels on the cellular membrane (Figure 1) (Clapham, 2007; Berridge et al., 2003). Additionally, a large quantity of intracellular calcium is stored in the endoplasmic reticulum (ER), where concentrations reach around 1 mM (Clapham, 2007; Berridge et al., 2003). This high concentration gradient across the ER membrane is maintained by the SERCA (Strehler & Treiman, 2004), which constantly clears calcium from the cytosol into the stores.

When a stimulus occurs to trigger calcium mobilization, the ion channels located on the ER membrane can open and permit a rapid stream of calcium into the cytosol



(Figure 1), where it can bind to and alter the function of a large variety of effector proteins (Clapham, 2007).

IP<sub>3</sub> receptors (IP<sub>3</sub>R) are of immense importance for the release of calcium from the ER. They can bind up to four molecules of inositol-1,4,5-trisphosphate (IP<sub>3</sub>) and will open upon activation (Alzayady et al., 2016; Prole & Taylor, 2019) to allow a quick influx of calcium into the cell (Figure 1), which makes IP<sub>3</sub> production one of the most important factors to regulate calcium mobilization. Because IP<sub>3</sub>R are inhibited by high intracellular calcium concentrations, they quickly close after releasing a small amount of calcium into the cytosol. Because of this, the calcium influx via these IP<sub>3</sub>R can follow a variety of intricate spatial and temporal patterns, such as calcium oscillations or waves (Prole & Taylor, 2019) that differ depending on the concentration and IP<sub>3</sub>. On the other hand, due to this negative feedback loop, a long-term increase in the cytosolic calcium concentration of a cell does not usually occur, even when IP<sub>3</sub> levels are kept high. Following a calcium signal, the cytosolic calcium is quickly cleared by re-uptake mechanisms, so that the resting state is restored and a new signal can occur (Clapham, 2007).

This mobilization of calcium from the ER can lead to a depletion of these cellular calcium stores, and thereby trigger the oligomerization of STIM1 proteins (Figure 1). These clusters of calcium-sensing proteins then interact with ORAI calcium channels on the cellular membrane, causing them to open and allow an influx of calcium from the extracellular space into the cytosol (Putney, 2005), which can both amplify an existing calcium signal and facilitate calcium store repletion via re-uptake mechanisms.

There are numerous other mechanisms that induce or amplify calcium signals, including the release of calcium from the intracellular stores via ryanodine receptors in skeletal or cardiac muscle cells. Here, an increase in intracellular calcium consequently activates ryanodine receptors expressed on the sarcoplasmic reticulum (Clapham, 2007), which amplifies a pre-existing calcium signal. However, this mechanism is not the focus of this work.

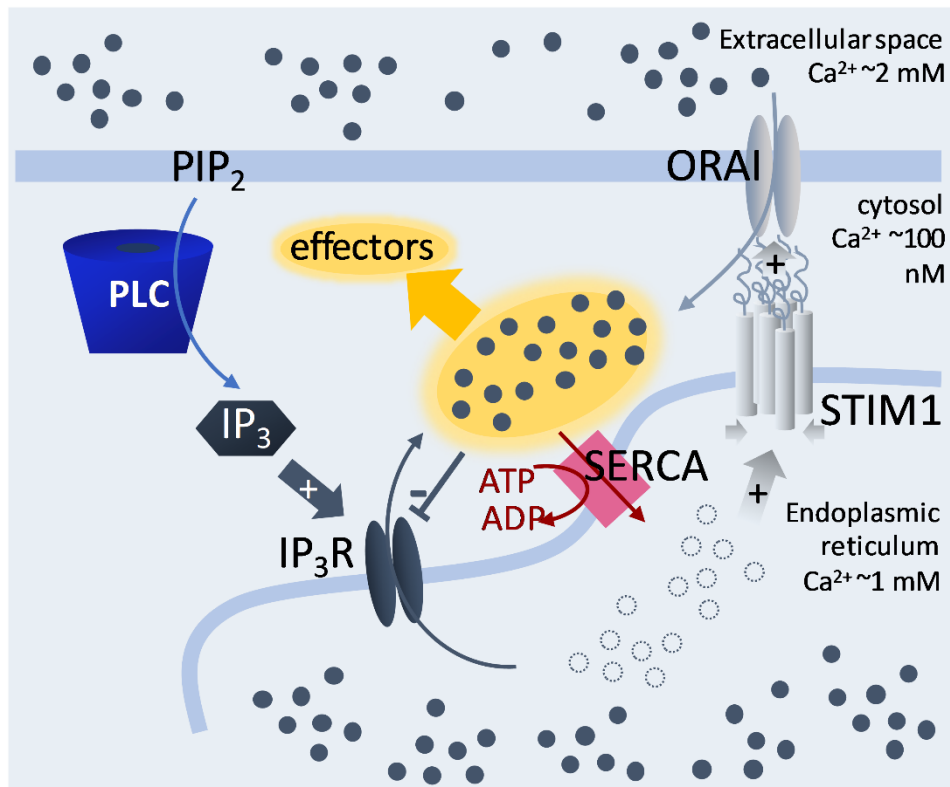


**Figure 1: Calcium mobilization from intracellular stores via IP<sub>3</sub> receptors.** Calcium is depicted as dark grey dots. At the resting state, the cytosolic calcium concentration is maintained at concentrations of around 100 nM, below those of the extracellular space, which usually reach approximately 2 mM. Calcium pumps, such as the SERCA (red), maintain this low intracellular calcium concentration by consuming ATP to move cytosolic calcium across the ER membrane into the intracellular calcium stores, where calcium concentrations reach up to 1 mM. Calcium mobilization, which refers to the increase of cytosolic calcium concentrations (yellow), is achieved either via an influx from the extracellular space, a release of calcium from the calcium stores, or a combination of both. Ligand-gated calcium channels called IP<sub>3</sub> receptors (IP<sub>3</sub>R, dark grey) located on the ER membrane open upon binding the ubiquitous second messenger IP<sub>3</sub> (dark grey), thereby allowing a release of calcium from the ER into the cytosol. These IP<sub>3</sub> receptors are inhibited by the presence of high calcium concentrations on the cytosolic side (dark grey), and thus close after a short calcium release, which can cause intricate patterns of calcium oscillations. A depletion of calcium in the ER triggers the oligomerization of STIM1 on the endoplasmic membrane (light grey), which in turn interacts with ORAI channels on the cellular membrane (light grey), thereby triggering an influx of calcium from the extracellular space into the cytosol. The intracellular calcium is quickly cleared by the SERCA again (red), which regenerates the stores and restores the low cytosolic calcium concentration of the resting state. IP<sub>3</sub> (dark grey), the molecule that triggers this entire calcium mobilization process, is produced by the phospholipase C (PLC, blue), which makes this family of enzymes one of the most important regulators of calcium release.

## The phospholipase C

Because of the ability of  $IP_3$  to open calcium channels, the enzyme family that produces  $IP_3$  is a central regulator of intracellular signaling. This family is the Phospholipase C (PLC) family, which catalyzes the hydrolysis of the membrane lipid Phosphoinositol-4,5-bisphosphate ( $PIP_2$ ) into membrane-bound diacylglycerol (DAG) and soluble  $IP_3$  (Figure 2, bottom) (Kadamur & Ross, 2013; Berridge et al., 2003). There are seven known PLC subtypes, all of which conduct the same enzymatic reaction in response to stimuli unique to the respective subtype (Figure 2, top). While the enzymatic activity of  $PLC\delta$ , the first subtype to evolve, is entirely regulated by the intracellular concentration of calcium and abundance of its substrate  $PIP_2$  in the membrane, the  $PLC\gamma$  family responds to phosphorylation via receptor tyrosin kinases (RTKs).  $PLC\zeta$  is constitutively active with no dependency on external stimuli and is expressed only in sperm. Upon fertilization, its release into the ovum triggers the calcium signaling cascade that is crucial for the initiation of mitosis and embryonic growth (Kadamur & Ross, 2013; Berridge et al., 2003). The recently discovered  $PLC\eta$  has been shown to play a role in neuronal signaling, but it is not yet clear how this isozyme is regulated (Cockcroft, 2006; Katan & Cockcroft, 2020).  $PLC\beta$ , and also  $PLC\epsilon$ , are regulated via GPCRs, and are thus sensitive to by far the most diverse range of stimuli. Because of this, the  $PLC\beta$  family is the primary focus of this study.

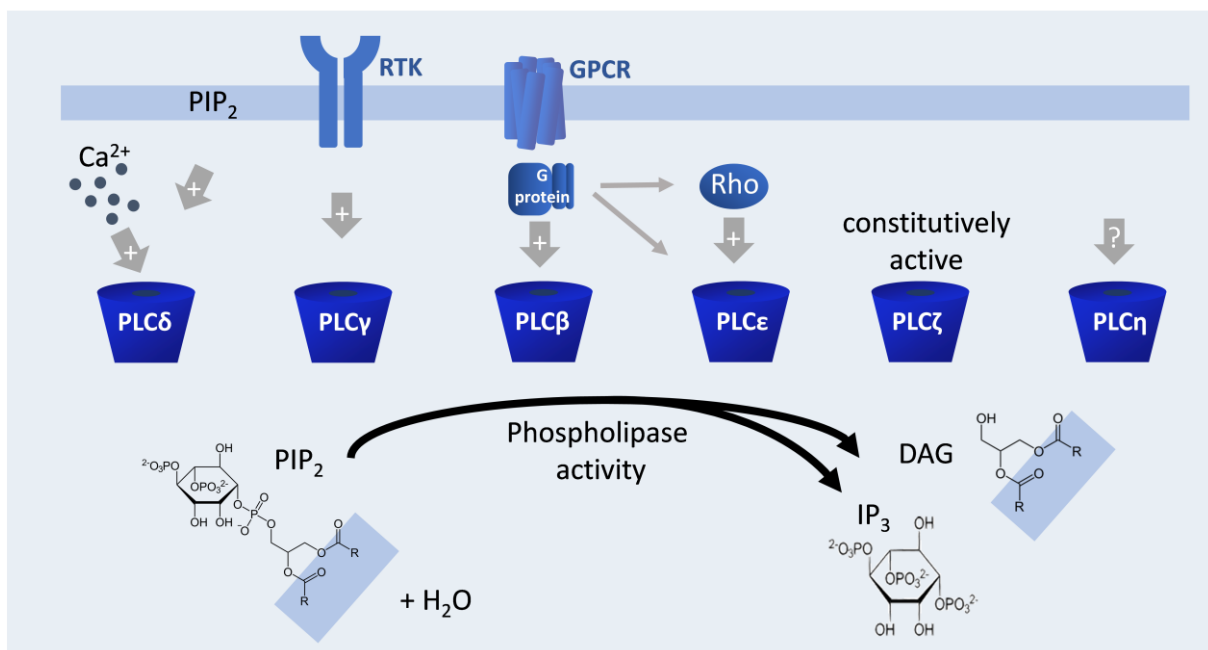


**Figure 2: The Phospholipase C family.** Based on (Kadamur & Ross, 2013; Cockcroft, 2006). Six subfamilies of PLC isozymes have been discovered to date (depicted in dark blue). The active site is more or less conserved across all subfamilies, and thus, they catalyze the same

## Introduction

enzymatic reaction (depicted below) of hydrolyzing the membrane lipid PIP<sub>2</sub> into hydrophobic DAG, which remains in the membrane, and hydrophilic IP<sub>3</sub>. However, because regulatory structural elements differ for each subfamily, their enzymatic activity is governed by different stimuli (depicted above).

## G protein-coupled receptors

G protein-coupled receptors (GPCRs) are the largest family of membrane proteins, with over 800 different receptors encoded in the human genome, and over 30% of drugs approved by the United States Food and Drug Administration directly target them (Hauser et al., 2017). They share the same basic structure featuring seven transmembranal helices, an extracellular N-terminus and an intracellular C-terminus, and three loops on either side of the membrane. When activated, a conformational change occurs, which is most prominent in the transmembranal helix 6 (Rosenbaum et al., 2009). In this way, they translate a huge variety of extracellular stimuli, from photons to protons to small molecule ligands to large peptides, into intracellular signals.

While more intracellular proteins are known to interact with activated GPCRs, their canonical mechanism of signal transduction is via the activation of guanine-nucleotide-bound proteins (G proteins) (Figure 3) (Rosenbaum et al., 2009; Oldham & Hamm, 2008). G proteins are heterotrimeric, meaning they consist of three subunits, which are commonly referred to as the G $\alpha$ , G $\beta$  and G $\gamma$  subunit. The G $\alpha$  subunit binds the guanine nucleotide, GDP or GTP, that gives G proteins their name, in a binding pocket located between their helical and RAS-like domain (Syrovatkina et al., 2016; Oldham & Hamm, 2008). Most G $\alpha$  subunits also carry a lipid anchor that increases their affinity to the cellular membrane. This membrane affinity of the heterotrimer is further increased by a prenylation of the G $\gamma$  subunit (Figure 3) (Oldham & Hamm, 2008; Syrovatkina et al., 2016).

In the resting state, G $\alpha$  is GDP-bound and has high affinity for the G $\beta$  and G $\gamma$  subunit (Figure 3A). Upon GPCR-activation, the G $\alpha$  subunit changes its conformation, causing it to “open” and the GDP to dissociate from its binding pocket (Figure 3B). In living cells, GDP is then immediately replaced by GTP (Figure 3B). The GTP-bound G $\alpha$  has a much lower affinity for the G $\beta\gamma$  subunits, causing the heterotrimer to dissociate into two subunits (Figure 3C). Each subunit then binds intracellular effector proteins and alters their properties, thereby transducing the extracellular stimulus recognized by the GPCR into an intracellular signaling cascade (Figure 3C, D). Next, because many

$G\alpha$  effectors are GTPase activating proteins (GAP), the  $G\alpha$ -bound GTP is hydrolyzed to GDP after a while (Figure 3C). Therefore, the  $G\alpha$  loses affinity for its effectors and regains affinity for the  $G\beta\gamma$  subunit, and the heterotrimer re-associates to re-establish the resting state and complete the G protein cycle (Figure 3A). In this state, the G protein is once again ready to be activated by a GPCR.

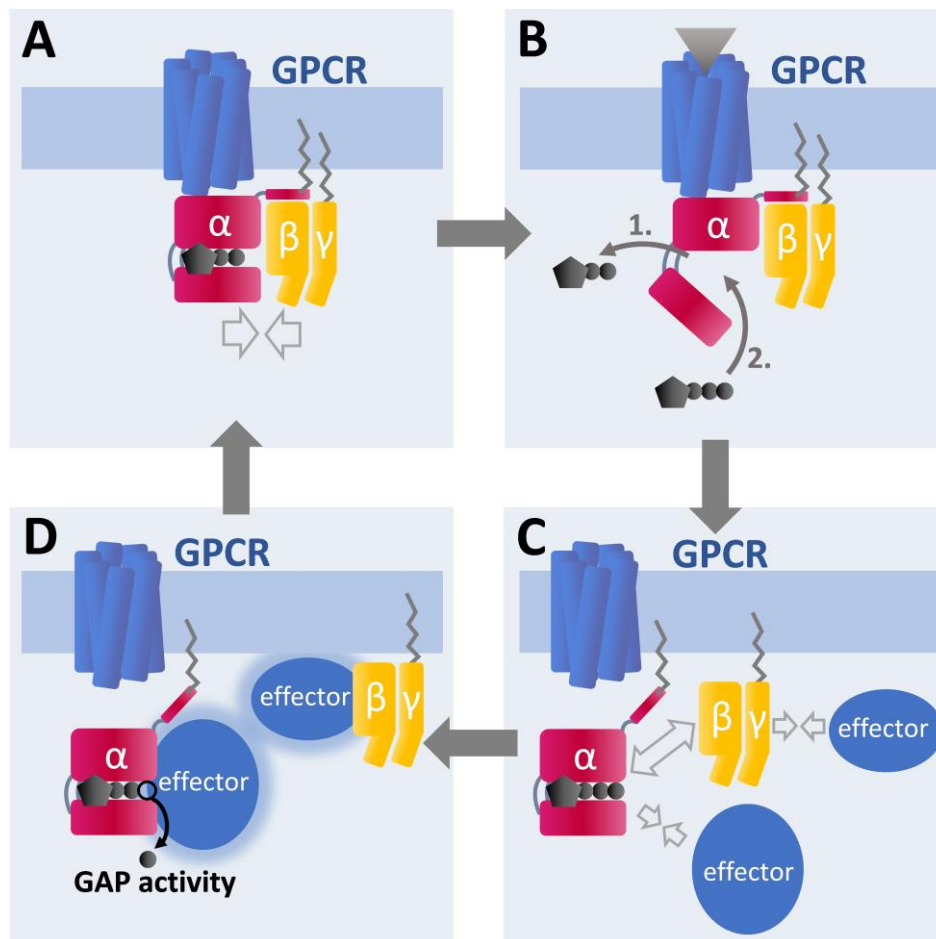


**Figure 3: G protein activation via G protein-coupled receptors.** Based on (Oldham & Hamm, 2008; Syrovatkina et al., 2016; Rosenbaum et al., 2009 and references therein). (A) In the inactive state, the GDP-bound  $G\alpha$  (red) and  $G\beta\gamma$  subunits form a heterotrimeric G protein, which is usually anchored to the cellular membrane by a prenylated residue in the  $G\gamma$  subunit as well as the  $G\alpha$  subunit. (B) Upon (ligand-mediated) GPCR activation, a conformational change is induced in the  $G\alpha$  subunit, which triggers the release of GDP from and binding of GTP to the nucleotide binding pocket (dark grey). (C) GTP-bound  $\alpha$  has a comparatively lower affinity to  $G\beta\gamma$ , causing the subunits to dissociate to bind and modulate intracellular effectors. (D) Both  $G\alpha$  as well as most  $G\alpha$  effectors are GTPase activating proteins, meaning they hydrolyze the  $\gamma$ -phosphate of GTP in the nucleotide binding pocket. The resulting GDP-bound  $G\alpha$  re-associates with  $G\beta\gamma$  (A) to restore the inactive state.

## G protein families and their signaling pathways

There are over 16  $G\alpha$ , five  $G\beta$  and 12  $G\gamma$  isoforms (McCudden et al., 2005; Smrcka, 2008), which in theory would make up enough heterotrimer combinations to provide a unique heterotrimer for each GPCR. However, they are instead grouped into four G-protein families, categorized by the  $G\alpha$  subunit they contain:  $G_s$ -,  $G_i$ -,  $G_q$ - and  $G_{12}$ -family heterotrimers. The  $G\alpha$  isoforms are grouped by homology, and each family is associated with a specific canonical signaling cascade triggered by the activated, GTP-bound  $G\alpha$ .

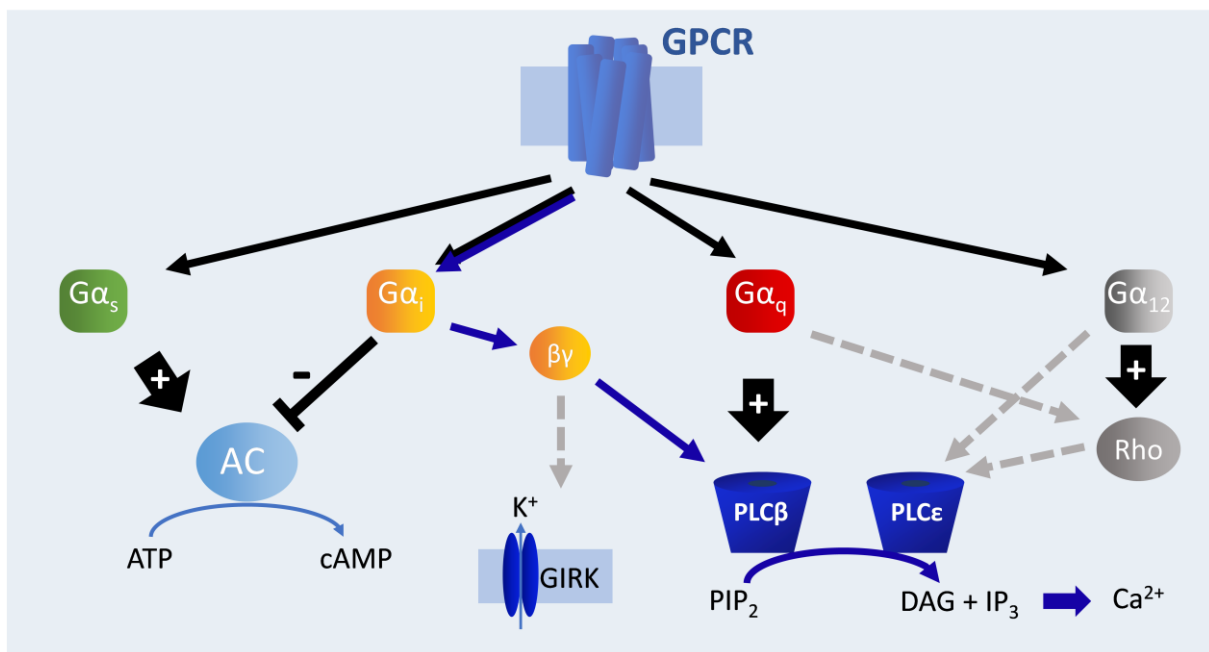


**Figure 4: G protein families and their signaling pathways.** Based on (McCudden et al. 2005 and references therein). Heterotrimeric G proteins can be grouped into four families, according to the sequence and function of their  $G\alpha$  subunits (green for  $G_s$ , yellow for  $G_i$ , red for  $G_q$  and grey for  $G_{12}$ ). The canonical signaling pathway of each  $G\alpha$  family is indicated in black. Examples of non-canonical signaling are depicted by dashed grey arrows. The dark blue arrows indicate the calcium pathway this project is centered on.

$G_{\alpha_s}$  and  $G_{\alpha_i}$  proteins both interact with the adenylyl cyclase (AC), an enzyme that converts ATP to cAMP (Figure 4).  $G_{\alpha_s}$ , also known as the stimulatory G protein, activates the AC, thereby increasing the intracellular cAMP concentration. On the other hand,  $G_{\alpha_i}$  inhibits the AC, thereby slowing the conversion of ATP to cAMP and decreasing the cellular cAMP levels. The  $G_i$  family is also known as PTX-sensitive G proteins (van der Ploeg et al., 1991), because all but one of its seven  $G\alpha$  are sensitive to inhibition with the  $G_i$  inhibitor PTX (Burns, 1988). The  $G_{12}/13$  family has been

found to regulate a variety of physiological processes by modulating Rho-kinase signaling (Suzuki et al., 2009) (Figure 4). The effectors of the G12/13 family include PLC $\epsilon$ , which links G12/13-activation to IP $_3$ /calcium signaling, possibly either through a direct intermolecular interaction with PLC $\epsilon$  or via the Rho signaling network.

The G $\alpha_q$  family canonically activates PLC $\beta$  and triggers calcium release, making it the most well-known, though not the only transducer of GPCR-mediated calcium mobilization. G $\alpha_q$  proteins have also been shown to regulate Rho signaling, which possibly links them to PLC $\epsilon$  as well (Syrovatkina et al., 2016) (Figure 4).

### G $\beta\gamma$ signaling.

Although the G $\alpha$  subunits are often portrayed as the main transducers of GPCR signaling, it has long been shown that the G $\beta\gamma$  subunits can also signal (Smrcka, 2008; McCudden et al., 2005). Despite five G $\beta$  and twelve G $\gamma$  subunits having been identified, we are only beginning to understand if and how their properties and physiological roles differ (McCudden et al., 2005; Khan et al., 2013). Not much is known about whether each G $\alpha$  family preferentially binds specific G $\beta\gamma$  combinations (Smrcka, 2008; Khan et al., 2013; Tennakoon et al., 2021; Masuho et al., 2021). However, G $\beta\gamma$  signaling is generally attributed to, and has been thoroughly demonstrated for, Gi-heterotrimers (McCudden et al., 2005; Smrcka, 2008; Kadamur & Ross, 2013). This includes the Gi-G $\beta\gamma$ -mediated activation of G protein-gated, inwardly rectifying potassium channels (GIRK) in neurons and cardiomyocytes (Smrcka, 2008; Lüscher & Slesinger, 2010), as well as Gi-G $\beta\gamma$  mediated activation of PLC $\beta$  to trigger IP $_3$  production and calcium release in the same manner as G $\alpha_q$  (Kadamur & Ross, 2013). This Gi-G $\beta\gamma$  calcium has been identified over 30 years ago (Sternweis & Smrcka, 1992; Cowen et al., 1990; Okajima & Ui, 1984; Goldman et al., 1985) and is considered an important process for immune cell activation (Li et al., 2000). The molecular mechanism of this pathway as well as its physiological relevance is historically based on two key findings: the observation of GPCR-mediated calcium that is abolished by the Gi inhibitor PTX (Okajima & Ui, 1984; Goldman et al., 1985; Cowen et al., 1990), and data showing that purified PLC $\beta$  can be activated by G $\beta\gamma$ , but not by G $\alpha_i$  (Smrcka & Sternweis, 1993; Sternweis & Smrcka, 1992). As such, the Gi-G $\beta\gamma$ -PLC $\beta$ -calcium mechanism is widely accepted as a well-established, independent signaling paradigm. However, despite its relative simplicity and unlike canonical G $\alpha_q$ -PLC $\beta$ -calcium,

demonstrating this  $G_i$  pathway has proven extremely challenging in most cases, which indicates that there might be an additional factor controlling it.

### PLC $\beta$ structure and activation

$G_q$ - as well as  $G_i$ -coupled GPCRs can mobilize calcium by activating the PLC $\beta$  enzyme family. PLC $\beta$  enzymes are large proteins of over 1000 amino acids (Kadamur & Ross, 2013; Hicks et al., 2008). The four members of this family (PLC $\beta$ 1-4) share a similar molecular structure (Figure 5A, B). From their N- to C-terminus, they consist of a Pleckstrin homology (PH) domain, followed by four EF domains that form two EF hands. The catalytic core is divided into two halves, the X and the Y domain, which form a TIM barrel and are separated by an acidic auto-inhibitory linker and followed by a C2 domain. The enzyme's C-terminus is divided into the proximal C terminal domain, which has regulatory functions, and the distal C terminal domain, which forms a coiled-coil structure and can anchor the enzyme to the membrane. The hydrolytic cleavage of membrane-bound PIP<sub>2</sub> takes place at a calcium ion bound to the TIM barrel. In the resting state, this position is covered by the XY linker, effectively auto-inhibiting the enzyme to ensure low basal activity. Another auto-inhibitory domain is a helix-turn-helix motif located in the proximal C-terminal domain. Both of these motifs hinder membrane association of PLC $\beta$  required for activation.



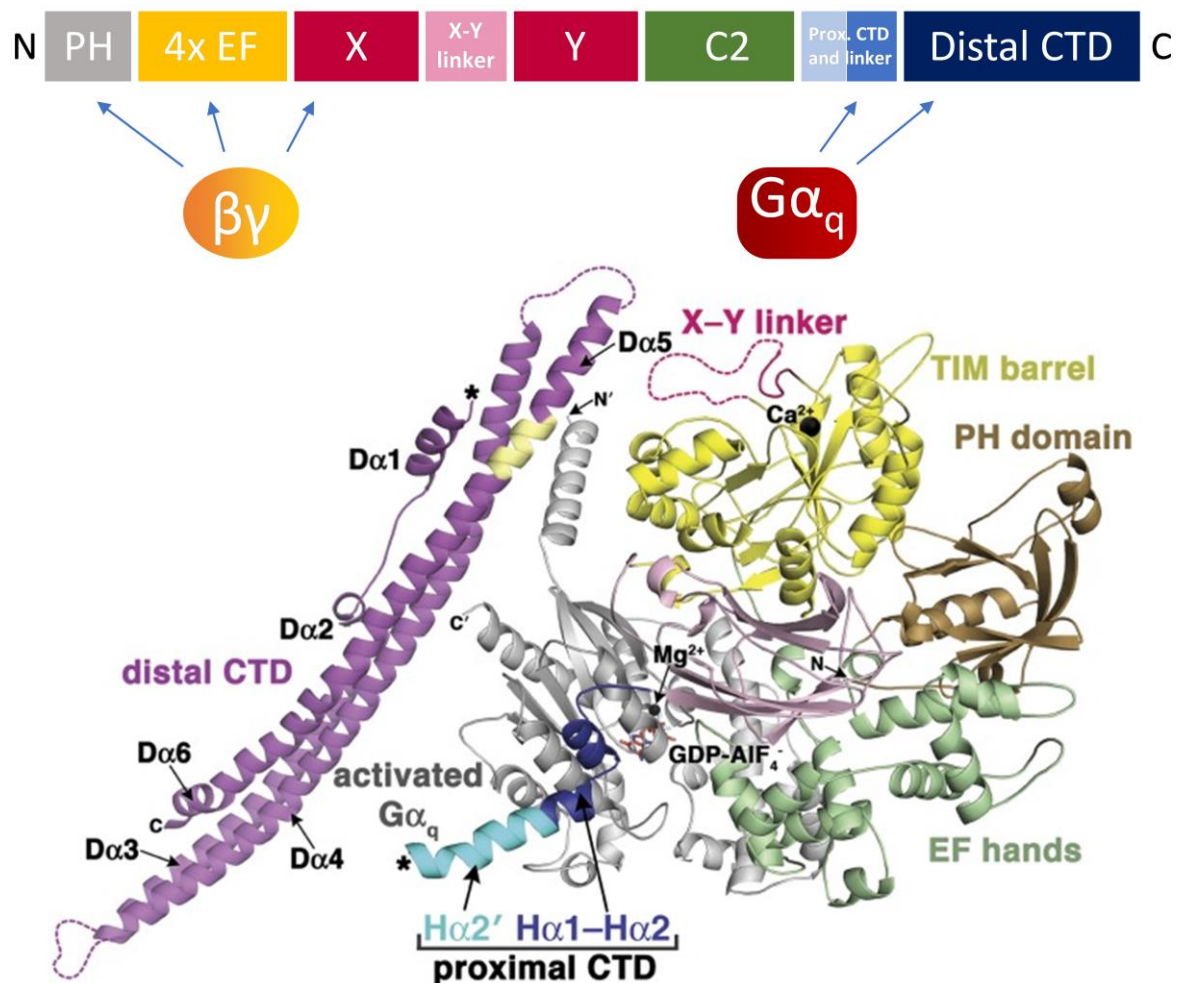


**Figure 5: The structure of the PLC $\beta$  family.** Based on (Hicks et al., 2008; Waldo et al., 2010; Lyon et al., 2011; Lyon et al., 2014; Kadamur & Ross, 2013). (A) PLC $\beta$  structural domains from N- to C-terminus. The regions that interact with G $\alpha_q$  and G $\beta\gamma$  are indicated with blue arrows. (B) PLC $\beta_3$  in complex with G $\alpha_q$ , (Lyon et al., 2011). The catalytic core, including the calcium ion (black), is located within the TIM barrel (yellow) and covered by a partially disordered X-Y linker (pink). G $\alpha_q$  engages the helix-turn-helix motif (H $\alpha_1$ -H $\alpha_2$ , HTH) as well as a portion of the distal C-terminal domain (CTD) (indicated in yellow).

As early studies with purified proteins have shown, PLC $\beta$  isozymes are activated by GTP-bound G $\alpha_q$  as well as G $\beta\gamma$  (Sternweis & Smrcka, 1992; Smrcka & Sternweis, 1993). A number of available crystal structures of PLC $\beta$  in complex with G $\alpha_q$  have located the binding position of G $\alpha_q$  to the enzymes c terminus (Figure 5A). One of the main points of G $\alpha_q$ -PLC $\beta$  interaction is located near the auto-inhibitory HTH motif of PLC $\beta$  (Lyon et al., 2011). Binding of G $\alpha_q$  to this region removes this auto-inhibitory domain and rearranges PLC $\beta$  at the membrane interface, causing the repulsion of the XY linker by the negatively charged membrane interface and revealing the catalytic site to facilitate substrate cleavage (Lyon et al., 2014).

## Introduction

In contrast to  $G\alpha_q$ , which activates all four  $PLC\beta$  isozymes,  $G\beta\gamma$  has been shown to activate only  $PLC\beta_2$  and  $PLC\beta_3$ , and sometimes  $PLC\beta_1$  to a small degree (Kadamur & Ross, 2013). The binding position of  $G\beta\gamma$  at  $PLC\beta$  is not entirely clear because so far, a crystal structure of  $G\beta\gamma$  in complex with  $PLC\beta$  is not yet available. However, a number of studies include molecular modeling- or mutational approaches that indicate  $G\beta\gamma$  interacts with regions of the PH-domain, the EF hands or the TIM barrel (Figure 5A). The C-terminal domains are not considered as important for  $G\beta\gamma$  binding because C-terminally truncated  $PLC\beta$  enzymes still respond to stimulation by  $G\beta\gamma$  (Kadamur & Ross, 2013).

It is important to note that compared with  $G\alpha_q$ ,  $G\beta\gamma$  is less potent in activating  $PLC\beta$  (Sternweis & Smrcka, 1992), which is often cited as a reason why  $G\beta\gamma$ -signaling is mainly or only  $G_i$ -mediated (Smrcka, 2008; Kadamur & Ross, 2013). According to this argument,  $G_i$  heterotrimers are generally more abundantly expressed and thus, unlike other G protein families, mobilize enough  $G\beta\gamma$  subunits to activate  $PLC\beta$ . There are also many findings indicating a synergistic activation of  $PLC\beta_3$  via  $G\alpha_q$  and  $G\beta\gamma$ , whereas  $PLC\beta_2$  shows a more additive activation (Rebres et al., 2011; Philip et al., 2010). This difference is thought to be rooted in two key differences between  $PLC\beta_2$  and  $PLC\beta_3$ . On the one hand,  $PLC\beta_2$  is less efficient than  $PLC\beta_3$ , in that its potential maximum speed of substrate conversion is considerably lower than that of  $PLC\beta_3$ . On the other hand, despite both isozymes being considerably auto-inhibited,  $PLC\beta_2$  shows a higher basal substrate conversion in the resting state. As a result, in the reconstituted system, activation of  $PLC\beta_2$  with either  $G\alpha_q$  or  $G\beta\gamma$  already increases its activity a significant portion of its peak speed, leaving no possibility of a further, over additive activation (Philip et al., 2010). Despite these differences in behavior of  $PLC\beta_2$  and  $PLC\beta_3$  in the reconstituted system, their activation via  $G_i$ - $G\beta\gamma$  is considered to be a fully competent, stand-alone signaling pathway for both isoforms.

## Variability of $G_i$ -calcium

Given the apparent mechanistic simplicity of the  $G_i$ - $G\beta\gamma$ - $PLC\beta$ -calcium paradigm, it is perhaps surprising that this pathway is sometimes considered a “quirk” of specific cell types or receptors, rather than a ubiquitous pathway. Often, this pathway is not demonstrated in studies that aim to characterize  $G_i$ -coupled GPCRs. Instead, studies might show calcium mobilization by these receptors upon transfection of a chimeric  $G\alpha_q/i$ -isoform that activates  $G\alpha_q$  effectors in response to  $G_i$ -GPCR activation

(Ravindranathan et al., 2009; Schmid et al., 2013; Binti Mohd Amir et al., 2018; Coward et al., 1999). Unlike Gi-Gβγ-GIRK activation, which depends on the expression of GIRK channels and is thus understandably only relevant in certain physiological systems, Gβγ-sensitive PLCβ isozymes are ubiquitously expressed and robustly activated by Gαq across a variety of backgrounds. The seemingly low interest in the Gi-Gβγ-PLCβ-calcium module is not due to a low relevance Gi-signaling in general either, because compared to the other G-protein families, Gi-coupled GPCRs comprise the largest group (Inoue et al., 2019). Thus, in principle, almost every cell type should be equipped with all the necessary components to mobilize Gi-calcium. Despite this, Gi-Gβγ-calcium is generally considered to be especially relevant for Gi-coupled GPCRs expressed in immune cells, while in other cells or organs, its role, consequences or even existence is barely described (Smrcka, 2008).

This perspective is not due to a disinterest in the Gi-Gβγ-PLCβ-calcium pathway, but because this signaling module is unexpectedly difficult to generate, and varies considerably across cell types and even laboratories. For example, stimulation of the Gi-coupled chemokine receptor CXCR2 triggers calcium release in neutrophils (Nasser et al., 2009), and also in HEK cells in one study (Fan et al., 2001), while another study using the same HEK background shows no CXCR2 calcium upon stimulation (Werry et al., 2003a). Interestingly, the authors then illustrate that stimulation of the cells with ATP immediately prior to CXCR2 stimulation restores the Gi-calcium. Many researches have published similar observations of restored Gi-calcium after stimulation of Gq-coupled GPCRs (Werry et al., 2003a, 2003b; Okajima & Kondo, 1992; Okajima et al., 1993; Gerwins & Fredholm, 1992; Dickenson & Hill, 1994; Megson et al., 1995; Connor & Henderson, 1996). Thrombocytes derived from Gq<sup>-/-</sup> mice show no calcium-dependent aggregation upon stimulation of Gi-coupled P2Y<sub>12</sub> (Offermanns et al., 1997). A recent investigation of the Gq inhibitor FR900359 (FR) (Schrage et al., 2015) demonstrates Gi-Gβγ-PLCβ mediated IP formation and calcium that is inexplicably fully blocked in the presence of the Gq inhibitor (Gao & Jacobson, 2016). Among many others, these findings have called into question the long-held tenet of Gi-Gβγ-PLCβ-calcium as an independent, fully competent signaling module. Instead, they seem to hint at a possible dependency of this module on Gq.

## Approach of this study

Based on the large quantity of evidence suggesting an involvement of Gq in the Gi-Gβγ-PLCβ-calcium mechanism, this study investigates the interdependency of these

## Introduction

two pathways. For this purpose, we make use of a set of both well-established as well as newly available, cutting edge tools and technology. We complement the use of the traditional Gi-inhibitor PTX with use of the more recently characterized specific Gq inhibitor FR (Schrage et al., 2015). We also use HEK cells that were genetically modified using CRIPRS/Cas9 technology (Grundmann et al., 2018; Milligan & Inoue, 2018), thus lacking functional alleles of  $G\alpha_q$  proteins (HEK- $\Delta Gq/11$ ), or depleted of functional PLC $\beta$ 1-4 isozymes (HEK PLC $\beta$ 1-4mut).

The aim of this study is to identify the mechanism underlying the variability of Gi-G $\beta\gamma$ -PLC $\beta$ -calcium. We hope to identify the factor that is required for G $\beta\gamma$  to activate PLC $\beta$  in living cells, and thereby provide a strategy to visualize and investigate this pathway in every cellular background. If successful, our investigations will provide the missing piece to a signaling pathway that has been considered paradigmatic for many years and potentially regulates calcium mobilization in almost every cell of the human body. Because calcium triggers a variety of physiological functions across different organs and cell types, our findings could lay the groundwork for new discoveries in a wide field of disease research.

# Material

## Chemicals and Reagents

**Table 1: Chemicals and reagents**

<b>Name</b>	<b>Source</b>	<b>ID#</b>
<b>5-HT</b>	Sigma-Aldrich	Cat# H9523-25mg
<b>A23187</b>	Sigma-Aldrich	Cat# C7522
<b>ADP</b>	Sigma-Aldrich	Cat# A2754-1g
<b>AR-C 66096</b>	Tocris	Cat# 3321/1
<b>ATP</b>	Sigma-Aldrich	Cat# A1852-1VL
<b>carbachol</b>	Sigma-Aldrich	Cat# C4382-1g
<b>Coelenterazine</b>	Carbosynth Limited	Cat# EC14031
<b>Coelenterazine h</b>	NanoLight	Cat# 301-1
<b>CXCL12</b>	Biozol	Cat# BYT-ORB544936
<b>Dk-PGD2</b>	Biozol	Cat# 12610
<b>Forskolin (FSK)</b>	Bachem	Cat# TRC-F701800
<b>FR900359</b>	G. König lab	N/A
<b>Fura2/AM</b>	Thermo Fisher Scientific	Cat# F1221
<b>Go6983</b>	Sigma-Aldrich	Cat# G1918-1mg
<b>Hanks' buffered salt solution (HBSS)</b>	Thermo Fisher Scientific	Cat# 14175129
<b>histamine</b>	Sigma-Aldrich	Cat# H7250-5g
<b>IL8</b>	PeproTech	Cat# 200-08M
<b>isobutylmethylxanthine (IBMX)</b>	Sigma-Aldrich	Cat# I5879

## Material

<b>m-3M3FBS</b>	Sigma-Aldrich	Cat# T5699
<b>MDL29,951</b>	Maybridge	Cat# SEW06645
<b>MRS 2179</b>	Tocris	Cat# 0900/10
<b>NECA</b>	Sigma-Aldrich	Cat# E2387
<b>PGD2</b>	Biomol	Cat# Cay12010-1
<b>poly-D-lysine</b>	Sigma-Aldrich	Cat# P2636
<b>PTX</b>	Thermo Fisher Scientific	Cat# PHZ1174
<b>Thallos AM dye</b>	TEFLabs	Cat# 902
<b>thapsigargin</b>	Sigma-Aldrich	Cat# T9033
<b>TM30089</b>	Sigma-Aldrich	Cat# SML2743-5mg
<b>UTP</b>	Sigma-Aldrich	Cat# U4125
<b>Primestar® GTX Polymerase</b>	Takara	Cat# R050B
<b>Taq Polymerase</b>	Asuka Inoue Lab, Sendai	N/A

## Cell Culture Media

### Base

**Table 2: Media bases**

<b>Name</b>	<b>Source</b>	<b>ID#</b>
<b>DMEM - Dulbecco's Modified Eagle Medium</b>	Thermo Fisher Scientific	Cat# 11965092
<b>MEM Alpha Medium (1x) + GlutaMAX™-I</b>	Thermo Fisher Scientific	Cat# 32561-039
<b>Medium 231</b>	Thermo Fisher Scientific	Cat# M231500
<b>Gibco™ RPMI 1640 Medium</b>	Thermo Fisher Scientific	Cat# 11560406

## Supplements

**Table 3: Media supplements**

Name	Source	ID#
Penicillin/streptomycin solution	Thermo Fisher Scientific	Cat# 15140
Fetal Bovine Serum (FBS)	Sigma Aldrich	Cat# -0804
G418 (Geneticin)	Gibco	Cat# 11811
Hygromycin B	Thermo Fisher Scientific	Cat# ant-hm-1
Blasticidin	Thermo Fisher Scientific	Cat# ant-bl-1
Horse Serum	Thermo Fisher Scientific	Cat# 26050070
Insulin	Thermo Fisher Scientific	Cat# 1258-014
Gentamicin	Thermo Fisher Scientific	Cat# 15750037
N2 supplement	Thermo Fisher Scientific	Cat# 1665870
3,3',5-Triiodo-L-thyronine sodium salt (T3)	Sigma Aldrich	Cat# T-2752
Sodium selenite	Sigma Aldrich	Cat# S-5261
L-thyroxine	Sigma Aldrich	Cat# T-2376
Smooth muscle growth supplement (SMGS)	Thermo Fisher Scientific	Cat# S00725

## Antibodies

**Table 4: Antibodies**

Name	Source	ID#
mouse anti-PLC $\beta$ 3	Santa Cruz Biotechnology	Cat# sc-133231; RRID: AB_2299534)
rabbit anti- $\beta$ -actin	BioLegend	Cat# 622102; RRID: AB_315946
goat anti-rabbit IgG Antibody HRP	antikoerper-online	Cat# ABIN102010; RRID: AB_10762386
goat anti-mouse IgG antibody HRP	Sigma-Aldrich	Cat# A4416; RRID: AB_258167

## Material

### Plasmids

**Table 5: Plasmids**

<b>Name</b>	<b>Source</b>	<b>ID#</b>
<b>3HA-hGPR17-pcDNA3.1</b>	Evi Kostenis Lab, Bonn	Plasmid #1021
<b>CXCR2-pcDNA3.1</b>	Evi Kostenis Lab, Bonn	Plasmid #1217
<b>DP2-pCAGGS</b>	Asuka Inoue Lab, Sendai	Plasmid #1521
<b>DP2-pcDNA3.1</b>	Asuka Inoue Lab, Sendai	Plasmid #704
<b>DP2<math>\Delta</math>ct-pcDNA3.1</b>	Evi Kostenis Lab, Bonn	Plasmid #705
<b>Gai1- pCAGGS</b>	Asuka Inoue Lab, Sendai	Plasmid #1527
<b>Gai2-pCAGGS</b>	Asuka Inoue Lab, Sendai	Plasmid #1528
<b>Gai3-pCAGGS</b>	Asuka Inoue Lab, Sendai	Plasmid #1529
<b>Gao1-pCAGGS</b>	Asuka Inoue Lab, Sendai	Plasmid #1559
<b>Gaq-pCAGGS</b>	Asuka Inoue Lab, Sendai	Plasmid #1530
<b>Gaq-pcDNA3.1</b>	Evi Kostenis Lab, Bonn	Plasmid #728
<b>Gaz-pCAGGS</b>	Asuka Inoue Lab, Sendai	Plasmid #1560
<b>G<math>\beta</math>1-pCAGGS</b>	Asuka Inoue Lab, Sendai	Plasmid #1455
<b>LgBiT-Gai1- pCAGGS</b>	Asuka Inoue Lab, Sendai	Plasmid #1496
<b>LgBiT-Gai2-pCAGGS</b>	Asuka Inoue Lab, Sendai	Plasmid #1497
<b>LgBiT-Gai3-pCAGGS</b>	Asuka Inoue Lab, Sendai	Plasmid #1498
<b>LgBiT-Gao1-pCAGGS</b>	Asuka Inoue Lab, Sendai	Plasmid #1499
<b>LgBiT-Gaz-pCAGGS</b>	Asuka Inoue Lab, Sendai	Plasmid #1500
<b>Gy2-GFP10-pcDNA3.1</b>	Evi Kostenis Lab, Bonn	Plasmid #1095
<b>G<math>\beta</math>1-pcDNA3.1</b>	Evi Kostenis Lab, Bonn	Plasmid #1093



<b>H1-pCAGGS</b>	Asuka Inoue Lab, Sendai	Plasmid #1443
<b>IP<sub>3</sub>-Sensor</b>	Gulyás et al., 2015	Plasmid #1561
<b>LgBiT-PLCβ1-pCAGGS</b>	Evi Kostenis Lab, Bonn	Plasmid #1450
<b>LgBiT-PLCβ2-pCAGGS</b>	Evi Kostenis Lab, Bonn	Plasmid #1451
<b>LgBiT-PLCβ3-pCAGGS</b>	Evi Kostenis Lab, Bonn	Plasmid #1452
<b>LgBiT-PLCβ4-pCAGGS</b>	Evi Kostenis Lab, Bonn	Plasmid #1453
<b>mGPR17-pcDNA3.1</b>	Evi Kostenis Lab, Bonn	Plasmid #1208
<b>pcDNA3.1</b>	Evi Kostenis Lab, Bonn	Plasmid #1218
<b>pCAGGS</b>	Asuka Inoue Lab, Sendai	Plasmid #1440
<b>PLCβ2-pcDNA3.1</b>	Evi Kostenis Lab, Bonn	Plasmid #1124
<b>PLCβ3<sup>F715A</sup>-pcDNA3.1</b>	Evi Kostenis Lab, Bonn	Plasmid #1533
<b>PLCβ3-pcDNA3.1</b>	Evi Kostenis Lab, Bonn	Plasmid #1354
<b>PLCβ3<sup>ΔXY</sup>-pcDNA3.1</b>	Evi Kostenis Lab, Bonn	Plasmid #1532
<b>PTX-S1-pCAGGS</b>	Asuka Inoue Lab, Sendai	Plasmid #1464
<b>rGPR17-pcDNA3.1</b>	Evi Kostenis Lab, Bonn	Plasmid #1223
<b>smBiT-Gy2-pCAGGS</b>	Asuka Inoue Lab, Sendai	Plasmid #1468
<b>sgPLCB1-pSpCas9(BB)-2A-GFP</b>	Asuka Inoue Lab, Sendai	Plasmid #1419
<b>sgPLCB2-pSpCas9(BB)-2A-GFP</b>	Asuka Inoue Lab, Sendai	Plasmid #1420
<b>sgPLCB3-pSpCas9(BB)-2A-GFP</b>	Asuka Inoue Lab, Sendai	Plasmid #1421
<b>sgPLCB4-pSpCas9(BB)-2A-GFP</b>	Asuka Inoue Lab, Sendai	Plasmid #1423
<b>Rluc8-Gαq-pcDNA3.1</b>	Evi Kostenis Lab, Bonn	Plasmid #1196
<b>Rluc8-Gαq<sup>H218A-R256A</sup>-pcDNA3.1</b>	Evi Kostenis Lab, Bonn	Plasmid #1562
<b>Gαq<sup>H218A</sup>-pcDNA3.1</b>	Evi Kostenis Lab, Bonn	Plasmid #1351
<b>Gαq<sup>R256A</sup>-pcDNA3.1</b>	Evi Kostenis Lab, Bonn	Plasmid #1352

## Material

---

<b>Gαq<sup>H218A-R256A</sup>-pcDNA3.1</b>	Evi Kostenis Lab, Bonn	Plasmid #1353
---	------------------------	---------------

---

## Bacterial strains

**Table 6: Bacterial strains**

<b>Name</b>	<b>Source</b>	<b>ID#</b>
<b>DH5α Competent Cells</b>	Thermo Fisher Scientific	Cat# 18265-017
<b>XL1-Blue Competent Cells</b>	Stratagene	Cat# 200130

## Experimental models

### Cell lines

**Table 7: Cell lines**

<b>Name</b>	<b>Source</b>	<b>ID#</b>
<b>Human: HEK</b>	ATCC	Cat# CRL-1573
<b>Human: native HEK</b>	A. Inoue lab	N/A
<b>Human: ΔGq/11 HEK</b>	A. Inoue lab	N/A
<b>Human: ΔG12/13 HEK</b>	A. Inoue lab	N/A
<b>Human: ΔGq/11/12/13 HEK</b>	A. Inoue lab	N/A
<b>Human: PLCβ1-4mut HEK</b>	A. Inoue lab	N/A
<b>Mouse: Oli-neu</b>	J. Trotter lab	N/A
<b>Human: HaCaT</b>	E. Gaffal lab	N/A
<b>Human: JURKAT</b>	ATCC	Cat# CRL-2063
<b>Mouse: brown adipocytes</b>	A. Pfeifer lab	N/A
<b>Mouse: PASC</b>	D. Wenzel lab	N/A
<b>Mouse: platelet</b>	B. Nieswandt lab	N/A

### Organisms

**Table 8: Organisms**

<b>Name</b>	<b>Source</b>	<b>ID#</b>
-------------	---------------	------------

<b>Mouse: C57Bl6/J</b>	Charles River	N/A
<b>Mouse: CD1</b>	Charles River	N/A

## Commercial Assay Kits

**Table 9: Commercial Assay Kits**

<b>Name</b>	<b>Source</b>	<b>ID#</b>
<b>ECL Prime Western blotting detection reagent</b>	GE Healthcare	Cat# RPN2236
<b>FLIPR<sup>®</sup> Calcium 5 Assay kit</b>	Molecular Devices	Cat# R8186
<b>HTRF-cAMP dynamic 2 kit</b>	Cisbio International	Cat# 62AM4PEC
<b>HTRF-IP One dynamic 2 kit</b>	Cisbio International	Cat# 62IPAPEC
<b>Pierce BCA Protein Assay</b>	Thermo Fisher Scientific	Cat# 23225
<b>black 96-well tissue culture plates with clear bottoms</b>	Corning	Cat# 3603

# Methods

## Cell culture

### Culture conditions

All cell lines were cultivated at 37°C in a 5% CO<sub>2</sub> humidified atmosphere, either in standard sterile cell culture dishes or flasks. Cells were passaged regularly to keep confluency below 90 % and replace the culturing media.

### Cell culture media

Each cell line was cultured in an appropriate media mixture to ensure optimal growth conditions.

**HEK parental and CRISPR/Cas9-edited cell lines, HaCaT and murine brown preadipocytes** cells were kept in the following media mixture:

**Table 10: HEK standard media**

Constituent	Volume [mL]	Final concentration
<b>Dulbecco's Modified Eagle Medium (DMEM)</b>	500	
<b>FBS</b>	50	~10%
<b>Penicillin-Streptomycin mixture</b>	5	~100 U/mL penicillin, 0.1 mg/mL streptomycin

**HEK-DP2-Δct, HEK-hGPR17, HEK-rGPR17 and HEK-mGPR17** were kept in the following media mixture:

**Table 11: HEK-GPCR cell line media**

Constituent	Volume [mL]	Final concentration
<b>Dulbecco's Modified Eagle Medium (DMEM)</b>	500	
<b>FBS</b>	50	~10%
<b>Penicillin-Streptomycin mixture</b>	5	~100 U/mL penicillin, 0.1 mg/mL streptomycin
<b>G418 (Geneticin)</b>	2.22	400 µg/mL

HEK-DP2-GIRK1/2 cells were kept in the following media mixture:

**Table 12: HEK-DP2-GIRK cell line media**

Constituent	Volume	Final concentration
<b>MEM Alpha Medium (1x) + GlutaMAX™-I</b>	500 mL	
<b>FBS</b>	50 mL	~10%
<b>Penicillin-Streptomycin mixture</b>	5 mL	~100 U/mL penicillin, 0.1 mg/mL streptomycin
<b>Puromycin</b>	33 µL	3 µg/mL
<b>Blasticidin</b>	278 µL	5 µg/mL
<b>G418 (Geneticin)</b>	2.22 mL	400 µg/mL

Oli-Neu cells were kept in the following media mixture:

**Table 13: Oli-Neu cell media**

Constituent	Volume	Final concentration
<b>Dulbecco's Modified Eagle Medium (DMEM)</b>	500 mL	
<b>FBS</b>	50 mL	~10%
<b>Penicillin-Streptomycin mixture</b>	5 mL	~100 U/mL penicillin, 0.1 mg/mL streptomycin
<b>Insulin</b>	625 µL	5 µg/mL
<b>Gentamicin</b>	250 µL	25 µg/mL
<b>N2 supplement</b>	5 mL	~1%
<b>T3</b>	400 µL	400 nM
<b>Sodium selenite</b>	370 µL	190 nM
<b>L-thyroxine</b>	65 µL	520 nM

## Methods

JURKAT cells were kept in the following media mixture:

**Table 14: JURKAT media**

Constituent	Volume [mL]	Final concentration
Gibco™ RPMI 1640 Medium	500	
FBS	50	~10%
Penicillin-Streptomycin mixture	5	~100 U/mL penicillin, 0.1 mg/mL streptomycin

Murine pulmonary arterial smooth muscle cells were kept in the following media mixture:

**Table 15: mPASMCMedia**

Constituent	Volume [mL]	Final concentration
Medium 231	500	
Smooth muscle growth supplement (SMGS)	50	~10%
Penicillin-Streptomycin mixture	5	~100 U/mL penicillin, 0.1 mg/mL streptomycin

## Transient Transfection

HEK cells were transiently transfected 48 h before the experiments using either FuGENE<sup>HD</sup> or Polyethylenimin (PEI, 1 mg/mL).

Using FuGENE, the transfection was performed according to the manufacturer's instructions. A total of 10 µg plasmid DNA was used in combination with 30 µL FuGENE for transfection of 4 mio cells in a 10 cm culture dish.

Transfection using PEI was performed using 10 µg plasmid DNA and 30 µL PEI solution, which was mixed in 500 µL PBS buffer and incubated for 15 min before adding it to 10 cm culture dish containing 4 mio cells.

If more or fewer cells were required for an experiment, the cell number, media volume, plasmid quantity, and transfection reagent quantity were adjusted to maintain the same ratio for transfections of higher or lower cell numbers.

## Generation of CRISPR/Cas9-edited HEK-PLC $\beta$ 1-4mut cell lines

To generate a HEK cell line that is lacking functional alleles encoding PLC $\beta$ 1, PLC $\beta$ 2, PLC $\beta$ 3 and PLC $\beta$ 4, HEK parental (wildtype) cells were genome-edited using CRISPR/Cas9 technology according to the previously published method (Milligan & Inoue, 2018).

### CRISPR/Cas9 method

The CRISPR/Cas9 gene editing system is derived from a bacterial defense mechanism that protects against re-infection with viral DNA. It works by using the RNA-guided Cas9-endonuclease to induce a double strand break in a selected gene region (Milligan & Inoue, 2018). Two factors are required in order for the Cas9 endonuclease to induce a double-strand break: i) the Cas9-bound RNA (CRISPR-RNA, crRNA) that guides the Cas9 complex to a complementary sequence of the target DNA, and ii) a short nucleotide sequence called the protospacer-associated motif (PAM) specific to the employed Cas9-protein that flanks the 3' end of the crRNA. For the streptococcus pyogenes-derived Cas9, which we use here, this PAM sequence is 5'-NGG-3'. Thus, by expressing a single guide RNA (sgRNA) of a desired sequence that mimics the function of the crRNA, along with a functional Cas9 endonuclease, the exact spot where the double strand break will occur can be reasonably well controlled.

### CRISPR/Cas9-edited genetic knockout strategy

Previously, this CRISPR/Cas9 method has been used by the Inoue lab to produce a genetic knockout of various G $\alpha$  isoforms or  $\beta$ -arrestins in HEK cells (Grundmann et al., 2018). This is possible because when a double-strand break occurs in the genome of a cell, the cellular repair mechanisms sometimes delete or insert a number of base pairs when repairing the cut. This can lead to premature stop-codons or frameshift mutations; thus, a functional protein will no longer be encoded. If this occurs in all alleles encoding for the target protein, the result is a complete genetic knockout of this protein.

The success of this strategy depends on a series of coincidences:

- 1) A cell within the pool of transfected HEK cells has to receive the plasmid encoding, and express the sgRNA and Cas9 endonuclease,
- 2) in this cell, double-strand breaks have to be induced in all alleles encoding the target proteins,

## Methods

3) when repairing those double strand breaks, deletions or insertions have been introduced into all of the alleles, and

4) all these deletions or insertions have to cause frameshift-mutations or encode stop-codons.

Therefore, the employed methodology has been optimized to increase the chance of achieving a knockout cell line as much as possible.

To allow selection of the cells that were successfully transfected with the plasmids encoding the CRISPR complex (see point 1), a vector that encodes an additional GFP-protein was selected. Because the chance of all alleles being targeted (see point 2) increases with the amount of expressed CRISPR-complex, fluorescence-activated single cell sorting (FACS) is then used to separate cells that expressed high quantities of GFP. These cells can then be cultured into individual monoclonal cell lines and be further screened.

To allow for selection of the cells where repair of the double strand break introduced insertions or deletions (see point 3), the sgRNA is designed to guide the cut to a restriction enzyme (RE) recognition site. When the region of the double strand break is amplified using a PCR, and then digested by a RE that recognizes the site of the double strand break, only the DNA that still contains the wildtype sequence will be digested. An agarose gel analysis of RE-digested PCR product from the lysates of each monoclonal cell line can then be used to identify the most promising cell lines for functional analysis and genetic sequencing (see point 4).

### Protocol to generate the HEK-PLC $\beta$ 1-4mut cell line

In order to target the genes encoding all four PLC $\beta$  isoforms, two consecutive “knockout rounds” were conducted. In the first round, PLC $\beta$ 1 and PLC $\beta$ 3 were targeted in HEK parental cells to generate a HEK-PLC $\beta$ 1/3mut cell line. In the second round, PLC $\beta$ 2 and PLC $\beta$ 4 were targeted in the resulting cell line, with the goal of achieving a PLC $\beta$ 1-4 quadruple knockout.



## sgRNA selection

The sgRNA we selected to target each PLC $\beta$  isoform, including their corresponding restriction enzyme and PCR primers flanking the target region were as follows:

**Table 16: PLC $\beta$ 1-4 CRISPR/Cas9 target regions**

Target	direction	PAM + 20 bases	sgRNA	RE	target region forward primer	target region reverse primer
PLC $\beta$ 1	sense	tgtggggaacatc gggcgctgg	CACCGtgtgggga acatcgggcgcc	Bsp T107 I	TTTGTGGAATGGG AGCCTTAAAC	TGGAAAGCCACG AGATTCAAATG
PLC $\beta$ 2	sense	accagaaacagcg ggactcctgg	CACCGaccagaaa cagcgggactcc	Hinf I	GCCCAAGGGATA TGGACCTG	TGGGGGACAGGA GATAGCTG
PLC $\beta$ 3	anti- sense	cctgatctgagca cggacatga	CACCGtcatgtccg tgctcagatcc	Mbo I	AGTATGAGCCCAA CCAGCAG	TGAGCAAATGGG CCAAAAGG
PLC $\beta$ 4	sense	acagttcggcggg aagtcttgg	CACCGacagttcgg cgggaagtctt	Mbo II	GCCCCAGTCTTCC TAGATCG	AAACTGAAGGGC ATCACACAC

## CRISPR/Cas9 transfection, FACS, and single clone culture

2 mio HEK cells were seeded into 10 cm culture dishes and allowed to attach overnight. The following day, these cells were transfected with a mixture of 5  $\mu$ g + 5  $\mu$ g of CRISPR plasmid targeting PLC $\beta$ 1 and PLC $\beta$ 3, respectively. 30  $\mu$ L PEI were used as the transfection reagent, according to the above-described method.

Around 48 h after transfection, the cells were detached, washed, resuspended in HBSS buffer and sorted using FACS to receive 50.000 cells with high green fluorescence. These cells were then spun down, resuspended in media, diluted and seeded into ten 96-well cell culture plates each at a concentration of 1 cell/well, 2 cells/well, and 5 cells/well.

After 14 days, the plates were evaluated to identify 100 wells containing a single, healthy-looking round colony that covered >50% of the available area. These clones were numbered, detached, and resuspended in a volume of 50  $\mu$ L Trypsin/EDTA. 20  $\mu$ L was moved to a correspondingly numbered well of a 6-well plate containing 3 mL of media per well to continue cell culture, the rest moved into a correspondingly numbered PCR plate containing 100  $\mu$ L media per well.

## Clone screening by PCR and RE-digest

The PCR plate containing the cell suspension was spun down to pellet the cells and aspirated to remove media. The cell pellets were resuspended in 45  $\mu$ L 50 mM NaOH

## Methods

per well and boiled at 96°C for 10 minutes to make cellular lysates. Next, the solution was neutralized using 5 µL 1M TRIS/HCl (pH 7.4) and frozen.

One or two days later, the cellular lysates were thawed and 5 µL per lysate was used to perform two PCRs amplifying each target region. The following PCR mixture was used for this:

**Table 17: CRISPR screening PCR mix (per 1 well)**

<b>Taq 5x buffer</b>	3 µL
<b>Taq polymerase</b>	0.1 µL
<b>Primer fw (100 µM)</b>	0.075 µL
<b>Primer rv (100 µM)</b>	0.075 µL
<b>dNTPs (10mM)</b>	0.3 µL
<b>MilliQ</b>	ad 13 µL

**Table 18: CRISPR screening PCR conditions**

<b>pre</b>	95°C	1 min	
<b>denat</b>	95°C	10 s	40 cycles
<b>anneal</b>	64°C	15 s	
<b>elong</b>	72°C	30 s	
<b>hold</b>	8°C	infinite	

Of the resulting PCR product, 5 µL were mixed with either 5 µL of RE-digestion mix or 5 µL water as a negative control, and digested for 2h.

**Table 19: CRISPR screening RE mix**

<b>Restriction Enzyme</b>	<b>DNA</b>	<b>10x NEBuffer</b>	<b>MilliQ water</b>
<b>1 unit</b>	(0.1 µg) 50 µL PCR product	1 µL	Ad 5 µL

The RE digest product was then loaded onto 3% agarose gels containing ethidium bromide, and run for ca. 30 min. Afterwards, undigested samples were identified under UV light to determine the HEK clones that contained mutated target sequences. Following this, these HEK cell clones were moved from 6-well plates into 10 cm dishes for further culturing, while the rest were discarded.

## Genetic sequencing

A PCR was performed to amplify each target region in each candidate cell line, using the Primestar polymerase according to the manufacturer's instructions. Furthermore,

we used 2  $\mu$ L cellular lysate and a total reaction volume of 50  $\mu$ L. Following this, a genetic sequencing service was used to analyze the mutations in all target regions of each clone. Because each HEK cell contains multiple alleles encoding each target gene, and not all alleles feature the exact same mutation, this usually reveals multiple overlapping sequences, which makes it difficult to determine the sequence of each individual allele (Figure M1). Thus, we focused on eliminating all clones that contained either wildtype or obvious in-frame mutations, and kept the rest for functional analyses.

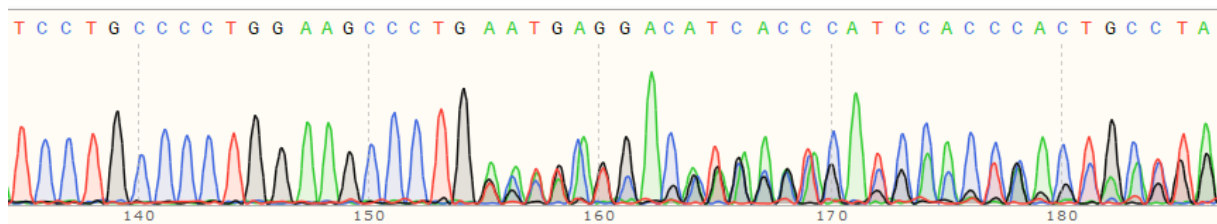


**Figure M1: Sanger Sequence of the PLC $\beta$ 3 CRISPR target region of one sample clone.** The left region of the SANGER sequence shows only one clear peak per position. However, starting at position 155, at least three overlapping sequences are visible. This is because a double strand break was introduced at this position that leads to different mutations in at least three alleles encoding PLC $\beta$ 3, all of which were amplified in the PCR of the target region and are thus present in the SANGER sequence diagram. The overlap makes it difficult to determine the genetic sequence of each allele from this diagram.

### Functional clone screening

PLC $\beta$  is the main transducer of GPCR-mediated calcium. Thus, after two knockout rounds targeting all PLC $\beta$  isoforms, we performed calcium measurements with the remaining clones to identify the cell lines that no longer mobilized calcium in response to GPCR-stimulation.

### What went wrong?

During our final functional screening, we only identified two cell lines that did not mobilize calcium in response to GPCR stimulation (data not shown). At this point, we again sent in the cells for genetic sequencing and found that both clones featured a 6BP deletion in one allele encoding for PLC $\beta$ 3, which had been introduced in the first knockout round and we had missed at the time. The mutations in each target gene of the selected cell line are as follows:

**Table 20: Genetic sequence of target regions in functional PLC $\beta$ 1-4 knockout HEK cell line**

Target	Allele	Mutation	Note	New sequence
<b>PLC<math>\beta</math>1</b>	1	16BP deletion	Frame-shift	TTTTGGATG()CCTGGAGCAGCG
	2	4BP deletion	Frame-shift	TTTTGGATGTGGGGAACATCG()CCTGG
<b>PLC<math>\beta</math>2</b>	1	1BP insertion: C	Frame-shift	CAGCGGGA(C)CTCCCG
	2	9BP deletion	In-frame	CAGCGG()CTTAACTC
<b>PLC<math>\beta</math>3</b>	1	1BP insertion: T	Frame-shift	GGAAGCCCTGGAT(T)CTGAGCAC
	2	6BP deletion	In-frame	GGAAGCCCTG()AGCAC
	3	2BP deletion	Frame-shift	GGAAGCCCTG()TCTGAGCAC
<b>PLC<math>\beta</math>4</b>	1	24BP deletion	In-frame	CACT()TCGGTAGAAATG
	2	WT Sequence	Wildtype	-

The Inoue lab has kindly performed another knockout round to target the 6BP deletion in the allele encoding PLC $\beta$ 3 of this cell line. The resulting cell line, which they kindly provided for us, still contains the 9BP-deletion in PLC $\beta$ 2 and wt-allele in PLC $\beta$ 4. Thus, it is not a genetic knockout, but a ‘functional knockout’, because it does not mobilize GPCR-dependent calcium unless a PLC $\beta$  isoform is re-transfected (see Figure 7, Results section). This cell line is referred to in this study as HEK-PLC $\beta$ 1-4mut.

## Isolation of primary cells

### Murine brown preadipocytes (mBAT)

Murine brown preadipocytes (mBAT) isolated from newborn pups of C57Bl6/J mice (Klepac et al., 2016; Pfeil et al., 2020) were kindly provided by the Alexander Pfeifer Lab, Bonn. The cells were unfrozen from cryoculture vials 48 h before the calcium measurement and immediately seeded into calcium measurement plates. Calcium measurements were then performed as described below.

### Murine pulmonary arterial smooth muscle cells (mPASMC)

Murine pulmonary arterial smooth muscle cells (mPASMC) isolated from CD1 mice (Matthey et al., 2017; Pfeil et al., 2020) were kindly provided by the Daniela Wenzel Lab, Bonn. The cells were unfrozen 2-3 weeks before the calcium measurements and cultivated in culture flasks according to the above-described procedure.

### Murine platelets

Murine platelets from CD1-mice were kindly isolated by the Bernhard Nieswandt Lab, Würzburg. Calcium and aggregatory measurements were performed using freshly isolated cells (Pfeil et al., 2020).

## Cell-based assays

Many of the following methodologies have been previously published in (Pfeil et al., 2020), because this publication describes many of the same data included in this work.

### Population-based calcium mobilization

For HEK cells, 60.000 cells were seeded in flat bottom 96 well cell culture plates and cultivated overnight. The next day, media was removed and cells were incubated with 50  $\mu$ L/well Calcium 5 dye (Molecular Devices, Sunnyvale, CA, USA) at 37°C for 45 minutes. Afterwards, the dye was diluted with 150  $\mu$ L for experiments with one ligand addition, or 100  $\mu$ L for experiments with two ligand additions, using HBSS supplemented with 20 mM HEPES. Calcium mobilization was measured as increase in fluorescence over time, using the FlexStation 3 MultiMode Bench Top reader (Molecular Devices, Sunnyvale, CA, USA). An initial baseline read of 20 s was performed, followed by a 50  $\mu$ L compound addition either once after 20 s or twice at 20 s and 140 s, respectively.

For other cell lines, the following modifications were used. Oli-neu-cells were seeded at 70.000 cells/well and cultured for 48 h in the presence of 1  $\mu$ M PD174265 before the start of the experiment. JURKAT cells were resuspended in Calcium 5 Dye and kept at 37°C for 45 min in the presence or absence of 10  $\mu$ M FR, then diluted with 3x the volume of HBSS + HEPES, seeded at 30.000 cells/well into non-PDL-treated 384 well plates, spun down and measured immediately. HaCaT cells were seeded into 96 well plates at 50.000 cells/well and cultured overnight. mPASMC were seeded into non-PDL-treated 96 well plates at 25.000 cells/well and cultured overnight. mBAT were

## Methods

seeded into PDL-treated 96 well plates at 16.000 cells/well and cultured for 48 h. 5  $\mu$ M A23187 was used as a viability control in all experiments. For all assays, the first compound addition was set to  $x=0$ ,  $y=0$ . The results show increase in intracellular calcium as RFU over time.

### Calcium mobilization and aggregometry in platelets

These experiments were kindly performed by the Nieswandt lab. Washed platelets (100  $\mu$ l at  $2 \times 10^5$ /mL) were loaded with 1  $\mu$ L Fura2/AM (F1221, Thermo Fisher Scientific; 3.3  $\mu$ M f.c.) in the presence of 0.2  $\mu$ g/mL pluronic F-127 for 20 min at 37°C. After one washing step, the platelet pellet was resuspended in 500  $\mu$ l HBSS and sample was transferred to a cuvette and placed into an FL-6500 Fluorimeter (Perkin Elmer). Inhibitors and calcium (1 mM f.c.) were added directly prior start of the measurement. The emission was measured at 509 nm under stirring conditions with excitations alternating between 340 nm and 380 nm. Baseline was recorded for 50 s before agonist addition. After each measurement calibration was performed with Triton X-100 (maximum signal) and EGTA (minimum) to calculate concentrations of free intracellular calcium (Grynkiewicz et al., 1985). 1  $\mu$ M Ionomycin was used as a viability control. For aggregometry, 50  $\mu$ l of PRP were mixed with 110  $\mu$ l Tyrode's-HEPES buffer containing 1 mM  $\text{CaCl}_2$  in an aggregometer cuvette in the presence of the indicated inhibitors. Light transmission was recorded on a four-channel aggregometer (Fibrinometer; ATRACT, Hamburg, Germany) for 10 min, with ADP being added 30 s after start of the measurement. The effect of ADP on platelets was quantified as max - min of the recorded optical response (Figure 4L) to quantify shape-change (initial decrease in light transmission) as well as aggregate formation (increase in light transmission), or by determining the maximum of the curve in direct response to agonist addition to visualize aggregation only (Figure S10). Results are expressed in arbitrary units, with platelet poor plasma (PPP) representing 100% light transmission.

### Singe cell calcium mobilization

200,000 cells were seeded onto fibronectin-coated 8 well  $\mu$  Slides (ibidi, Fitchburg, WI, USA) and cultivated overnight. The next day, media was removed and cells were incubated with 100  $\mu$ L/well Calcium 5 Dye (Molecular Devices, Sunnyvale, CA, USA) for 45 min at 37°C, then diluted with 300  $\mu$ l HBSS supplemented with 20 mM HEPES. Calcium mobilization was measured as increase in each cell's median fluorescence over time, using the Axio observer Z.1 microscope equipped with the LD Plan-Neofluar 20x/0,4 Korr M27 objective and the filter set 38. An initial baseline read of 20 s was

performed, followed by 50  $\mu$ L compound addition. The results show increase in cytosolic calcium as RFU over time.

### IP<sub>1</sub> accumulation

IP<sub>1</sub> quantifications were performed using the Cisbio HTRF kit (Cisbio Codolet, France) according to the manufacturer's instructions, with the following modifications: 25,000 HEK cells per well were used. Cells were stimulated with agonist at 37°C for the duration of 30 min. At this point, lysis buffer and HTRF components were added and left at room temperature for at least 1 h. HTRF values were determined using the Mithras LB 940 multimode plate reader (Berthold Technologies, Bad Wildbad, Germany). Using a standard curve generated from the IP<sub>1</sub> standard solutions provided by the manufacturer, all HTRF ratios were converted to IP<sub>1</sub> concentrations in nM.

### cAMP accumulation

For cAMP assays, the Cisbio HTRF kit (Cisbio Codolet, France) was used according to manufacturer's instructions, with the following modifications: 25.000 cells/well were stimulated with the indicated concentration of forskolin with or without varying concentrations of receptor agonist for 45 min. Then, lysis buffer and HTRF components were added and incubated at room temperature for at least 1 h. The Mithras LB 940 multimode plate reader (Berthold Technologies, Bad Wildbad, Germany) was used to record HTRF values. Using a standard curve generated from the cAMP standard solutions provided by the manufacturer, all HTRF ratios were converted to nM cAMP concentrations.

### NanoBiT

Cells cultured in 6 cm dishes were transfected with all components (see TS1) 24 h before the experiment, and measured according to previously published protocols (Shihoya et al., 2018; Dixon et al., 2016). Briefly, on the day of the experiment, cells were harvested and resuspended in 2 mL of HBSS supplemented with 5 mM HEPES and 0.01% BSA, then seeded in a 96 well plate using 80  $\mu$ L per well. Cells were loaded with 20  $\mu$ L of the same buffer supplemented with 50  $\mu$ M coelenterazine, followed by a 2 h incubation at room temperature. Using a SpectraMax L reader (Molecular Devices, Sunnyvale, CA, USA), five readings per well were performed to determine a baseline, followed by ligand addition and 10 min of luminescence read at 20 s intervals. The results show proximity of G $\beta\gamma$  and PLC $\beta$ 3 after ligand addition as fold increase of luminescence over time, or the proximity of G $\alpha$ i with G $\beta\gamma$  over time.

## Methods

### IP<sub>3</sub> BRET

BRET measurements using the IP<sub>3</sub> sensor (Gulyás et al., 2015) were performed according to the published protocol, with the following modifications: HEK cells were transfected in 10 cm dishes 24h before the measurements and trypsinized on the day of the measurements, washed, and resuspended using HBSS + HEPES to seed 80 µL with 80,000 cells/well into a white-bottom 96-well plate. 10 µL Coelenterazine h were used as the BRET substrate. The emission at 485 nm and 535 nm was measured for 40 s using the PHERAstar microplate reader (BMG labtech, Ortenberg, Germany), before injecting 10 µL agonist or buffer. The data were processed as previously described (Gulyás et al., 2015) and buffer-corrected, then quantified by determining the mean BRET decrease after compound addition.

### Gαq-Gβγ dissociation BRET

BRET measurements to determine Gαq-Gβγ rearrangement were performed according to the previously published protocol (Schrage et al., 2015). Briefly, HEK-ΔGq/11 cells were transfected with Rluc8-Gαq<sup>wt</sup> or Rluc8-Gαq<sup>H218AL254A</sup> and GFP-Gγ2, along with rGPR17 and Gβ1 48h before the experiment. On the day of the measurement, cells were trypsinized, washed and resuspended in HBSS + HEPES to seed 100 µL with 180.000cells/well into a white-bottom 96-well plate. 10 µL agonist was added immediately prior to the measurement at the respective time interval. The Mithras LB 940 multimode plate reader (Berthold Technologies, Bad Wildbad, Germany) was used to inject 10 µL BRET2 substrate Deepblue C and then record the emission at 395 nm and 515 nm wavelength.

### DMR

Dynamic mass redistribution assays were performed using the Corning Epic biosensor (Corning, NY, USA) according to a previously published protocol (Schröder et al., 2011). Briefly, 18,000 cells/well were seeded in 384 well plates on top of an optical biosensor and cultured overnight. The next day, cells were washed with HBSS supplemented with 20 mM HEPES and allowed to equilibrate for 1 h or until measurements stabilized. Then, a new measurement was started to record at least 5 min of baseline read followed by the addition of compounds using the Cybi-SELMA semi-automated electronic pipetting system (Analytik Jena AG, Jena, Germany) and 60 more min of measurement. The experiments show dynamic mass redistribution following ligand activation as pm shift in reflected wavelength over time.



### Thallium Flux

Activation of GIRK channels was measured using a Thallo AM dye-based thallium flux assay kit and recorded with the FlexStation 3 MultiMode Bench Top reader (Molecular Devices, Sunnyvale, CA, USA) according to the previously published protocol (Krebs et al., 2018), which is a modified version of (Wydeven et al., 2014). Briefly, the day before the experiment, 20,000 cells/well were seeded in 384 well plates. On the day of the experiment, cells were incubated with Thallo AM dye for 45 min. Thereafter, the dye was replaced by 40  $\mu$ L of HBSS supplemented with 20 nM HEPES. All compounds were diluted in the same buffer additionally supplemented with thallium sulfate to reach a final concentration of 0.75 mM thallium in each well. The experiment shows GIRK channel activation as increase in fluorescence over time.

### Western Blot

All lysates were collected from the same batch of transfected cells that were used for calcium measurements. Cells were lysed on the day of the calcium measurements, 48 h after transient transfection. After running the gels and blotting onto nitrocellulose membranes, protein expression was detected as follows. To detect  $\beta$ -actin, anti- $\beta$ -actin antibody was diluted in RotiBlock (1:1,000) to treat membranes overnight at 4°C. Anti-rabbit in RotiBlock (1:20,000) was used as the second antibody and incubated for 1 h at room temperature. After  $\beta$ -actin detection using ECL detection reagent, the membranes were washed and blocked for 60 min at room temperature. Afterwards, to detect PLC $\beta$  expression, the membranes were incubated in anti-PLC $\beta$ 3 mouse monoclonal antibodies diluted in RotiBlock (1:500) at 4°C overnight. Anti-mouse antibody diluted in RotiBlock (1:20,000) was used as the second antibody, and detected.

### Data processing

Data were processed using Microsoft Excel and analyzed using GraphPad Prism 8. All kinetic data were baseline-corrected to a buffer control by subtracting the value of the buffer-stimulated curve from the respective ligand-stimulated curve for every timepoint. Data were then analyzed as indicated in the respective y-axis title of each panel.

# Results

## Chapter 1: Does Gi-calcium depend on Gq?

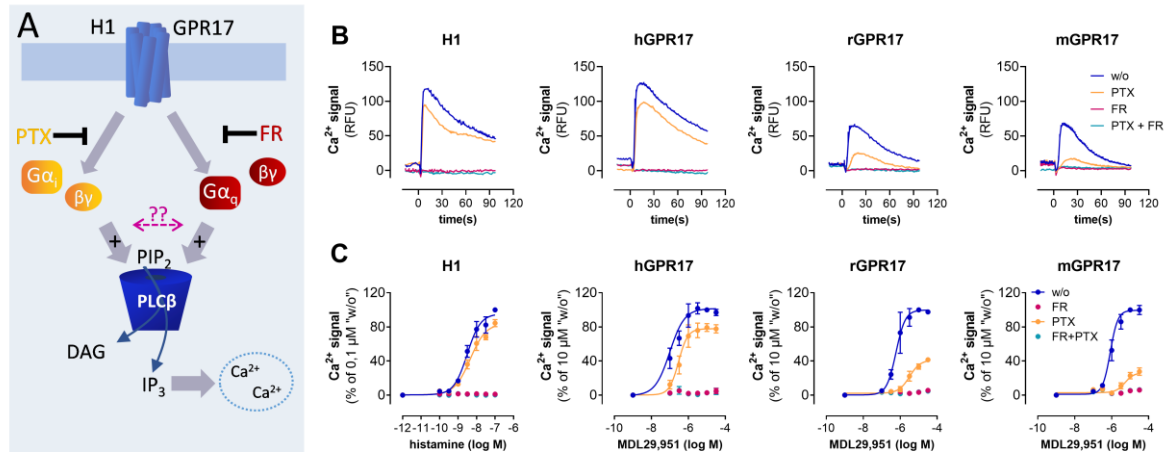


**Figure 6: Gi-calcium is completely blocked by Gq inhibitor FR.** (A) calcium measurements were performed in HEK cells using receptors that activate both Gi and Gq. The specific inhibitors PTX for Gi and FR for Gq were used to selectively inhibit each pathway and uncover a potential interdependency of the two signaling stimuli. (B) Representative calcium kinetics obtained with 100 nM histamine for H1 and 10  $\mu$ M MDL29,951 for GPR17. Calcium mobilization was partially blocked in cells treated with PTX, and fully absent in the presence of FR. (C) quantification of three biologically independent experiments of (B), shown as mean  $\pm$  SEM.

### Gi-calcium is completely blocked by Gq inhibitor FR

The first goal of this work was to investigate a potential interaction or interdependency of Gq-calcium and Gi-G $\beta\gamma$ -calcium in living cells. To gain insight into this, we used a set of GPCRs that activate both Gq and Gi and observed their capacity to mobilize calcium (Figure 6A). As our model receptors, we used the histamine receptor H1, along with its endogenous ligand histamine (Inoue et al., 2019), and three species orthologs of GPR17, an orphan GPCR that can be conveniently activated by the surrogate agonist MDL29,951 (Simon et al., 2016). To visualize the Gi- and Gq-contribution to the resulting calcium mobilization, we used the Gi-inhibitor PTX and the Gq inhibitor FR (Figure 6A). Upon stimulation with their cognate agonists, all four model receptors mobilized calcium in a concentration-dependent manner (Figure 6B, C). PTX-treatment revealed varying Gi-contributions for each receptor, with H1 and hGPR17 showing a small, rGPR17 a more balanced and mGPR17 a high Gi-component (Figure 6C). Interestingly, treatment with FR completely abolished all calcium

mobilization, including the Gi-dependent component, for all receptors (Figure 6B, C). This result indicated a complete dependency of Gi-G $\beta\gamma$ -calcium on Gq in living cells, a surprising finding given that Gi-G $\beta\gamma$ -calcium has been shown to be an independent signaling pathway in the reconstituted system.

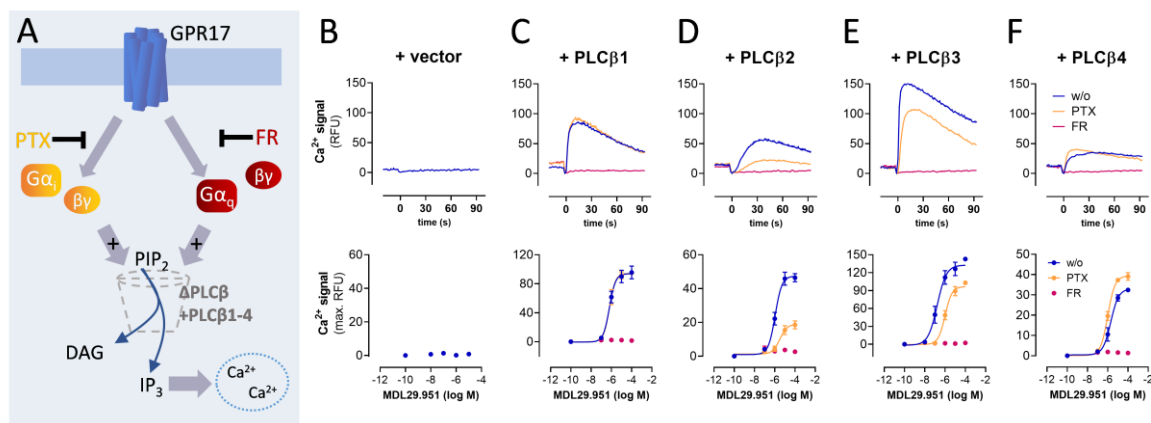


**Figure 7: FR-sensitive Gi-calcium is mobilized via PLC $\beta$ 2 and PLC $\beta$ 3.** (A) HEK PLC $\beta$ 1-4mut cells transfected with rGPR17, along with either control vector (B) or each PLC $\beta$  isoform (C-F), were observed in a calcium mobilization experiment. (B-F) the top panels show the representative calcium traces upon stimulation with 10  $\mu$ M MDL, quantified as mean  $\pm$  SEM of three biologically independent experiments in the bottom panels. rGPR17 only mobilized calcium in HEK-PLC $\beta$ 1-4mut cells where a PLC $\beta$  isoform was re-expressed (B vs C-F), and this calcium was partially Gi-dependent only in the presence of PLC $\beta$ 2 and PLC $\beta$ 3 (D, E). In cells transfected with PLC $\beta$ 4, PTX-treatment led to an increase in the slope and maximal calcium mobilization (F). All calcium mobilization was completely abolished in the presence of FR (C-F).

### FR-sensitive Gi-calcium is mobilized via PLC $\beta$ 2 and PLC $\beta$ 3

Gi-G $\beta\gamma$ -calcium is usually mediated via PLC $\beta$ 2 and PLC $\beta$ 3, while G $\alpha_q$  activates all four PLC $\beta$  isozymes (Kadamur & Ross, 2013; Smrcka, 2008). However, Gi-G $\beta\gamma$  has also been shown to interfere with various other pathways that control calcium mobilization, including the PLC $\gamma$ , PLC $\epsilon$  and PLC $\eta$  pathways. Therefore, our next step was to confirm the origin of our Gi-G $\beta\gamma$ -calcium. To this end, we generated a HEK PLC $\beta$ 1-4mut cell line. In this cell line, CRISPR/Cas9 technology has been used to target the alleles encoding the four PLC $\beta$  isozymes (Figure 7A). As expected, HEK PLC $\beta$ 1-4mut cells showed no rGPR17-mediated calcium mobilization (Figure 7B), which indicated that in our hands, GPCR-calcium is PLC $\beta$ -mediated. Re-transfection of each PLC $\beta$  subtype restored the rGPR17-mediated calcium mobilization (Figure 7C-F), with PLC $\beta$ 2- and PLC $\beta$ 3- dependent calcium displaying partial inhibition by PTX (Figure 7D, E).

## Results

Interestingly, PLC $\beta$ 4-transfected cells showed an increased calcium mobilization via GPR17 in the presence of PTX that was reflected in both a steeper calcium kinetic and a higher calcium peak (Figure 7F). Since PTX inhibits Gi and thus increases intracellular cAMP levels, this increased calcium mobilization in PTX-treated cells could indicate a dependency of PLC $\beta$ 4 on the cAMP pathway, which is an interesting basis for further investigation. Regardless, the partial PTX-sensitivity of PLC $\beta$ 2 and PLC $\beta$ 3 confirms that Gi-G $\beta\gamma$ -PLC $\beta$ -calcium is mediated via these two PLC $\beta$  subtypes, which is perfectly in line with the Gi-calcium signaling paradigm. Additionally, for all PLC $\beta$  subtypes, the calcium was completely abolished by the Gq inhibitor FR (Figure 7B-F), underlining the complete dependency of Gi-G $\beta\gamma$ -calcium on the Gq pathway.

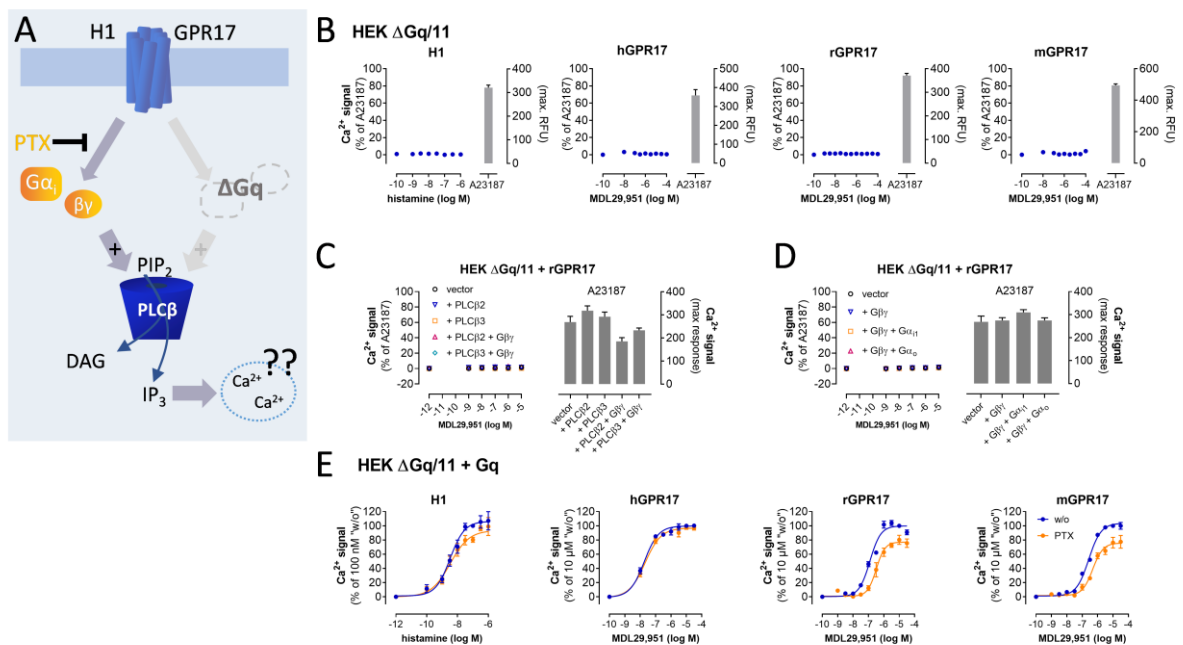


**Figure 8: Gq is required and sufficient to restore Gi-calcium in HEK- $\Delta$ Gq/11 cells.** (A) HEK- $\Delta$ Gq/11 cells, which do not express G $\alpha_q$  subunits, were investigated for Gi-calcium. (B) The mean  $\pm$  SEM show no H1- or GPR17-dependent calcium in this cellular background (blue data points), despite intact viability controls (grey bars). (C, D) Overexpression of (C) PLC $\beta$ , or (D) Gi-heterotrimers did not restore rGPR17-mediated Gi-calcium, but cells remained responsive to the viability control. (E) Mean  $\pm$  SEM of restored, PTX-sensitive calcium responses upon re-transfection of G $\alpha_q$ . All experiments show three biologically independent experiments.

### Gq is required and sufficient to restore Gi-calcium in HEK- $\Delta$ Gq/11 cells

While these findings made a compelling case for a dependency of Gi-G $\beta\gamma$ -calcium on Gq, previous investigations have reported a similar finding. As a result, the specificity of FR, a generally very well-characterized molecule, has been doubted (Gao &

Jacobson, 2016). Thus, the loss of Gi-calcium upon Gq-inhibition has to be further examined before any final conclusion can be drawn. In order to corroborate the data obtained with the pharmacological Gq inhibitor FR, we made use of the genetically modified HEK- $\Delta$ Gq/11 cell line. This cell line has been genetically modified with CRISPR/Cas9 technology to lack functional alleles encoding G $\alpha$ q and G $\alpha$ 11 (Grundmann et al., 2018). As G $\alpha$ 14 and G $\alpha$ 16 are not expressed in HEK cells (Atwood et al., 2011), the HEK- $\Delta$ Gq/11 cell line no longer expresses any G-proteins of the Gq family, and therefore perfectly complements the pharmacological tool FR (Figure 8A). In this cellular background, neither H1 nor any GPR17 species ortholog triggered detectable calcium mobilization upon stimulation (Figure 8B). Even upon transfection of PLC $\beta$ 2 or PLC $\beta$ 3 to boost overall PLC $\beta$  signaling (Figure 8C), or heterotrimeric Gi proteins to increase Gi-signaling (Figure 8D), rGPR17 failed to induce detectable Gi-calcium. However, reintroduction of Gq was sufficient to re-establish both Gq- and Gi-calcium for all receptors (Figure 8E). Thus, both the pharmacological (Figure 6) as well as the genetic tool (Figure 8) point towards the same conclusion: Gq is required and sufficient for Gi-G $\beta\gamma$ -calcium.

## Results

### Excursion 1.1: Gq overexpression shifts Gi/Gq balance of calcium signals towards Gq

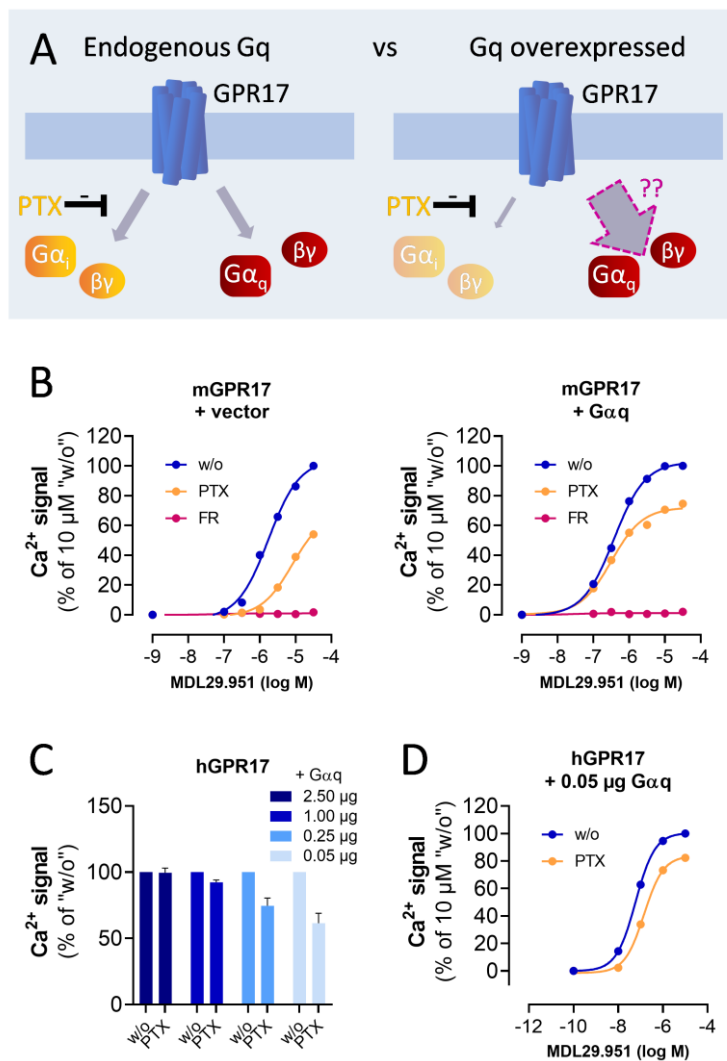


**Figure 9: Gq overexpression shifts Gi/Gq balance of calcium signals towards Gq.** (A) In HEK cells, we tested whether transfection of larger quantities of Gαq would diminish the PTX-sensitivity of a calcium signal by providing less Gi- and more Gq protein activation. (B) preliminary calcium mobilization data (n=1) obtained with a stable HEK-mGPR17 cell line transfected with either vector control (left panel) or Gαq (right panel). The PTX-sensitive Gi-component of the calcium signal was reduced when Gαq was overexpressed, and no calcium was detected in the presence of FR. (C) 100 nM MDL29,951-mediated calcium mobilization via hGPR17 in HEK-ΔGq/11 shows a decreasing Gi-component when transfected

with increasing quantities of Gαq. (D) Concentration response curve of hGPR17 mediated calcium mobilization upon re-transfection of only 0.05 μg Gαq plasmid, in the absence and presence of PTX.

Notably, the Gi-dependent calcium obtained upon re-transfection of Gq into HEK-ΔGq/11 cells was smaller for all receptors than that obtained in the wt-background (compare Figure 8E with Figure 6C), with hGPR17-dependent calcium showing almost no PTX-sensitivity. It seems like, under these conditions of Gαq overexpression, all four model receptors favored the Gq pathway. A possible explanation could be that the increased expression level of Gq after transient overexpression (a) increases Gq-coupling of GPR17, or (b) saturates the PLCβ-pathway, leaving less room for enhancement via Gi-Gβγ. To examine whether the quantity of Gαq expression would

really increase the Gq- and decrease the Gi-component of GPR17-mediated calcium (Figure 9A), we performed calcium measurements with HEK cells stably expressing mGPR17. We transfected this cell line with either control vector to maintain endogenous Gq expression (Figure 9A, B, left panels), or Gαq to achieve overexpression of Gq (Figure 9A, B, right panels). Indeed, after transfection of Gq, the PTX-sensitive Gi-contribution to calcium mobilization by this receptor decreased (Figure 9B). Thus, we reasoned that in the HEK-ΔGq/11, transfection of lower amounts of Gq should better visualize Gi-calcium. Careful titration of the transfected amount did indeed reveal PTX-sensitivity of hGPR17 (Figure 9C). Because of this finding, the amount of transfected Gα subunit in all following experiments was optimized to ensure a robustly restored calcium signal with an observable PTX-sensitive component.

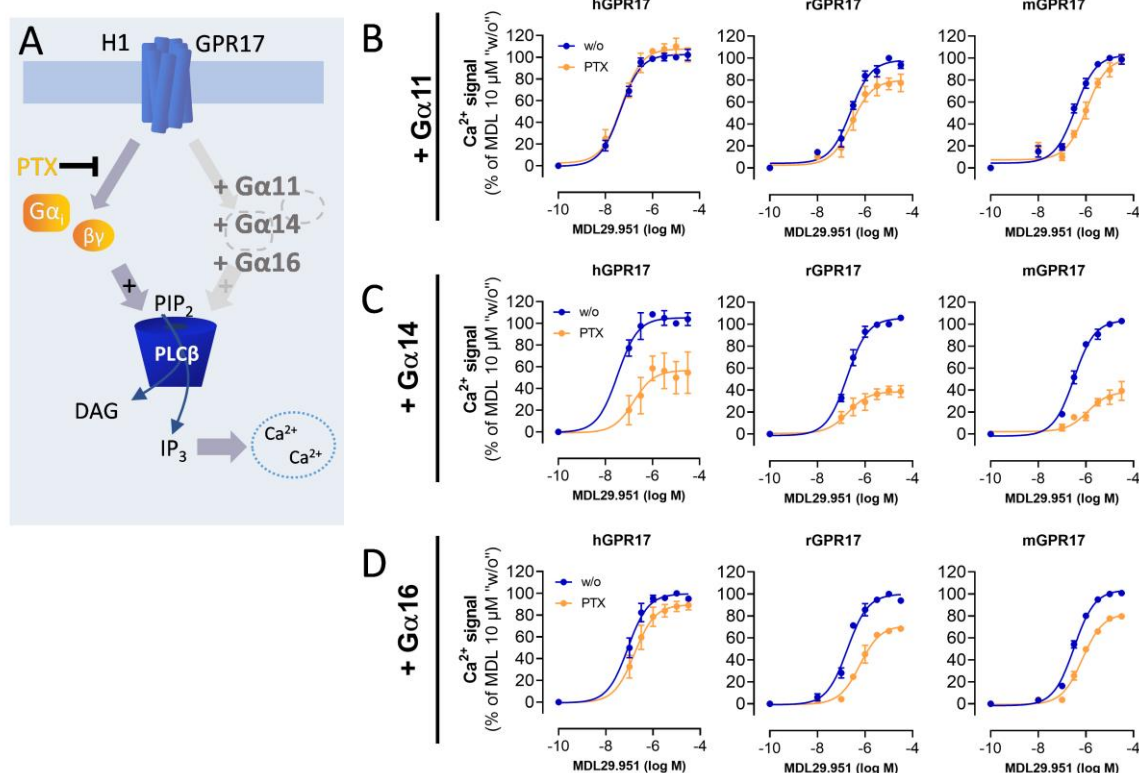


**Figure 10: All Gαq family subunits restore Gi-calcium.** (A) In HEK-ΔGq/11 cells, each ortholog of GPR17 was co-expressed with Gα11, Gα14 or Gα16. Upon stimulation with MDL29,951, calcium mobilization was observed in the absence and presence of PTX to detect Gi-calcium. (B-D) summarized mean ± SEM of three independent experiments shows no PTX-sensitive calcium for hGPR17 with Gα11 (B), but PTX-sensitive calcium for rGPR17 and mGPR17 in the presence of Gαq (B), and for all three species in the presence of Gα14 (C) and Gα16 (D).

## Results

### All Gαq family subunits restore Gi-calcium

After observing the rescue of Gi-calcium by re-transfection of Gαq, we were curious to see if all Gα-isoforms of the Gq family would restore Gi-calcium. The Gq family consists of four isoforms: Gq, G11, G14 and G15/16 (Figure 4A), the latter referring to the non-human (G15) and human (G16) ortholog of the same Gα subunit (McCudden et al., 2005). Like Gαq, transfection Gα11 (Figure 4B), Gα14 (Figure 4C) and Gα16 (Figure 4D) restored the calcium signal for all three species orthologs of GPR17. PTX-sensitivity varied, with Gα11 restoring the smallest, and Gα14 restoring the largest Gi-component to the signal. This might very well be due to a difference in expression between the Gαq subunits (see Figure 9), which we did not investigate in this context. Regardless, all Gq family members were capable of restoring a PTX-sensitive Gi-calcium.

Taken together, these results demonstrate that there is a complete dependency of Gi-calcium on Gq in HEK cells, in that Gi-calcium is undetectable when Gαq-isoforms are not expressed or pharmacologically inhibited, and can only be restored upon re-expression of a Gαq-isoform.

## Chapter 2: The Gq requirement for specifically Gi-coupled receptors

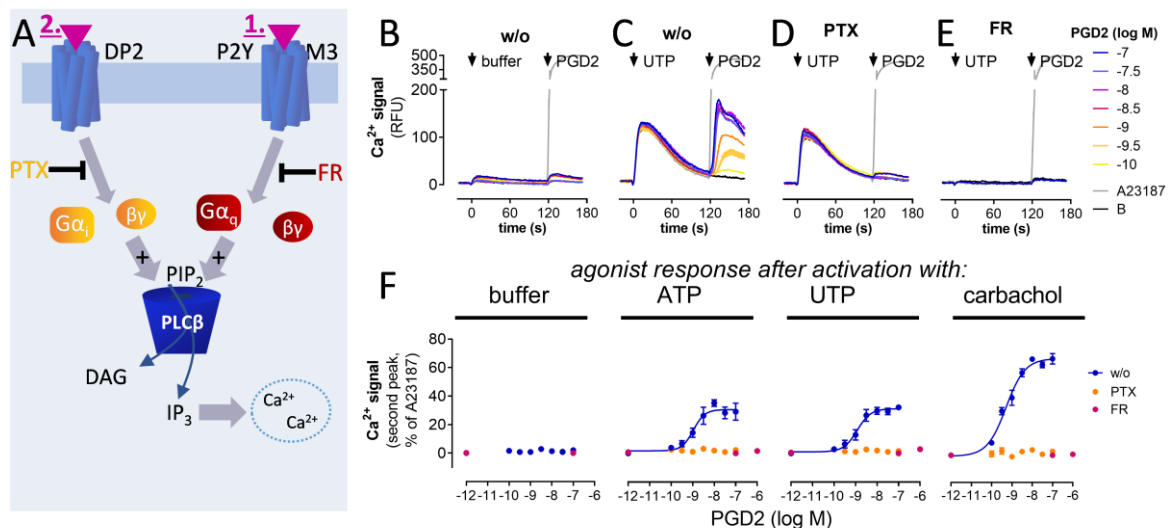


**Figure 11: Specifically Gi-coupled DP2 requires additional Gq input to mobilize Gi-calcium.**

(A) in HEK cells stably expressing Gi-coupled DP2, calcium mobilization was measured using the cognate agonist PGD2. Prior to the Gi-stimulus, either buffer or 100 μM UTP/ATP, or 100 μM CCh was used to stimulate endogenous Gq-coupled P2Y or M3 receptors to provide Gq input. (B-E) representative calcium kinetics, depicted as mean + SEM, show no calcium



mobilization when only DP2 is stimulated with PGD2 (B), but restored PGD2-dependent calcium when the cells are pre-stimulated with UTP (C). This PGD2-mediated calcium is entirely blocked by PTX (D) and absent when FR is used to abolish the UTP-stimulus (E). (F) The mean  $\pm$  SEM of three experiments reveals no PGD2-dependent calcium when cells are pretreated with buffer, but robust, PTX- and FR-sensitive calcium responses induced by PGD2 when the cells are pre-stimulated with ATP, UTP or CCh.

Specifically Gi-coupled DP2 requires additional Gq input to mobilize Gi-calcium. Gi-calcium is a hallmark feature of chemokine and chemoattractant receptors expressed in immune cells. These Gi-GPCRs do not couple to Gq, which made us interested in testing if they also dependent on G $\alpha$ q to mobilize their paradigmatic Gi-calcium (Figure 11A). To investigate this, we selected a variant of the D-type prostanoid receptor 2 (DP2, formerly chemoattractant receptor homologous molecule expressed on T-Helper cells type 2, CRTH2) that lacks the c-terminal domain to improve signaling in recombinant systems (DP2- $\Delta$ ct) (Schröder et al., 2009). However, stimulating HEK cells stably expressing this receptor with PGD2, its cognate agonist (Sedej et al., 2012) did not produce a calcium response (Figure 11B), even though Gq was expressed in this cellular background. Because the receptors that activate Gq in addition to Gi had mobilized Gi-calcium in the presence of Gq (Figure 6-10), we hypothesized that Gi calcium might be dependent not only on Gq presence, but Gq-activation. Unlike H1 and GPR17, DP2 would not generate this potentially required Gq activation on its own. To test if Gq activation would restore DP2- $\Delta$ ct-mediated Gi-calcium, we stimulated the cells with UTP to activate the endogenously expressed Gq-coupled P2Y receptors prior to addition of the DP2-agonist PGD2 (Figure 11A). Indeed, in this setup, PGD2 triggered concentration-dependent calcium release (Figure 11C) that was entirely Gi-dependent (Figure 11D). Incubation of the cells with FR abolished the Gq-activation provided by UTP, and thus, no Gi-calcium was observed (Figure 11E). In order to exclude a possible UTP-specific effect on the DP2 receptor, or P2Y-DP2-specific crosstalk responsible for the restored Gi-calcium, we also tried priming the cells with ATP, a different P2Y agonist, and carbachol (CCh), which is an agonist at the endogenously expressed Gq-coupled muscarinic M3 receptors. All three options restored similar, PTX- sensitive PGD2 calcium that was absent in the presence of FR (Figure 11F). This data indicates that mobilization of Gi-calcium via the Gi-specific DP2 receptor requires additional Gq activation via another GPCR.

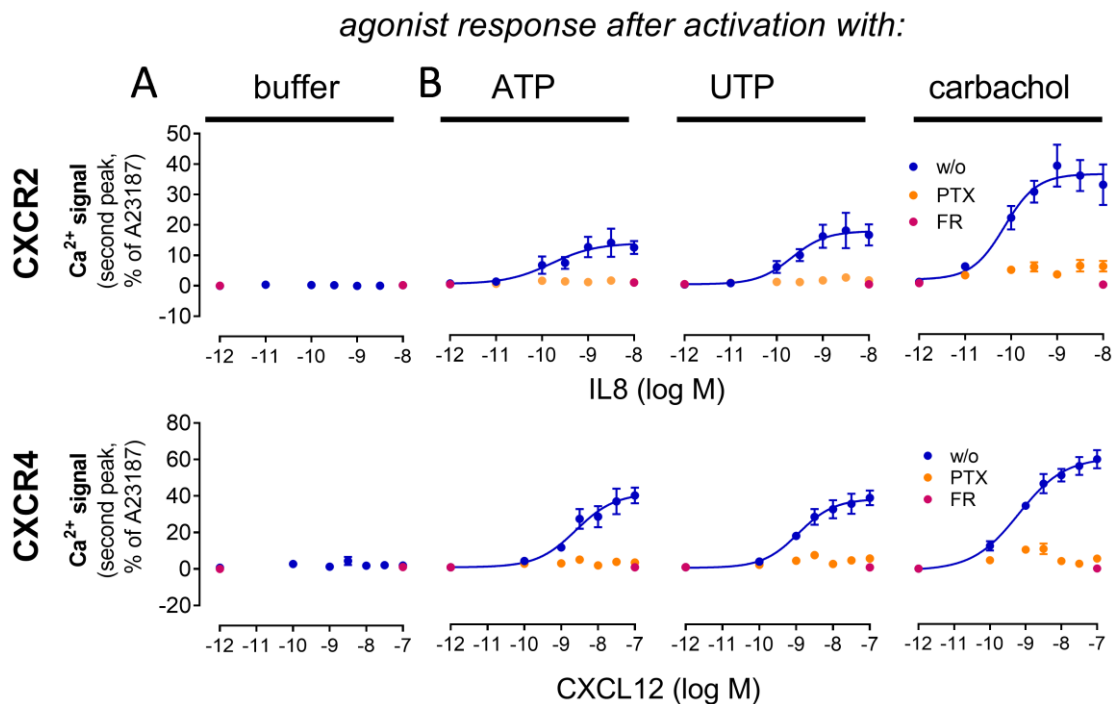


**Figure 12: Gi-calcium via CXCR2 and CXCR4 requires Gq input.** (A, B) HEK cells stably expressing CXCR2 (top panels) or endogenously expressing CXCR4 (bottom panels) do not mobilize calcium in response to IL8 or CXCL12 when pre-treated with buffer (A), but display concentration-dependent, PTX- and FR-sensitive calcium mobilization in response to IL8 and CXCL12 when pre-stimulated with ATP, UTP or CCh. All data are shown as mean  $\pm$  SEM of three biologically independent experiments.

### Gi-calcium via CXCR2 and CXCR4 requires Gq input

If Gi-calcium always depends on Gq-activation, this would mean that any Gi-coupled receptor that does not activate Gq will not mobilize any calcium when stimulated on its own in HEK cells. Therefore, to corroborate our findings with DP2, we tested two other Gi-coupled GPCRs. Because Gi-calcium is a hallmark feature of chemokine signaling (Premack & Schall, 1996), we chose two chemokine receptors that are associated with physiological Gi-calcium signaling, CXCR2 and CXCR4. Interestingly, neither stably transfected CXCR2 nor endogenously expressed CXCR4 induced Gi-calcium upon stimulation with their cognate agonists in HEK cells (Figure 12A). Indeed, like DP2, their ability to mobilize Gi-calcium was completely dependent on prior Gq-stimulation (Figure 12B). Because all three specifically Gi-coupled receptors required stimulation of a Gq-coupled GPCR to mobilize Gi-calcium, we concluded that Gi-calcium in living cells is always dependent not only the presence of Gq, but on activation of the Gq pathway, which can be achieved either via the same receptor that

stimulates  $G_i$  (see Figure 6-10) or via any other available Gq-coupled receptor (Figure 11, Figure 12).

### *Excursion 2.1: Both basal and acute Gq activation restore Gi-calcium, but acute Gq stimulation does so more reliably*

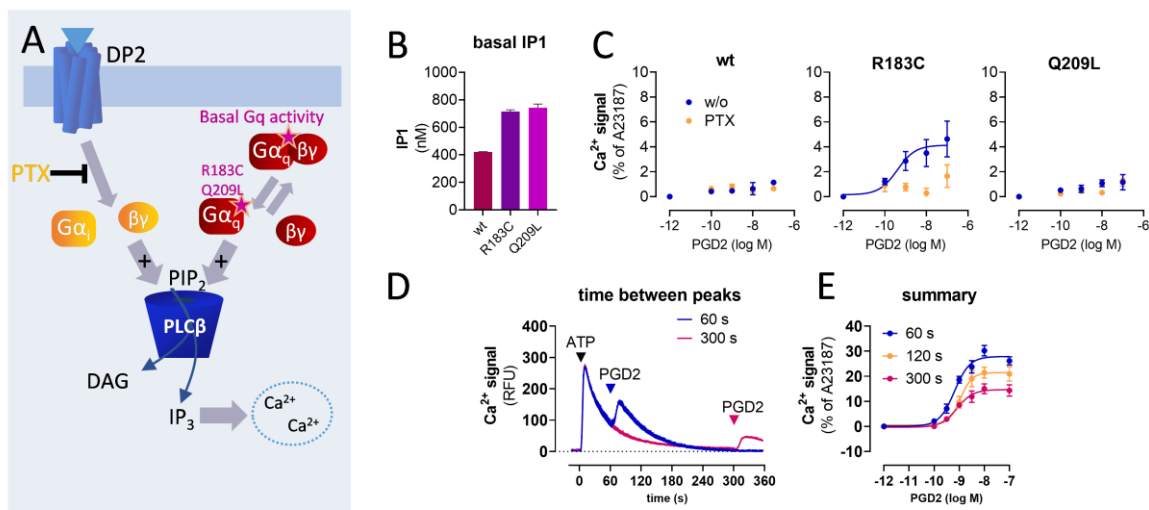


**Figure 13: Both basal and acute Gq activation restore Gi-calcium, but acute Gq stimulation does so more reliably.** (A-C) HEK cells were transiently transfected with DP2, along with either  $G\alpha_q^{wt}$  or the constitutively active  $G\alpha_q^{R183C}$  or  $G\alpha_q^{Q209L}$  mutant. (B) The basal  $IP_1$  production, shown as mean + SEM of one representative experiment, is increased upon transfection of the constitutively active  $G\alpha_q^{R183C}$  or  $G\alpha_q^{Q209L}$  mutants. (C) in response to PGD2, PTX-sensitive calcium is mobilized only in cells transfected with the  $G\alpha_q^{R183C}$  mutant. This data shows mean  $\pm$  SEM of four biologically independent experiments. (D, E) In HEK-DP2- $\Delta$ ct cells, the time between the acute Gq input provided by ATP and the Gi-stimulus PGD2 was varied. Representative kinetics (D) are shown as mean + SEM, summarized as mean  $\pm$  SEM of three experiments in (E), revealing higher Gi-calcium peaks for more recent Gq-input.

We have already demonstrated that the Gq-activity required for Gi-calcium can be provided by the same or other GPCRs. Next, we wondered if an increase in basal Gq activity would also restore Gi-calcium. To provide basal Gq activation, we used two constitutively active mutants of Gq, the  $G\alpha_q^{R183C}$  and the  $G\alpha_q^{Q209L}$  variants. Both of these variants of Gq are oncogenes that occur naturally (Singh et al., 2011; Sisley et al., 2011; Luke et al., 2015; Bastian, 2014; Carvajal et al., 2017; Annala et al., 2019; Kostenis et al., 2020). Their GTPase-deficiency makes these mutants constitutively active (Figure 13A, and they drive the growth and migration of various tumors, including that of uveal melanoma. Upon transfection of these mutants into HEK- $\Delta$ Gq/11 cells, we witnessed increased basal  $IP_1$  levels compared to control vector or

## Results

$G\alpha^{wt}$ , confirming the constitutive activity of both  $G\alpha$  mutants (Figure 13B). However, stimulation of DP2 in these cells only lead to a miniscule mobilization of Gi-calcium for  $G\alpha^{R183C}$  and a barely detectable Gi-calcium for  $G\alpha^{Q209L}$  (Figure 13C). This measurement window was the result of many attempts at optimization (data not shown), and although we cannot exclude the possibility that the signal could be further improved by changing the methodology, we wondered if Gi-calcium perhaps is more robustly restored by an acute Gq stimulus instead of long-term, basal activation. Indeed, an experiment using the pre-stimulation setup, but varying the timepoint of Gi-stimulation (Figure 13D), revealed a clear time-dependent aspect of the Gq requirement (Figure 13D, E). Taken together, these results imply that Gi-calcium is most efficiently mobilized when it immediately follows the required Gq-stimulus. However, more investigations would be necessary to draw conclusions on how this would play out in a physiological context.

## Chapter 3: Which Gi-pathways require Gq?

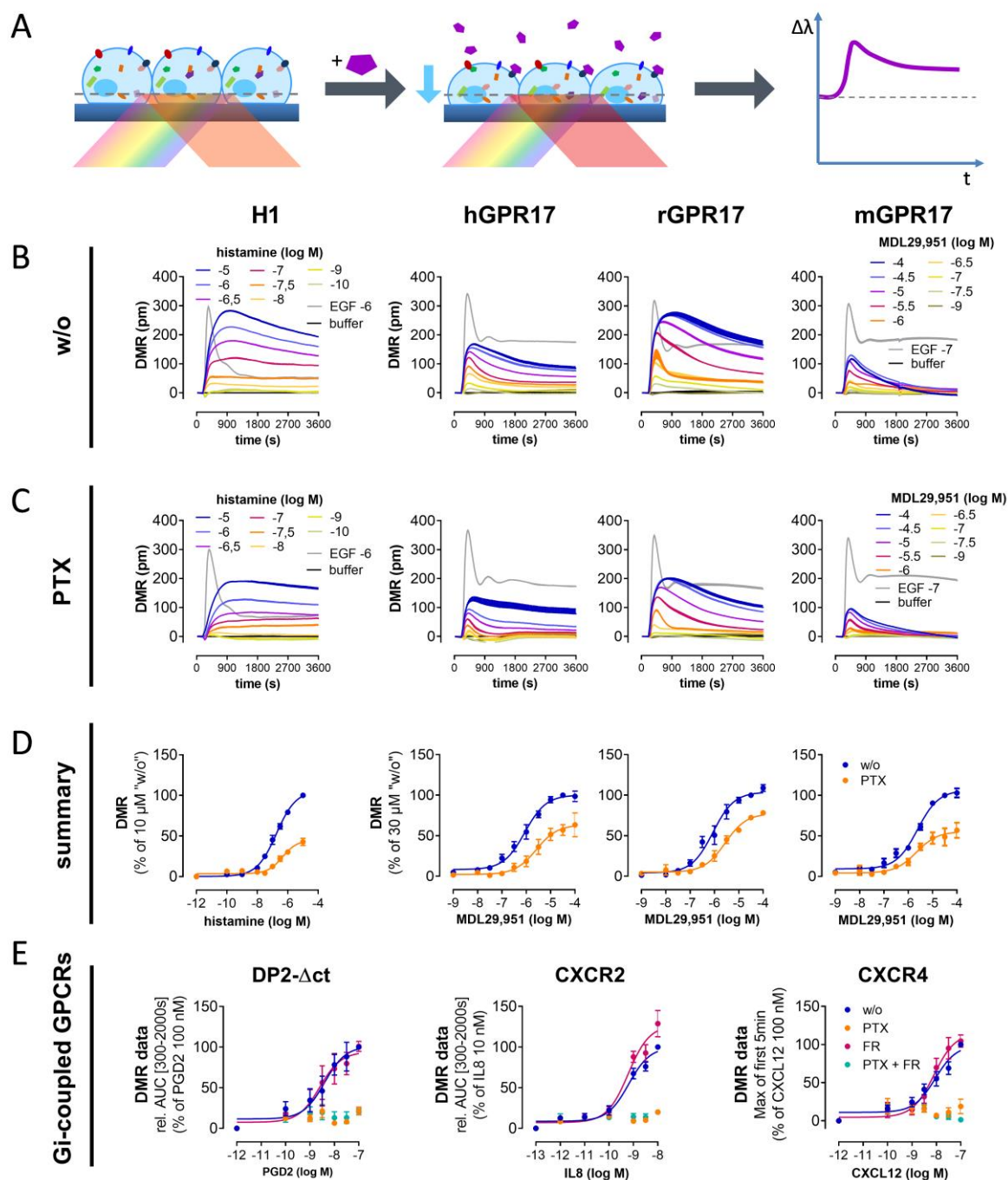


**Figure 14: All model GPCRs are expressed and couple to Gi without Gq.** (A) Upon GPCR activation, a signaling cascade induces cell shape changes that are registered by an optical biosensor as a change in the reflected wavelength, which represents dynamic mass redistribution (DMR). If this DMR response is sensitive to inhibition by PTX, this confirms that it is triggered via the Gi signaling cascade. (B-C) Representative mean + SEM DMR kinetics obtained in HEK- $\Delta$ Gq/11 cells transfected with H1 or GPR17 (see Figure 3B) in the absence (B) or presence (C) of PTX, summarized in (D) as mean  $\pm$  SEM of three experiments. All four

## Results

receptors signal in a concentration-dependent, PTX-sensitive manner in the HEK- $\Delta$ Gq/11 background. (E) The mean  $\pm$  SEM DMR of three biologically independent experiments confirms intact, fully PTX-sensitive signaling via DP2- $\Delta$ ct, CXCR2 and CXCR4 (compare Figure 6 and 7) in the absence and presence of FR.

### All model GPCRs are expressed and couple to Gi without Gq

Gi-calcium, a paradigmatic pathway that has long been considered stand-alone, is fully dependent on Gq in our living HEK cell system. Thus, we wondered if any other Gi-signaling pathways also share this previously unrecognized Gq requirement. Our first step was to investigate if general Gi-signaling via our model receptors was dependent on Gq. To this end, we examined the promiscuous H1 and GPR17 receptors' capacity to trigger Gi-dependent dynamic mass redistribution (DMR) in absence of Gq. DMR measurements are a holistic, real-time readout of cellular cytoskeletal changes (shape changes) in response to ligand stimulation (Figure 14A). This method registers GPCR stimulation of all G-protein subfamilies (Schröder et al., 2011; Schröder et al., 2010), but also some other stimuli such the activation of some ion channels (Krebs et al., 2018). In this readout, stimulation of H1 or GPR17 expressed in HEK- $\Delta$ Gq/11 yielded clear, concentration dependent signals that were partially PTX-sensitive (Figure 14B-D). This confirmed the expression of all four model GPCRs and their capacity to signal via Gi in the absence of Gq, despite the fact that no Gi-calcium was mobilized (see Figure 8). The remaining, PTX-insensitive signal most likely represented Gs-activation via these GPCRs. Similarly, despite not mobilizing Gi-calcium, the specifically Gi-coupled model receptors DP2, CXCR2 and CXCR4 also triggered DMR that was entirely PTX-sensitive and remained intact in the presence of Gq-inhibitor FR (Figure 14E). We concluded that Gq is not required for all Gi-GPCR-dependent signaling pathways.

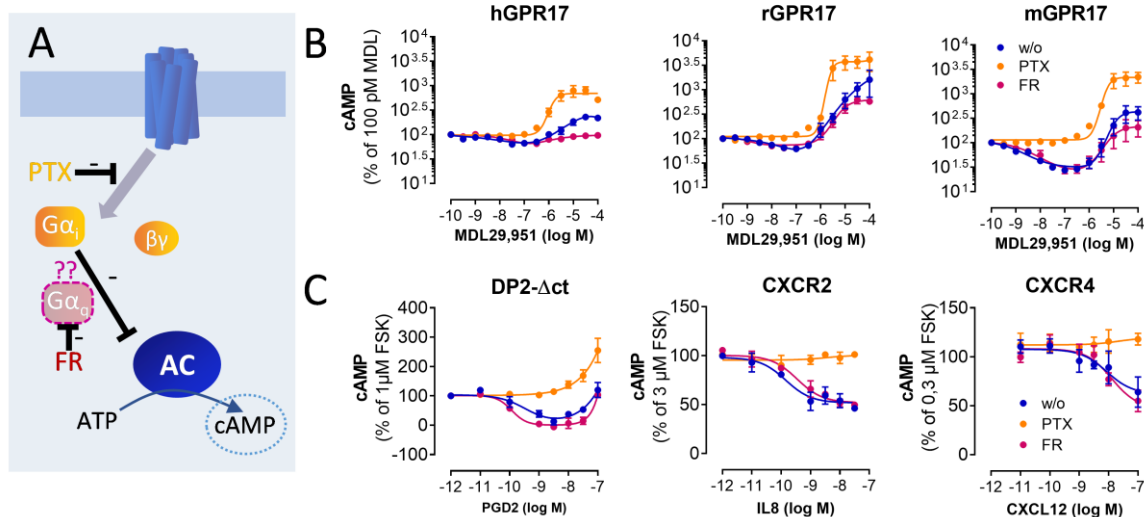


**Figure 15:  $G\alpha_i$ -mediated cAMP depression does not require  $Gq$ .** (A)  $G\alpha_i$  inhibits the adenylyl cyclase-dependent cAMP production. If this process required  $Gq$  like  $G_i$ -calcium does, it should be blocked in the presence of FR. (B) cAMP measurements of HEK cells stably expressing each GPR17 species ortholog, shown as mean  $\pm$  SEM of three biologically independent experiments, show PTX-sensitive inhibition of FSK-induced cAMP production for lower agonist concentrations that is intact in the presence of FR. (C) HEK cells stably expressing DP2- $\Delta$ ct, CXCR2 or endogenously expressing CXCR4 show PTX-sensitive cAMP depression that remains in the presence of FR, depicted here as mean  $\pm$  SEM of three biologically independent experiments.

### $G\alpha_i$ -mediated cAMP depression does not require $Gq$

Next, we examined the canonical  $G\alpha_i$ -mediated cAMP depression for a potential dependency on  $Gq$  (Figure 15A). When stimulated with low agonist concentrations, HEK cells stably expressing hGPR17, rGPR17, or mGPR17 showed an inhibition of forskolin (FSK)-mediated cAMP accumulation that reflected  $G_i$ -activation (Figure 15B). We also detected an increase in cAMP production for high concentrations of agonist, again congruent with  $G_s$ -activation. While the  $G_i$ -mediated cAMP-depression was entirely abrogated by preincubation with PTX, the cAMP profile of each receptor was only slightly modulated by  $Gq$ -inhibitor FR, with the  $G_i$ -dependent part remaining intact (Figure 15B). The specifically  $G_i$ -coupled model receptors displayed more classical  $G_i$ -cAMP-profiles, with a clear depression of FSK-mediated cAMP for all ligand concentrations (Figure 15C). Again, this was completely blocked by PTX, but unaffected by FR. We concluded that canonical  $G\alpha_i$ -AC signaling is not dependent on  $Gq$ .

## Results

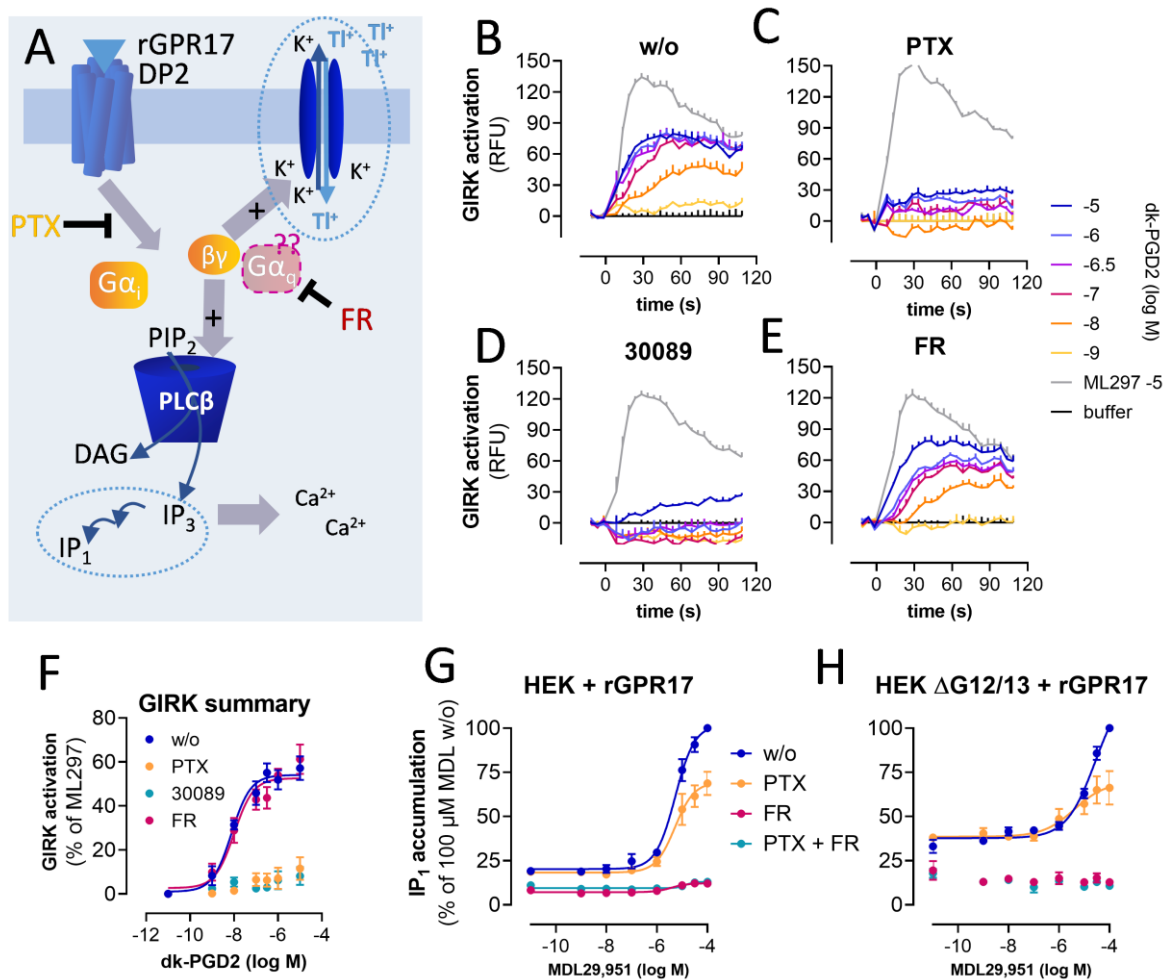


**Figure 16: Gi-G $\beta\gamma$ -PLC $\beta$  signaling, but not Gi-G $\beta\gamma$ -GIRK activation, fully depends on Gq.** (A) Gi-G $\beta\gamma$  can activate the PLC $\beta$  to trigger IP production and calcium release, as well as GIRK channels to allow K<sup>+</sup> flux. FR can be used to investigate whether each signaling process depends on Gq. (B-E) mean + SEM of representative thallium flux kinetics show GIRK activation in response to the direct GIRK activator ML297 and also via stimulation of DP2 with dk-PGD2. The DP2-mediated GIRK activation is sensitive to PTX (C) and DP2 antagonist TM30089 (D), but intact in the presence of FR. Three biologically independent experiments were summarized as mean  $\pm$  SEM in (F). (G, H) rGPR17-induced IP<sub>1</sub> accumulation, shown as mean  $\pm$  SEM of three experiments, is partially PTX-sensitive and almost fully FR-sensitive (G). The remaining IP<sub>1</sub> accumulation in the presence of FR shows no PTX sensitivity (G), but is undetectable in cells lacking G12 and G13 (H).

Gi-G $\beta\gamma$ -PLC $\beta$  signaling, but not Gi-G $\beta\gamma$ -GIRK activation, fully depends on Gq.

Unlike Gi-cAMP-signaling, Gi-calcium is triggered by the G $\beta\gamma$  subunit released from the Gi-heterotrimer, which activates PLC $\beta$ . We considered whether Gq might be required for Gi-G $\beta\gamma$ -signaling. To investigate this notion, we selected two Gi-G $\beta\gamma$ -signaling



readouts (Figure 16A). The first one visualizes activation of the GIRK channel using a fluorescent dye to detect thallium influx upon opening of the channel. HEK cells stably expressing the GIRK1/2 subunit combination along with DP2 showed a concentration-dependent GIRK activation upon stimulation with the specific DP2 agonist dk-PGD2 (Figure 16B). As expected, this response was not detected in the presence of PTX (Figure 16C) or DP2-antagonist TM30098 (Uller et al., 2007) (Figure 16D). However, GIRK activation was unaffected by FR (Figure 16E, F). Notably, the direct GIRK activator ML297 (Wydeven et al., 2014) elicited GIRK responses that were independent of inhibitor-treatment, confirming the cell viability under all conditions (Figure 16B-E). The second Gi-Gβγ-readout we selected was IP<sub>1</sub>-accumulation, which is triggered by Gi-Gβγ-dependent activation of PLCβ, and lies just upstream of the Gq-dependent Gi-calcium (Figure 16A). HEK cells expressing rGPR17, selected here as a representative GPCR of our promiscuous model receptors, showed concentration-dependent IP<sub>1</sub> accumulation, with partial PTX-sensitivity confirming Gi-involvement in the signal. Like Gi-calcium, a downstream readout of the same cascade, but unlike Gi-Gβγ-GIRK-activation, this Gi-Gβγ IP<sub>1</sub> accumulation was almost entirely blocked in the presence of FR, with only a small, PTX-insensitive IP<sub>1</sub> production remaining. This PTX-insensitive IP<sub>1</sub> accumulation was absent in HEK-Δ12/13 cells (Figure 16H), indicating that it is most likely G12/13-PLCε-mediated. In these cells, FR completely abolished all rGPR17-dependent IP<sub>1</sub> accumulation, including the PTX-sensitive Gi-Gβγ-dependent component. These results indicate that Gi-Gβγ-GIRK does not require Gq, while Gi-Gβγ-PLCβ-activation is entirely dependent on Gq activation.

*Excursion 3.1: The effect of Gq-activation on Gi-Gβγ-GIRK activation.*

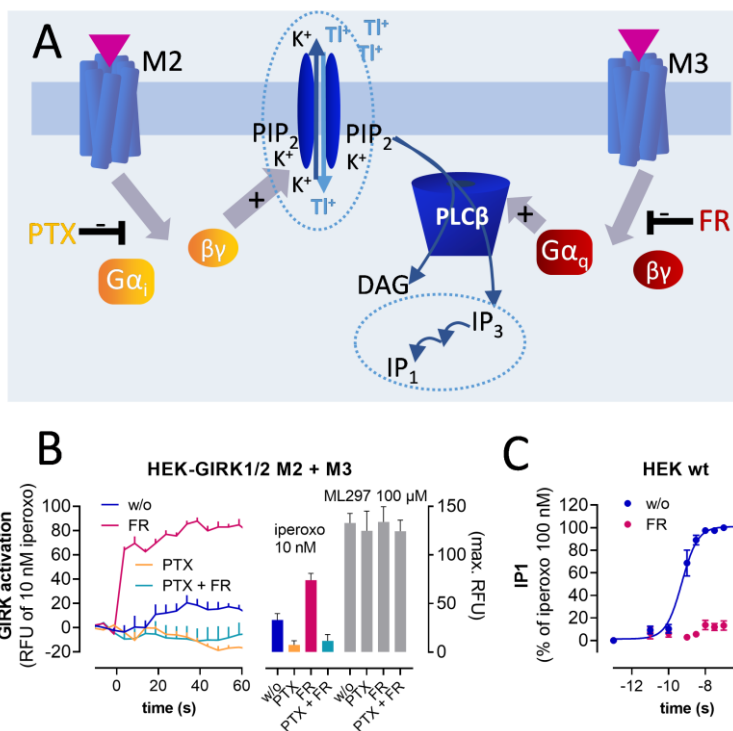


**Figure 17: Gq hampers Gi-Gβγ-GIRK activation by depletion of GIRK co-factor PIP<sub>2</sub>.** (A) Activation of Gi-coupled M2 activates GIRK channels via Gi-Gβγ. In HEK cells, the same ligand also activates Gq-coupled M3 receptors, which leads to PLCβ-dependent hydrolysis of the GIRK co-factor PIP<sub>2</sub> to IP<sub>3</sub> and DAG, thereby decreasing GIRK ion Flux in a Gq-dependent manner. (B) Representative GIRK kinetics and quantification of three

experiments show GIRK activation via M2/3 receptor stimulation that is completely PTX-sensitive and boosted in the presence of FR. All data are shown as mean + SEM. (C) mean ± SEM of three IP<sub>1</sub> accumulation experiments in HEK wt cells show complete FR-sensitivity of IP production via M3.

We also measured Gi-Gβγ-GIRK activation upon simultaneous Gi and Gq-stimulation. To this end, we used a HEK cell line stably expressing GIRK1/2 and the M2 receptor. In addition to this Gi-coupled M2 receptor, HEK cells also endogenously express the Gq-coupled M3 receptor (Figure 17A). Stimulating this cell line with iperoxo, a super-agonist that activates both muscarinic receptors (Dallanocce et al., 1999), we witnessed only minute GIRK-activation (Figure 17B). However, upon blocking the Gq pathway with FR, the iperoxo-mediated GIRK-activation increased significantly (Figure 17B). This is due to the effect of Gq-stimulation on PIP<sub>2</sub>, a co-factor required for GIRK activation (Wydeven et al., 2014). In the absence of FR, activation of Gq via the M3 receptor results in PLCβ-mediated conversion of PIP<sub>2</sub> into IP<sub>3</sub> and DAG, which can be observed as IP<sub>1</sub>-accumulation (Figure 17C). When FR is present, this cleavage of PIP<sub>2</sub> does not take place (Figure 17C), leaving more PIP<sub>2</sub> available to boost the GIRK-current, thus explaining the more robust GIRK-response (Figure 17B). Therefore, it can be concluded that Gi-Gβγ-GIRK activation not only does not require Gq, it is actually

negatively affected by Gq activation. This presents a stark contrast to the complete dependency of Gi-Gβγ-PLCβ signaling on Gq.

In summary, we have demonstrated that neither Gi-activation in general (Figure 14), nor canonical G<sub>ai</sub>-signaling (Figure 15), nor Gi-Gβγ-GIRK signaling (Figure 16, 17) depend on Gq. Instead, Gq seems to be a specifically required ‘master switch’ for the Gi-Gβγ-PLCβ-pathway only.

## Chapter 4: the canonical Gq pathway: which step allows Gi-calcium?

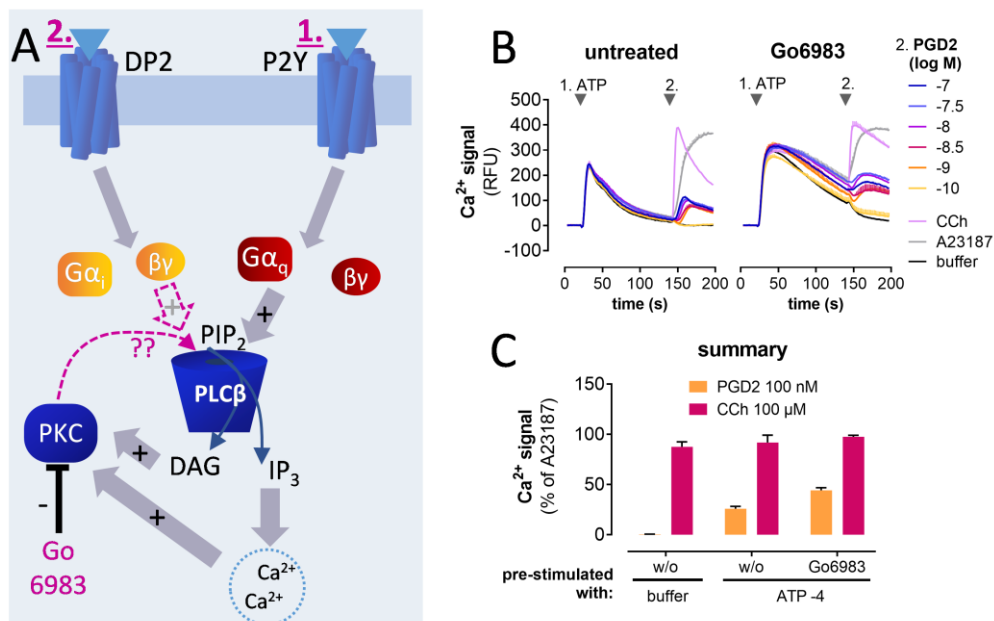


**Figure 18: Gi-Gβγ-PLCβ-calcium does not require Gq-PKC-activation.** (A) The PKC, which is activated downstream of Gq stimulation, is known to interact with PLCβ. If this step was required for Gi-Gβγ-PLCβ signaling, then the pan PKC inhibitor Go6983 should abolish Gi-calcium. (B) representative calcium kinetics, displayed as mean + SEM, show priming of the cells with P2Y agonist ATP and subsequent DP2-mediated Gi-calcium (left panel) that remains intact in the presence of PKC inhibitor Go6983 (right panel). (C) Three biologically independent experiments were summarized as mean + SEM. DP2 agonist PGD2 only induced calcium when cells were pre-stimulated with ATP, and this calcium response remained intact in the presence of Go6983, while the Gq stimulus CCh was stable under all three conditions.

### Gi-Gβγ-PLCβ-calcium does not require Gq-PKC-activation

So far, we have shown that Gq activation is specifically required for Gi-Gβγ-PLCβ-calcium. In order to better understand the mechanistic basis for this requirement, we aimed to narrow down the exact step of the canonical Gq signaling cascade that fulfills

## Results

this condition. We started by investigating one of the very downstream effectors of Gq-activation, the protein kinase C (PKC). This kinase is activated by the Gq-dependent calcium release, as well as by the production of DAG by PLC $\beta$ . PKC then phosphorylates various effectors, providing the starting point for kinase signaling. PKC has been shown to phosphorylate PLC $\beta$ , a process that is usually considered a “negative feedback mechanism” to down-regulate PLC $\beta$ -signaling (Filtz et al., 1999; Xu et al., 2001; Kadamur & Ross, 2013). We wondered if this interaction, or any other PKC-dependent process, might provide the basis for Gi-G $\beta\gamma$  to activate PLC $\beta$  (Figure 18A). If this were the case, we reasoned that the pan-PKC-inhibitor Go6983 should abolish Gi-calcium. Thus, we examined the effect of Go6983 on HEK cells stably expressing DP2, primed with ATP to allow DP2-mediated Gi-calcium (Figure 18B). However, Gi-calcium was clearly detectable upon PKC-inhibition (Figure 18B, C), with the signal even being slightly prolonged, possibly due to the impaired negative feedback mechanisms (Figure 18B). In conclusion, PKC-activation is dispensable for Gi-G $\beta\gamma$ -calcium.

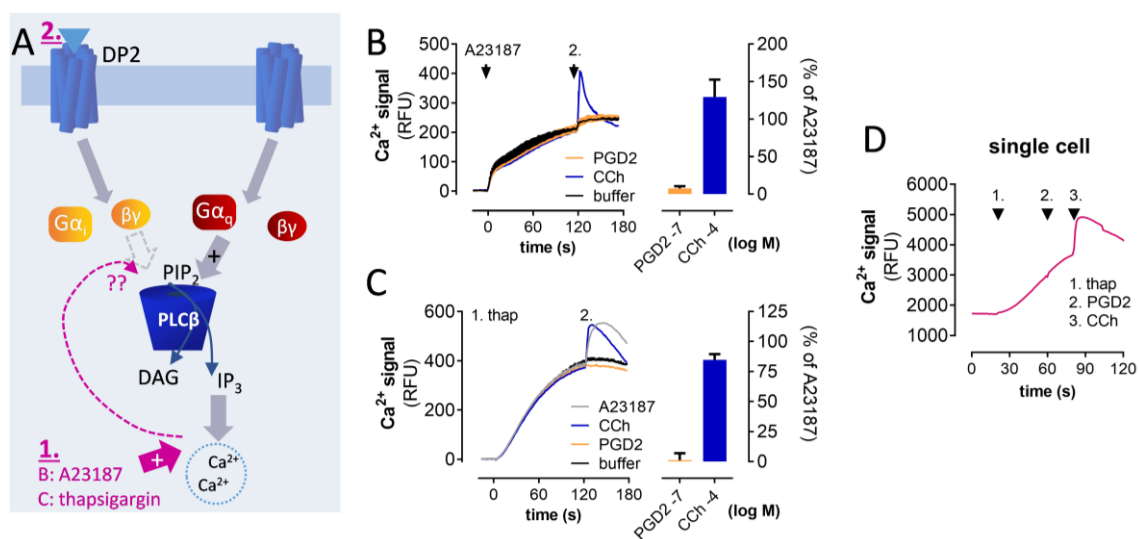


**Figure 19: An acute increase in intracellular calcium is not sufficient to allow Gi-calcium.**

(A) The Gq (pre-)stimulation required for Gi-G $\beta\gamma$ -PLC $\beta$ -calcium triggers an acute increase of intracellular calcium. If this calcium release alone were sufficient to allow Gi-G $\beta\gamma$ -PLC $\beta$ -calcium, then a Gq-independent calcium stimulus, such as A23187 or thapsigargin, should restore Gi-calcium without Gq activation. (B, C) representative calcium kinetics obtained in HEK-DP2- $\Delta$ ct cells (left panels) and their quantified summary (right panels), both displayed as mean + SEM. Priming of the cells with 500 nM A23187 (B) or 30  $\mu$ M thapsigargin (C) increases the intracellular calcium levels. The cells respond to the subsequent CCh stimulus, but no PGD2 calcium response is detectable. (D) A single cell calcium kinetic, representing three biologically independent measurements performed with 25 replicates each, shows increased intracellular

calcium levels in response to 10  $\mu\text{M}$  thapsigargin, followed by no response to 100 nM PGD2 stimulation, followed by an intact calcium response to Gq stimulus CCh (100  $\mu\text{M}$ ).

An acute increase in intracellular calcium is not sufficient to allow Gi-calcium

The next consequence of Gq-activation we examined was calcium release. Since there are multiple calcium-binding domains in the structure of PLC $\beta$ , including two EF hands and a crucial domain in the catalytic center, an increased intracellular calcium concentration might be the 'master switch' that unlocks PLC $\beta$  activation via Gi-G $\beta\gamma$  (Figure 19A). To test this, we used A23187 to generate Gq-independent calcium release. A23187 produced a relatively steady calcium increase, but the following DP2-stimulation with PGD2 did not produce any observable Gi-calcium, although the cells were still responsive to the Gq stimulus CCh (Figure 19B). We also tested the effect of thapsigargin, a SERCA-inhibitor that blocks the re-uptake of calcium into the stores, causing a slow leakage into the cytosol. However, again, no subsequent Gi-calcium was detected. In both cases, the cells still mobilized calcium upon Gq-stimulation with CCh. However, since this was a population-based experiment, the responsiveness to CCh does not reliably demonstrate that the cells with increased intracellular calcium were still responsive at the time of the second compound addition. It could be argued that there might have been other cells that did not respond to A23187- or thapsigargin- stimulation, respectively, and therefore were responsive to Gq-stimulation, while the cells with increased intracellular calcium were completely depleted and thus unable to mobilize Gi-calcium or respond to control. In order to exclude this possibility and draw a definitive conclusion whether increased intracellular calcium allows Gi-G $\beta\gamma$ -PLC $\beta$ -activation, we repeated the thapsigargin-prestimulation in a single cell setup. Here, we clearly observed increased intracellular calcium, no response to Gi-stimulation, followed by an intact response to Gq-stimulation within the same cell, thus proving that a calcium increase alone does not meet the requirement for Gi-G $\beta\gamma$ -PLC $\beta$ -calcium.

## Results

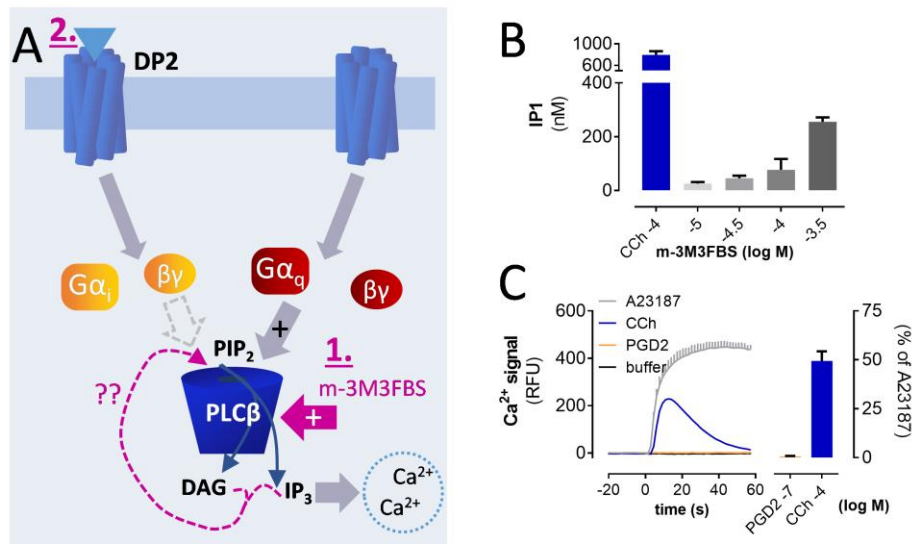


**Figure 20: Increased intracellular IP production does not restore Gi-Gβγ-PLCβ-calcium.** (A) m-3M3FBS is published as a G<sub>q</sub>-independent PLC activator. We investigated if this compound would restore Gi-calcium in absence of G<sub>q</sub> input. (B) HEK-DP2-Δct cells pre-incubated with high concentrations of m-3M3FBS for 45 min showed increased IP<sub>1</sub> accumulation. Data are shown as mean + SEM of three independent experiments. In a calcium experiment (C), the same cells showed intact responses to control stimuli, but no calcium mobilization in response to PGD<sub>2</sub>. Representative kinetics (left panel) are mean + SEM, summarized as mean + SEM of three biologically independent experiments (right panel).

### Increased intracellular IP production does not restore Gi-Gβγ-PLCβ-calcium

Next, we asked if Gi-Gβγ-PLCβ-calcium would be restored by G<sub>q</sub>-independent PIP<sub>2</sub> conversion cleavage to IP<sub>3</sub> and DAG (Figure 20A). We achieved this by using the unspecific PLC activator m-3M3FBS (Bae et al., 2003) in HEK-DP2-Δct cells. Notably, only the highest concentration of m-3M3FBS caused a detectable increase in IP<sub>1</sub> accumulation (Figure 20B) over the course of 45 min. However, the same cells failed to mobilize Gi-calcium in response to PGD<sub>2</sub> after this treatment (Figure 20C). Admittedly, there might be doubts as to the specificity of such a high concentration of any compound, and while the accumulation of IP<sub>1</sub> might be visible because further degradation of IP<sub>1</sub> is prevented through the addition of Li<sup>+</sup> to this assay setup, the levels of the biologically active but quickly degradable IP<sub>3</sub> might be virtually unchanged. Keeping these limitations in mind, we took this data as an indication that PIP<sub>2</sub> conversion might not be the event that allows Gi-Gβγ-PLCβ-calcium.

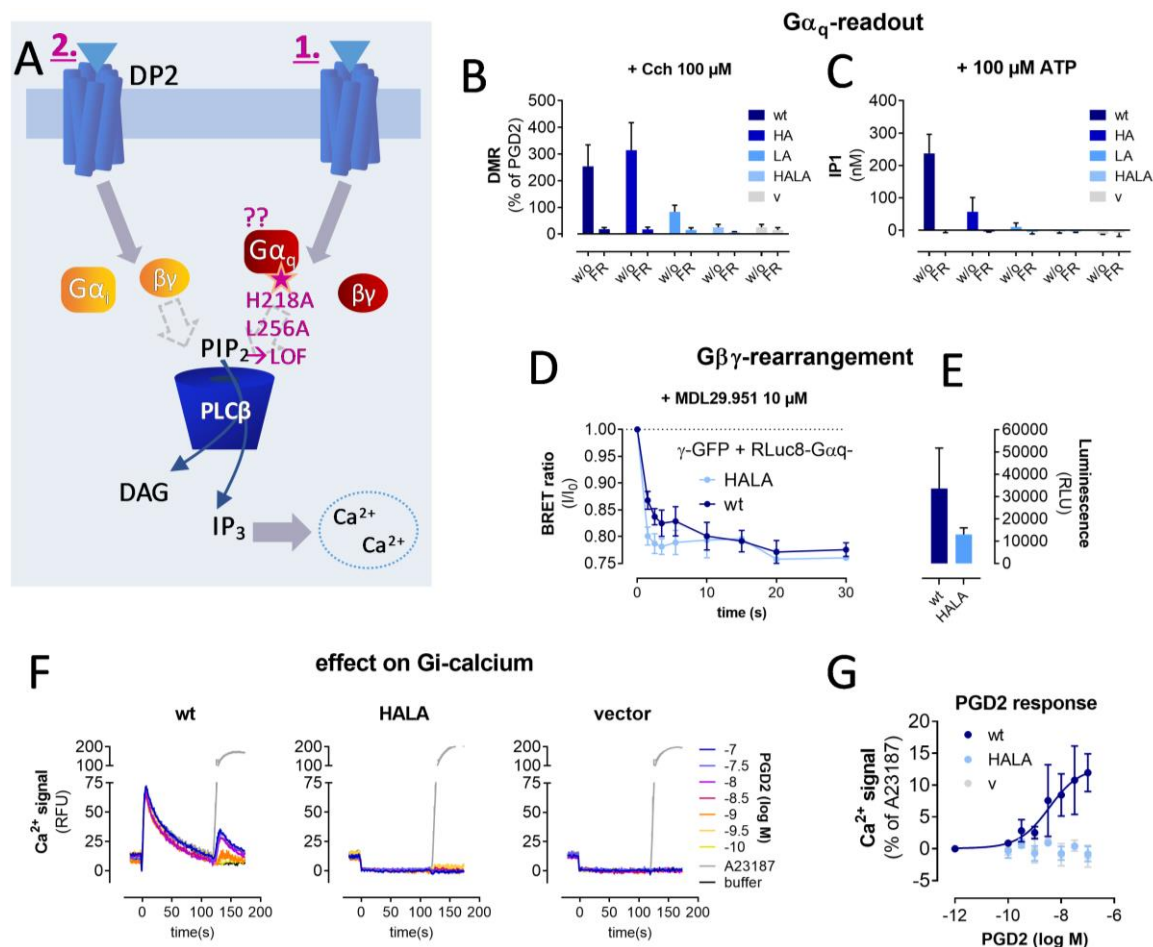


**Figure 21: Gα<sub>q</sub>-PLCβ interaction, rather than Gq-Gβγ-signaling, is required for Gi-Gβγ-PLCβ-calcium.** (A) HEK-ΔGq/11 cells were transfected with DP2, along with a Gα<sub>q</sub> protein carrying the H218A and/or L254A mutations to abrogate PLCβ interaction. These mutations are „loss of function“ (LOF) regarding their capacity to bind PLCβ, but retain their ability to form heterotrimeric G-proteins and mobilize Gβγ upon activation. We investigated if pre-stimulation of these Gq heterotrimers would restore Gi-Gβγ-PLCβ-calcium. (B, C) Mean + SEM of three DMR (B) and IP<sub>1</sub> accumulation (C) experiments show a reduced signaling capacity by the Gα<sub>q</sub>-LOF single mutants and a complete loss of function for the Gα<sub>q</sub>-LOF double mutant, in response to CCh (B) or ATP (C), respectively. (D) mean + SEM of the basal luminescence (395 nm) upon expression of RLuc8-Gα<sub>q</sub><sup>wt</sup> and -Gα<sub>q</sub><sup>H218A-L256A</sup>, respectively, shows lower expression of the double mutant upon transfection. (E) BRET measurements show a decrease in Gα<sub>q</sub>-RLuc8 and GFP-Gγ2 BRET upon stimulation of rGPR17 that is comparable for the Gα<sub>q</sub>-LOF double mutant and Gα<sub>q</sub><sup>wt</sup>. Data are depicted as mean ± SEM of three biologically independent experiments, normalized to the unstimulated values. (F, G) calcium measurements in HEK-ΔGq/11 cells show PGD2 calcium after pre-stimulation of the cells with ATP when Gα<sub>q</sub><sup>wt</sup> is transfected, but no detectable PGD2 calcium when Gα<sub>q</sub>-LOF double mutant is transfected. (F) Representative calcium measurements shown as men + SEM, summarized in (G) as mean ± SEM of three biologically independent experiments.

## Results

### Gαq-PLCβ interaction, rather than Gq-Gβγ-signaling, is required for Gi-Gβγ-PLCβ-calcium

Since we excluded most canonical downstream-consequences of the Gq cascade regarding being the ‘master switch’ for Gi-Gβγ-PLCβ-calcium, we concluded that it must be the heterotrimeric Gq protein itself that is required. A heterotrimeric G protein consists of two signaling transducers, the Gα and the Gβγ subunit. We hypothesized that it is probably the direct interaction of the Gαq-subunit with PLCβ that allows PLCβ to be activated by Gi-Gβγ. On the other hand, it could also be argued that the Gq-Gβγ subunit might be involved with the ability of Gi-Gβγ to activate its effector. To discriminate between these two possibilities, we again used G-proteins carrying specific mutations to change their signaling properties. In this case, we modified the positions H218A and L256A, which are essential for Gαq’s effector interaction (Waldo et al., 2010). Gαq proteins carrying either of these mutations have been described as being complete loss-of-function regarding their capacity to activate PLCβ (Waldo et al., 2010), but we reasoned that they should still be activated by GPCRs and thus retain their Gβγ-releasing behavior (Figure 21A). Interestingly, HEK-ΔGq/11 cells transfected with the single mutants still showed clearly detectable, FR-sensitive DMR in response to CCh (Figure 21B) and IP<sub>1</sub> accumulation upon stimulation with ATP (Figure 21C). However, cells transfected with the double-mutant promisingly showed no detectable Gq signaling (Figure 21B, C). On the other hand, a BRET assay showed intact rGPR17-mediated rearrangement between the Rluc8-tagged version of Gαq<sup>H218A-L256A</sup> and GFP-G<sub>γ2</sub>, which was not impaired compared to that of Rluc8-tagged Gαq<sup>wt</sup> (Figure 21D). On the contrary, it could be argued that Gαq<sup>H218A-L256A</sup>-Gβγ rearrangement occurs even faster than that of Gαq<sup>wt</sup> heterotrimers. However, this could also be a result of the lower expression levels of Rluc8-Gαq<sup>H218A-L256A</sup> (Figure 21E). We concluded that this Gαq double mutant is defective regarding its Gαq signaling, but capable of mobilizing Gβγ upon activation. If an interaction of the Gαq subunit with PLCβ was required for Gi-Gβγ-PLCβ-calcium, this Gαq<sup>H218A-L256A</sup> mutant should no longer restore Gi-calcium. To test this, we performed calcium measurements in HEK-ΔGq/11 cells expressing Gαq<sup>H218A-L256A</sup> along with the DP2 receptor. As expected, there was no detectable Gq-calcium upon stimulation of the Gαq<sup>H218A-L256A</sup>- or vector-transfected cells with ATP, while the response in Gq<sup>wt</sup>-transfected cells was intact (Figure 21F, G). And indeed, there was also no detectable Gi-calcium mobilization upon PGD<sub>2</sub>-stimulation in the presence of the double mutant (Figure 21E, F). Notably, because Rluc8-Gαq<sup>H218A-</sup>



L256A showed impaired expression compared to  $G\alpha^{wt}$ , a reduced expression of  $G\alpha^{H218A}$ . L256A might be in part responsible for this absence of Gi-calcium. Thus, while the expression of  $G\alpha^{H218A-L256A}$  would have to be confirmed to draw a definitive conclusion, these data seem to indicate that the interaction of  $G\alpha$  with  $PLC\beta$  is essential for Gi- $G\beta\gamma$ - $PLC\beta$ -calcium.

Keeping all limitations in mind, our conclusion from these investigations was that it is the active, effector-binding  $G\alpha$  subunit itself, rather than canonical Gq downstream consequences or Gq- $G\beta\gamma$ -signaling, that is a 'master switch' for Gi- $G\beta\gamma$ - $PLC\beta$ -calcium.

## Chapter 5: Identifying the molecular mechanism - what does $G\alpha$ do?

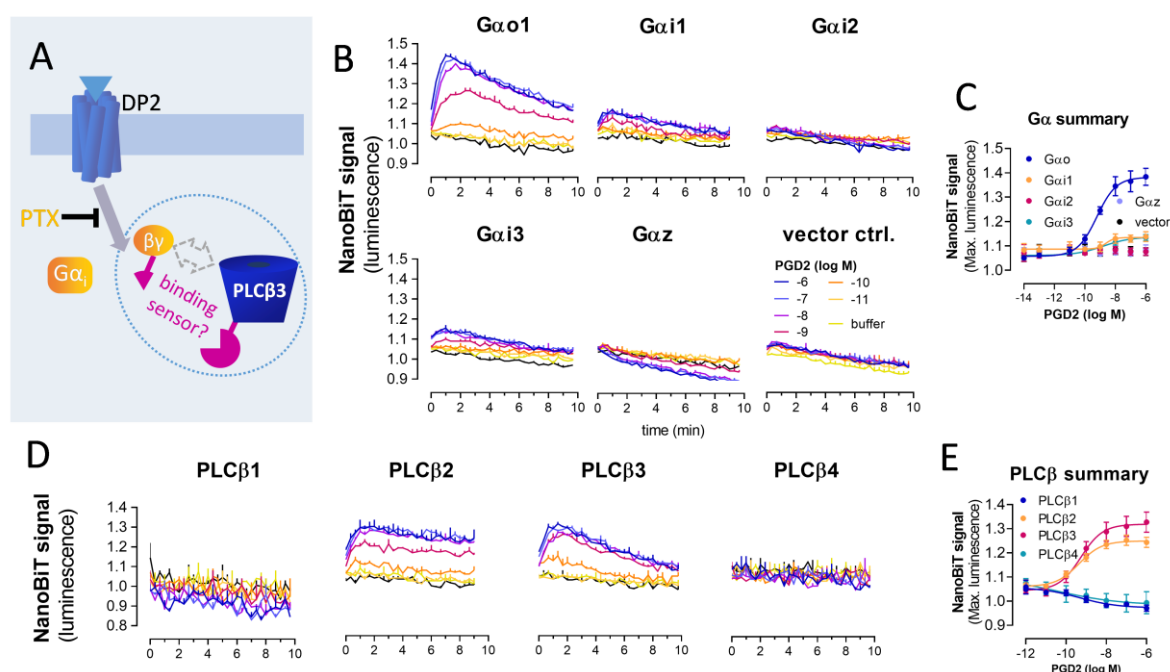


**Figure 22. NanoBIT sensor displays  $G\beta\gamma$ - $PLC\beta$  binding.** (A) To detect  $G\beta\gamma$  binding to  $PLC\beta$ , a small fragment of the nanoluciferase was fused to  $G\gamma 2$  (smBiT- $G\gamma 2$ ) and the corresponding large fragment was fused N-terminally to  $PLC\beta$  (LgBiT- $PLC\beta$ ). We tested if this sensor was suitable to detect binding of  $G\beta\gamma$  to  $PLC\beta$  upon activation of Gi-coupled DP2 in HEK cells. (B, C) Representative mean + SEM luminescence kinetics recorded in HEK cells expressing the smBiT- $G\gamma 2$  LgBiT- $PLC\beta 3$  sensor, along with  $G\beta 1$ , DP2 and the indicated  $G\alpha i$  subunit, summarized in (C) as mean  $\pm$  SEM of three experiments. In the presence of  $G\alpha o$ ,  $G\alpha i 1$  and  $G\alpha i 3$ , stimulation with PGD2 produced concentration-dependent increased luciferase activity. The  $pEC_{50}$  value of PGD2 was 9.21, 8.62 and 8.80 for  $G\alpha o 1$ ,  $G\alpha i 1$ ,  $G\alpha i 3$ , respectively, which matches the  $pEC_{50}$  values of PGD2-mediated  $Ca^{2+}$  responses (8.97, 8.92 and 9.29 for ATP-, UTP- and CCh-

## Results

prestimulated cells, respectively, see also Figure 11). (D, E) In HEK cells expressing  $G_{\alpha o}$ ,  $G_{\beta 1}$ , smBiT-G $\gamma 2$  and LgBiT fused to the respective PLC $\beta$  isoform, representative kinetics (D) summarized in (E) show PGD2 induced increased luciferase activity only in the presence of PLC $\beta 2$  and PLC $\beta 3$ , but not PLC $\beta 1$  and PLC $\beta 4$ .  $pEC_{50}$  values were 9.36 and 9.27 for PLC $\beta 2$  and PLC $\beta 3$ , respectively.

### NanoBiT sensor displays $G_{\beta\gamma}$ -PLC $\beta$ binding.

We intended to disentangle the precise role the activated  $G_{\alpha q}$  subunit has in allowing Gi- $G_{\beta\gamma}$ -PLC $\beta$  activation. To do this, we first had to identify the step of Gi- $G_{\beta\gamma}$ -PLC $\beta$  activation that fails without  $G_q$ . We came up with two hypotheses to account for the absence of IP $_1$  accumulation or calcium release via Gi- $G_{\beta\gamma}$  alone. Either, without priming by  $G_{\alpha q}$ , the  $G_{\beta\gamma}$ -subunit released from Gi is not capable of binding to PLC $\beta$ , or it binds to PLC $\beta$  without triggering substrate conversion. To visualize binding of  $G_{\beta\gamma}$  to PLC $\beta$ , we developed a nanoBiT sensor (Dixon et al., 2016) that detects the proximity of two proteins as increased luminescence. We designed a construct by fusing the smallBiT (smBiT) of the split luciferase to the N-terminus of  $G_{\gamma 2}$  (smBiT-G $\gamma 2$ ) using a flexible linker, and tagged PLC $\beta 3$  N-terminally with the corresponding large BiT (LgBiT-PLC $\beta$ ) (Figure 22A). HEK cells were then transfected with this sensor, along with the DP2 receptor,  $G_{\beta 1}$  and either control-vector or the indicated  $G_{\alpha i}$ -subunit (Figure 22B). Upon stimulation with PGD2, the cells transfected with  $G_{\alpha o}$ ,  $G_{\alpha i 1}$  and  $G_{\alpha i 3}$  showed a concentration-dependent increase in luminescence, indicating Gi-dependent binding of  $G_{\beta\gamma}$  to PLC $\beta 3$  (Figure 22B). Because the highest signal was obtained for  $G_{\alpha o}$ , we selected this  $G_{\alpha i}$ -isoform for further examinations of Gi- $G_{\beta\gamma}$  binding to PLC $\beta$ . Next, to validate the sensor, we compared binding of Gi- $G_{\beta\gamma}$  to different isoforms of PLC $\beta$ . We transfected similarly tagged versions of PLC $\beta 1$  (LgBiT-PLC $\beta 1$ ), PLC $\beta 2$  (LgBiT-PLC $\beta 2$ ), and PLC $\beta 4$  (LgBiT-PLC $\beta 4$ ) and detected their binding to  $G_{\beta\gamma}$ . Upon stimulation of the DP2 receptor, we observed concentration-dependent binding to PLC $\beta 2$  and PLC $\beta 3$ , with no or negative signals for PLC $\beta 1$  and PLC $\beta 4$  (Figure 22D, E). Therefore, the sensor faithfully recapitulates both our findings that Gi- $G_{\beta\gamma}$ -PLC $\beta$ -calcium is mediated via PLC $\beta 2$  and PLC $\beta 3$  as well as the well-established Gi-calcium paradigm (Kadamur & Ross, 2013). Additionally, the  $pEC_{50}$  values of PGD2 for  $G_{\beta\gamma}$ -PLC $\beta$  binding reflected those observed in our calcium measurements. This underlined that this newly-developed sensor is well-suited and trustworthy in visualizing  $G_{\beta\gamma}$  binding to PLC $\beta$ .

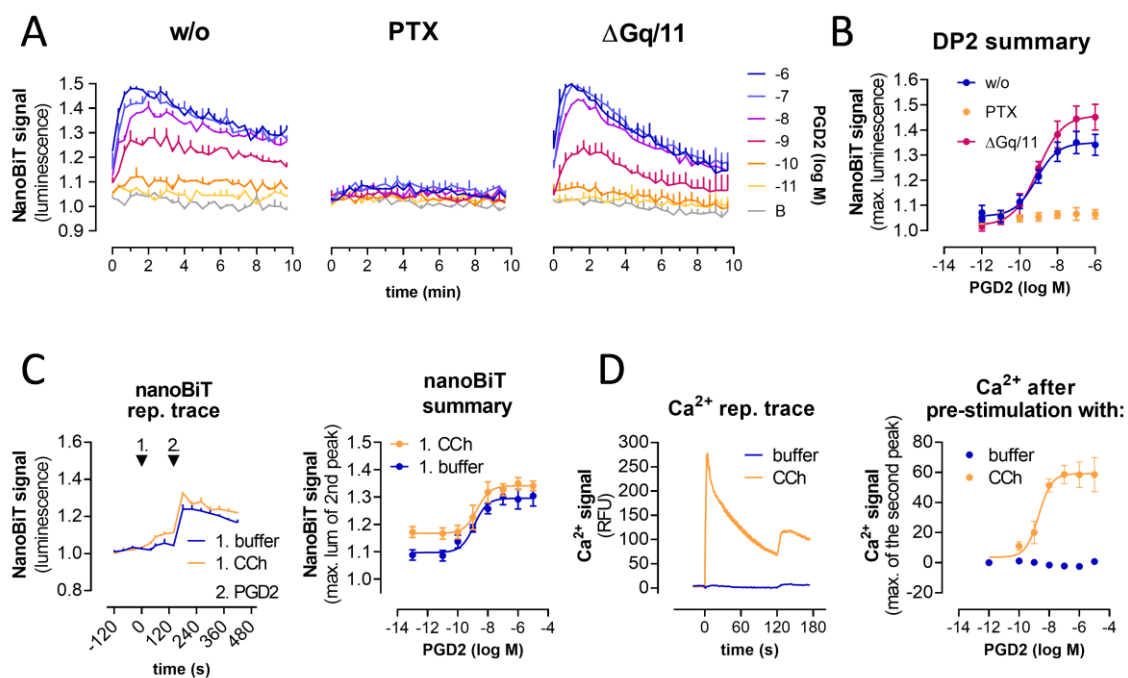


**Figure 23: Gq does not enhance Gβγ-PLCβ binding.** (A, B) In HEK cells, the nanoBiT Gβγ-PLCβ3 sensor shows PGD2-dependent luminescence increase that is blocked by co-transfection of PTX-S1, but intact in cells lacking Gαq/11. The representative kinetics depicted as mean + SEM in (A) were summarized as mean ±SEM of three biologically independent experiments in (B). (C) Representative (left panel) and summarized (right panel) nanoBiT signals show no increase in PGD2-mediated luminescence when the cells are pre-stimulated with CCh. (D) In the same cells, representative (left panel) and summarized (right panel) calcium data shows PGD2-mediated responses only after CCh priming.

### Gq does not enhance Gβγ-PLCβ binding

Using this nanoBiT sensor, we investigated if Gi-Gβγ binding to PLCβ was Gαq-dependent. As expected, the robust, DP2-mediated Gβγ-PLCβ3 interaction was fully blocked in cells transfected with the active PTX-S1 subunit to inhibit Gi-activation (Figure 23A, B). On the other hand, binding of Gβγ to PLCβ remained intact in HEK-ΔGq/11 cells (Figure 23A, B). These findings underline that Gi-Gβγ does not require Gq in order to bind PLCβ. Next, we tested whether Gαq-activation would enhance binding of Gβγ to PLCβ, thereby facilitating Gi-Gβγ-PLCβ-calcium. However, prestimulation of the cells with CCh to provide Gq input did not enhance PGD2-mediated binding of Gβγ to PLCβ3 (Figure 23C), although the same cells responded with robust PGD2-mediated calcium-mobilization only after CCh-prestimulation (Figure 23D). Interestingly, we detected a slight increase of luminescence upon CCh

## Results

addition (Figure 23C), which most likely arises from  $G\beta\gamma$  subunits freed upon activation of M3 receptors. From these data we concluded that Gi-derived  $\beta\gamma$  binding to  $PLC\beta$  is neither dependent on nor facilitated by  $Gq$ .

### *Excursion 5.1: Why is there no binding of $Gai2$ - $G\beta\gamma$ or $Gaz$ - $G\beta\gamma$ to $PLC\beta3$ ?*

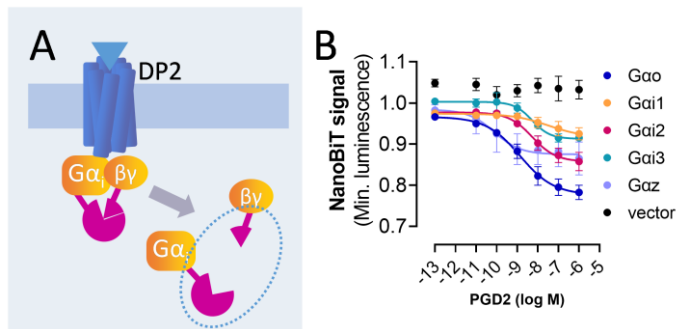


**Figure 24: DP2 activates all  $Gai$  subunits.** (A) A nanoBiT sensor to detect G protein dissociation was conceived by fusing the large fragment of a nanoluciferase to the  $G\alpha_i$  subunit (lgBiT- $G\alpha_i$ ) and the corresponding small fragment to  $G\gamma_2$  (smBiT- $G\gamma_2$ ).

Upon dissociation of the G protein in response to GPCR-activation, the intact nanoluciferase is disrupted and no longer active, causing a decrease in luminescence. (B) mean  $\pm$  SEM of two biologically independent nanoBiT experiments in HEK cells transfected with DP2,  $G\beta_1$ , smBiT- $G\gamma_2$  and the indicated lgBiT- $Gai$  subunit show a PGD2 dependent luminescence decrease for all  $Gai$  subunits.

We did not detect any increase in luminescence upon stimulation of DP2 when cells were transfected with  $Gai2$  or  $Gaz$ . Our first interpretation of this result was that DP2 did not activate these heterotrimers. However, we observed robust rearrangement between  $Gai2$  or  $Gaz$  and  $G\beta\gamma$  upon DP2-stimulation (Figure 24A, B). We also double-checked the cDNA concentration of the plasmid-stocks used for and their activity upon transfection in a cAMP-experiment (data generated by Yuki Ono for an unrelated project), but were unable to find a problem. We came up with three tentative explanations for the lack of observable  $G\beta\gamma$ - $PLC\beta3$  interaction, (i) that the  $G\beta\gamma$  subunits from these Gi-heterotrimers are not able to bind to  $PLC\beta3$ , (ii) that the N-terminally tagged  $G\gamma_2$  is not incorporated well into heterotrimers containing untagged  $Gai2$  or  $Gaz$ , or (iii) that the transfection conditions we used were not sufficiently optimized. Clearly, more investigations will be necessary to allow drawing a conclusion.

### Excursion 5.2: Does Gq-G $\beta\gamma$ bind to PLC $\beta$ ?

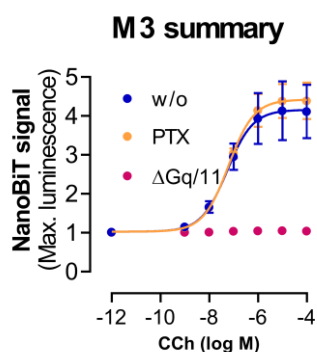


**Figure 25: Gq-G $\beta\gamma$  binds to PLC $\beta$  upon stimulation of M3 receptors.** In HEK cells transfected with M3, the nanoBiT G $\beta\gamma$ -PLC $\beta$  sensor shows CCh-dependent luminescence increase that is unaffected by co-transfection of PTX-S1, but absent in cells lacking G $\alpha_q/11$ . Data are depicted as mean  $\pm$ SEM of three biologically independent experiments.

Upon stimulation of the endogenously expressed M3 receptor in HEK cells transfected with the G $\beta\gamma$ -PLC $\beta$  binding nanoBiT sensor, we surprisingly detected a slight increase in luminescence (Figure 23C). We were intrigued by this observation, because the M3 receptor is known to be predominantly Gq-coupled, and Gq-derived G $\beta\gamma$  is not commonly associated with PLC $\beta$  binding or activation. Thus, we transfected HEK cells with M3, G $\alpha_q$ , the nanoBiT sensor, and tested for G $\beta\gamma$ -PLC $\beta$  binding upon M3 activation. Indeed, we detected concentration-dependent increases in luminescence upon addition of CCh, which were unaffected by co-transfection of PTX-S1 and absent in HEK- $\Delta Gq/11$  cells (Figure 25), underlining their Gq-G $\beta\gamma$  origin. In conclusion, not only Gi-G $\beta\gamma$  but also Gq-G $\beta\gamma$  can bind to PLC $\beta$  upon activation of a Gq-coupled GPCR.

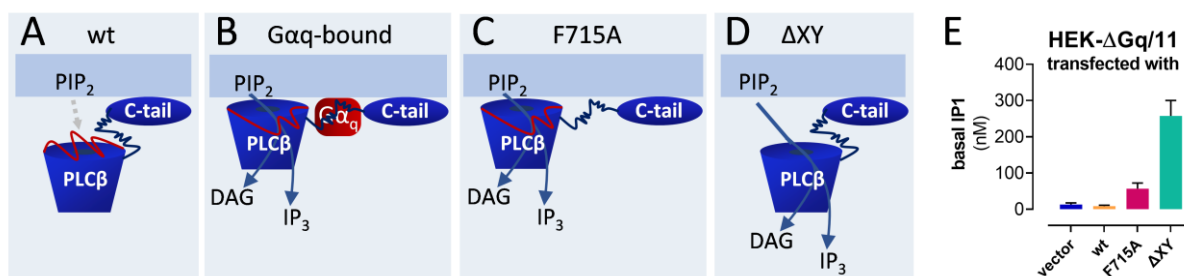


**Figure 26: PLC $\beta$ 3 constructs are not auto-inhibited and thus constitutively active.** Based on (Charpentier et al. 2014; Lyon et al. 2011; Hicks et al. 2008; Lyon et al. 2014). (A) PLC $\beta$ 3<sup>wt</sup> is auto-inhibited by an auto-inhibitory linker (XY-linker, depicted in red) that covers the catalytic site and prevents substrate cleavage. A HTH motif near the proximal C terminal domain also contributes to this auto-inhibition by hindering membrane access. Due to these two auto-inhibitory domains, the PLC $\beta$ 3<sup>wt</sup> enzyme shows close to no basal activity. (B) When G $\alpha_q$ -GTP binds near this HTH motif, it rearranges PLC $\beta$  at the membrane, causing repulsion of the XY linkers acidic region by the negatively charged membrane interface to reveal the catalytic site and allow substrate cleavage. (C) the PLC $\beta$ 3<sup>F715A</sup> mutant carries a mutation disturbing the interaction of the HTH with the TIM barrel of PLC $\beta$ 3, making the HTH more

## Results

flexible and thus promoting membrane collision with the XY linker to release auto-inhibition. This mutant shows low constitutive activity. (D) The PLC $\beta$ 3 $^{\Delta XY}$  mutant lacks the entire auto-inhibitory XY-linker, leaving the catalytic site freely accessible to PIP<sub>2</sub> and thus greatly increasing the PLC $\beta$ 3 enzymes basal activity. (E) HEK- $\Delta$ Gq/11 cells transfected with PLC $\beta$ 3 $^{F715A}$  or PLC $\beta$ 3 $^{\Delta XY}$  show increased IP<sub>1</sub> production compared to those transfected with vector control or PLC $\beta$ 3 $^{wt}$ . Data are shown as mean + SEM of three biologically independent experiments, each performed in triplicate.

PLC $\beta$ 3 constructs are not auto-inhibited and thus constitutively active.

If Gi-G $\beta$  $\gamma$  can bind to PLC $\beta$ , but no activation is detected without Gq, the activated G $\alpha$ q must make a crucial contribution that allows the catalytic reaction of PLC $\beta$ . The catalytic site of PLC $\beta$ , like that of most PLC subfamilies, is covered by an auto-inhibitory XY linker in a “plug-and-cap” like manner, which prevents substrate access (Hicks et al., 2008; Waldo et al., 2010; Gresset et al., 2010; Lyon et al., 2014) (Figure 26A). A critical step for activation of PLC $\beta$  is when this XY linker is repulsed by the membrane interface to uncover the catalytic site. This removal occurs when activated G $\alpha$ q binds to a helix-turn-helix (HTH) domain and thereby rearranges PLC $\beta$  at the membrane interface (Figure 26B). Disturbance of the Gq binding HTH domain using a single point mutation (PLC $\beta$ 3 $^{F715A}$ , Figure 26C) or genetic deletion of the XY linker (Lyon et al., 2011) (PLC $\beta$ 3 $^{\Delta XY}$ , Figure 26C) or also reveal the enzyme’s catalytic site and are known to cause constitutive activity (Charpentier et al., 2014). We performed an IP<sub>1</sub> accumulation assay that confirmed increased PLC $\beta$  activity in HEK cells transfected with either of the two modified PLC $\beta$  constructs, compared to control-vector or wildtype-PLC $\beta$ 3 (Figure 26E).

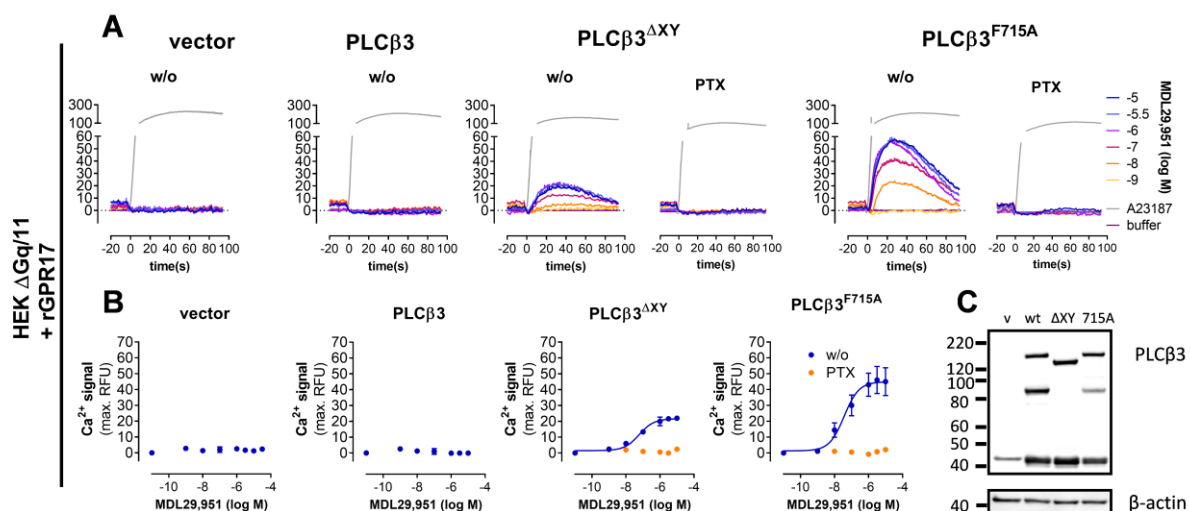


**Figure 27: Gi-Gβγ-PLCβ-calcium via crippled auto-inhibition PLCβ3 mutants does not require Gq.** (A) HEK-ΔGq/11 cells were transfected with rGPR17 and either control vector or PLCβ3<sup>wt</sup>, PLCβ3<sup>ΔXY</sup> or PLCβ3<sup>F715A</sup> as indicated. The mean + SEM representative calcium kinetics (A), summarized as mean ± SEM of three experiments (B), show no calcium response to rGPR17 agonist MDL29,951 when vector or PLCβ3-wt was transfected. In the presence of PLCβ3<sup>ΔXY</sup> or PLCβ3<sup>F715A</sup>, MDL29,951 elicits concentration-dependent calcium responses that are entirely PTX-sensitive (A, B). (C) A representative western blot of cellular lysates obtained from the cells used in (A, B) shows comparable expression of PLCβ3<sup>wt</sup> and the PLCβ3<sup>ΔXY</sup> and PLCβ3<sup>F715A</sup> constructs.

Gi-Gβγ-PLCβ-calcium via crippled auto-inhibition PLCβ3 mutants does not require Gq.

We reasoned that without Gq, binding of Gi-βγ alone might not sufficiently relieve auto-inhibition of PLCβ via the HTH or XY-linker, which would leave the catalytic site inaccessible and prevent substrate hydrolysis. If this were the case, Gi-Gβγ would activate PLCβ3<sup>F715A</sup> or PLCβ3<sup>ΔXY</sup> in absence of Gq, because the catalytic site is more easily accessible in these constructs. We were excited to find that, indeed, a calcium assay revealed rGPR17-mediated calcium mobilization in HEK-ΔGq/11 cells expressing PLCβ3<sup>ΔXY</sup> and PLCβ3<sup>F715A</sup> (Figure 27A, B). This concentration-dependent response was entirely Gi-dependent, as PTX treatment abrogated the signal completely. Notably, a western blot revealed similar expression levels of PLCβ3<sup>wt</sup> and the modified versions (Figure 27C), so the gain of Gi-calcium was not due to a boost in signal upon overexpression of PLCβ3.

## Results

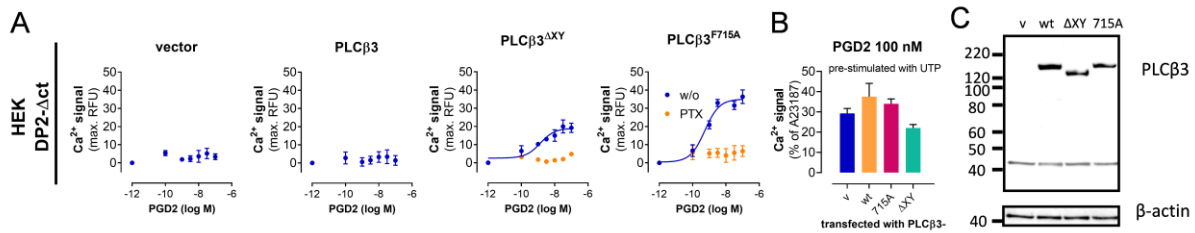


**Figure 28: When PLCβ3 auto-inhibition is disturbed by mutation, Gi-calcium no longer requires Gq input.** (A, B) Three independent calcium measurements were conducted in HEK-DP2-Δct cells transfected with vector, PLCβ3<sup>wt</sup>, PLCβ3<sup>ΔXY</sup> or PLCβ3<sup>F715A</sup> as indicated, and summarized here as mean ± SEM. Upon stimulation with DP2 agonist PGD2 without prior Gq stimulation, only cells expressing PLCβ3<sup>ΔXY</sup> or PLCβ3<sup>F715A</sup> mobilized calcium, which was blocked in the presence of PTX. (B) When primed with UTP, all cells displayed PGD2-dependent calcium mobilization (left panel), and all cells responded to A23187 (right panel). (C) A representative Western blot of lysates obtained from the experiments in (A, B) shows comparable expression of all transfected PLCβ3 constructs.

Additionally, we transiently expressed PLCβ3<sup>ΔXY</sup> and PLCβ3<sup>F715A</sup> in HEK-DP2-Δct cells, and observed concentration-dependent, Gi-mediated responses to PGD2 without prior Gq activation (Figure 28A). Notably, following Gq-stimulation with UTP, all cells mobilized calcium via DP2 (Figure 28B), confirming that transfection of the control plasmid or PLCβ3 did not interfere with DP2 receptor functionality. Again, all PLCβ3 isoforms were expressed at comparable levels in the transfected cells (Figure 28C).

From this data, we conclude that PLCβ3 constructs with crippled auto-inhibition no longer require Gq for Gi-βγ-PLCβ activation. This indicated that Gαq is necessary for Gi-Gβγ-PLCβ-calcium because it relieves the auto-inhibition of PLCβ and allows substrate hydrolysis, which is not sufficiently achieved by Gβγ alone.

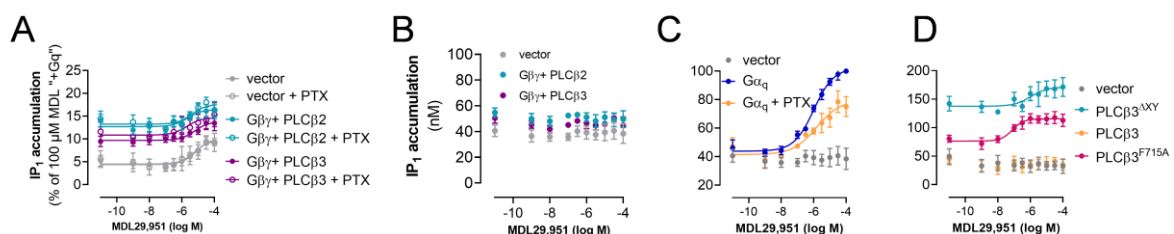


**Figure 29: Without Gq, Gβγ slightly increases basal cellular PLCβ activity, but does not mediate Gi-GPCR induced activation.** (A) In HEK-ΔGq/11 or HEK-ΔGq/11/12/13 cells, PLCβ activation by Gβγ was measured by overexpressing PLCβ2 or PLCβ3 with Gβ1 and Gγ2 and accumulating the cellular IP<sub>1</sub> production per 30 min. (B, C) HEK-ΔGq/11 cells transfected with rGPR17, along with Gβγ and PLCβ2 or PLCβ3 showed increased basal IP<sub>1</sub> accumulation



compared to vector-transfected cells. (B) Stimulation with MDL29.952 induced a slight increase in IP<sub>1</sub> production that was not enhanced in Gβγ-PLCβ-transfected cells and not sensitive to PTX, but absent in HEK-ΔGq/11/12/13 cells (C). MDL29,951-mediated, PTX-sensitive IP<sub>1</sub> production was restored by Gq expression (D) and in the presence of crippled auto-inhibition PLCβ3-constructs (E). All data are depicted as the mean ± SEM of three biologically independent experiments.

Without Gq, Gβγ slightly increases basal cellular PLCβ activity, but does not mediate Gi-GPCR induced activation.

Experiments using purified proteins have established Gβγ as a stand-alone activator of PLCβ. However, in living cells, Gi-Gβγ depends on Gαq to trigger calcium mobilization via PLCβ. This raised the pressing question whether Gβγ is no activator of PLCβ in living cells. A widely-used way to measure PLCβ activation via Gβγ (or Gαq) in living cells is by co-transfecting both and measuring the resulting accumulation of hydrolysis product (Hicks et al., 2008; Waldo et al., 2010; Wu et al., 1992). However, so far this hasn't been done in cells completely lacking Gαq proteins. When we transfected HEK-ΔGq/11 cells with Gβγ and PLCβ2 or PLCβ3, respectively, we indeed observed increased basal IP<sub>1</sub> accumulation compared to the control-transfected cells (Figure 29A), indicating that the Gβγ-PLCβ module is intact without Gq. Stimulation of the co-transfected rGPR17 with MDL29,951 led to a slight concentration-dependent increase in IP<sub>1</sub> levels. However, this was not PTX-sensitive and thus not Gi-Gβγ-mediated (Figure 29A). Thus, to remove this confounding IP<sub>1</sub> production and better assess rGPR17-mediated Gi-Gβγ-PLCβ activation, we used HEK cells lacking functional alleles of Gα12 and Gα13 (HEK-ΔGq/11/12/13). In these cells, rGPR17 stimulation did not trigger Gi-Gβγ-PLCβ activation, even when Gβγ and PLCβ2 or PLCβ3 were overexpressed (Figure 29B). In line with Gi-Gβγ-PLCβ-calcium mobilization, co-transfection of either Gq (Figure 29C) or PLCβ3 constructs with crippled auto-inhibition (Figure 29D) were required and sufficient to restore agonist-mediated Gi-Gβγ-PLCβ-dependent IP<sub>1</sub> accumulation.

## Results

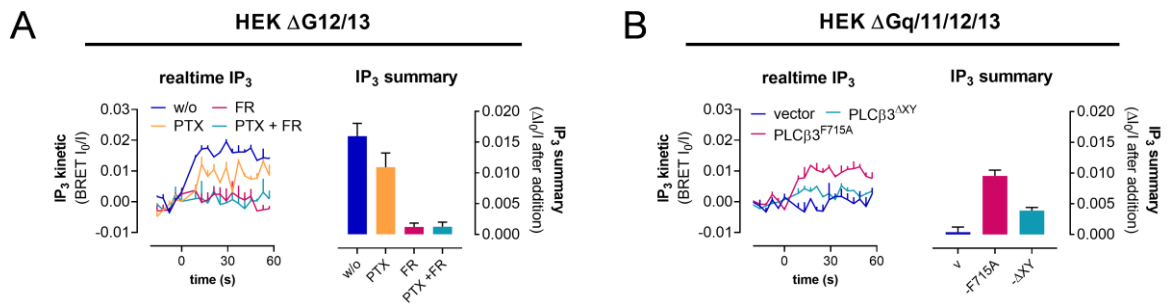


**Figure 30: Gi-G $\beta$  $\gamma$ -PLC $\beta$  activation does not trigger real-time IP<sub>3</sub> increase without Gq.** In HEK- $\Delta$ G12/13 cells or HEK- $\Delta$ Gq/11/12/13 cells, the IP<sub>3</sub> levels were monitored in real-time using a BRET IP<sub>3</sub> sensor that changes conformation upon binding of IP<sub>3</sub>. (A) representative real-time IP<sub>3</sub> kinetics (left panels) and their quantification (right panels) show an acute, partially PTX-sensitive increase in IP<sub>3</sub> upon stimulation of GPR17 that is fully blocked by FR. In the absence of Gq/11 (B), the lack of rGPR17-dependent IP<sub>3</sub> production is restored when PLC $\beta$ 3 $\Delta$ XY or PLC $\beta$ 3<sup>F715A</sup> is expressed. All data are depicted as mean + SEM, all quantifications show three biologically independent experiments.

### Gi-G $\beta$ $\gamma$ -PLC $\beta$ activation does not trigger real-time IP<sub>3</sub> increase without Gq

The lack of GPCR-induced Gq-independent G $\beta$  $\gamma$ -PLC $\beta$  activation is in line with the absence of Gi-calcium without Gq because to trigger calcium-release via PLC $\beta$  requires an acute (i.e. GPCR-induced) increase of intracellular IP<sub>3</sub>. To visualize Gi-GPCR-induced changes in IP<sub>3</sub> levels with and without Gq in real-time, we employed a BRET-sensor (Gulyás et al., 2015). In cells expressing Gq, activation of rGPR17 produced an immediate increase in IP<sub>3</sub> that was partially PTX-sensitive (Figure 30A). In line with our calcium- and IP<sub>1</sub>-data, this IP<sub>3</sub>-increase was entirely abrogated in cells treated with FR (Figure 30A) or lacking Gq (Figure 30B), and restored in cells expressing the crippled-auto-inhibition PLC $\beta$ 3 constructs (Figure 30B).

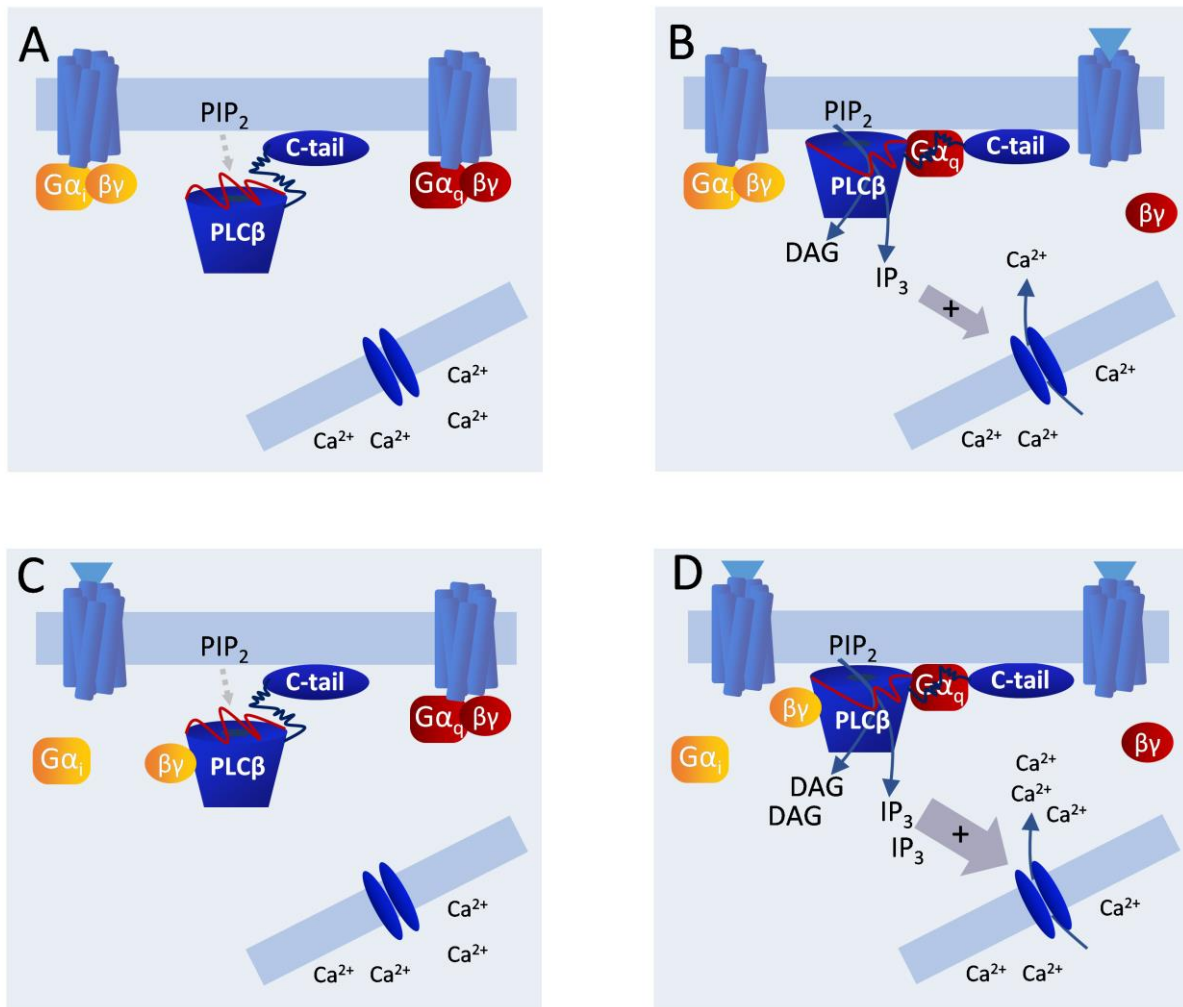


**Figure 31: Mechanistic model for Gi-Gβγ-PLCβ-calcium in living cells.** (A) In the resting state, PLCβ isozymes are strictly auto-inhibited by their XY-linker, which occludes the catalytic site and prevents substrate cleavage. The HTH motif located in the proximal C-terminal domain also contributes to this auto-inhibition by preventing repulsion of the XY-linker by the membrane interface. (B) Upon Gq-GPCR stimulation, the activated Gαq-GTP binds near the HTH motif and re-arranges PLCβ at the membrane. As a result, the XY linker is repulsed, revealing the catalytic site, and allowing substrate hydrolysis. (C) When a Gi-GPCR is stimulated, Gβγ is released from the heterotrimers and binds to PLCβ, but this does not sufficiently relieve auto-inhibition of the enzyme, and thus, no substrate cleavage occurs. (D) When the auto-inhibition of PLCβ is released by Gαq, Gi-Gβγ can induce further activation of PLCβ and thus subsequent calcium release.

### Mechanistic model for Gi-Gβγ-PLCβ-calcium in living cells

Taking all these findings together, we propose the following mechanistic model (Figure 31) of how Gi-Gβγ-PLCβ-signaling is triggered in living cells: in principle, Gi-Gβγ can activate PLCβ2 and PLCβ3 in living cells, even without Gq. However, because

## Results

PLC $\beta$  enzymes are strictly auto-inhibited (Figure 31A) and G $\beta\gamma$  does not sufficiently overcome this, there is no acute PLC $\beta$ -activation by Gi-G $\beta\gamma$  alone (Figure 31C). Therefore, G $\alpha_q$ -GTP (Figure 31B) (or a structural alteration of PLC $\beta$ ) is required to relieve this auto-inhibition and allow acute, GPCR-mediated Gi-G $\beta\gamma$ -PLC $\beta$  activation and subsequent Gi-calcium (Figure 31D).

Chapter 6: from HEK cells to physiological systems – is the Gq requirement conserved?

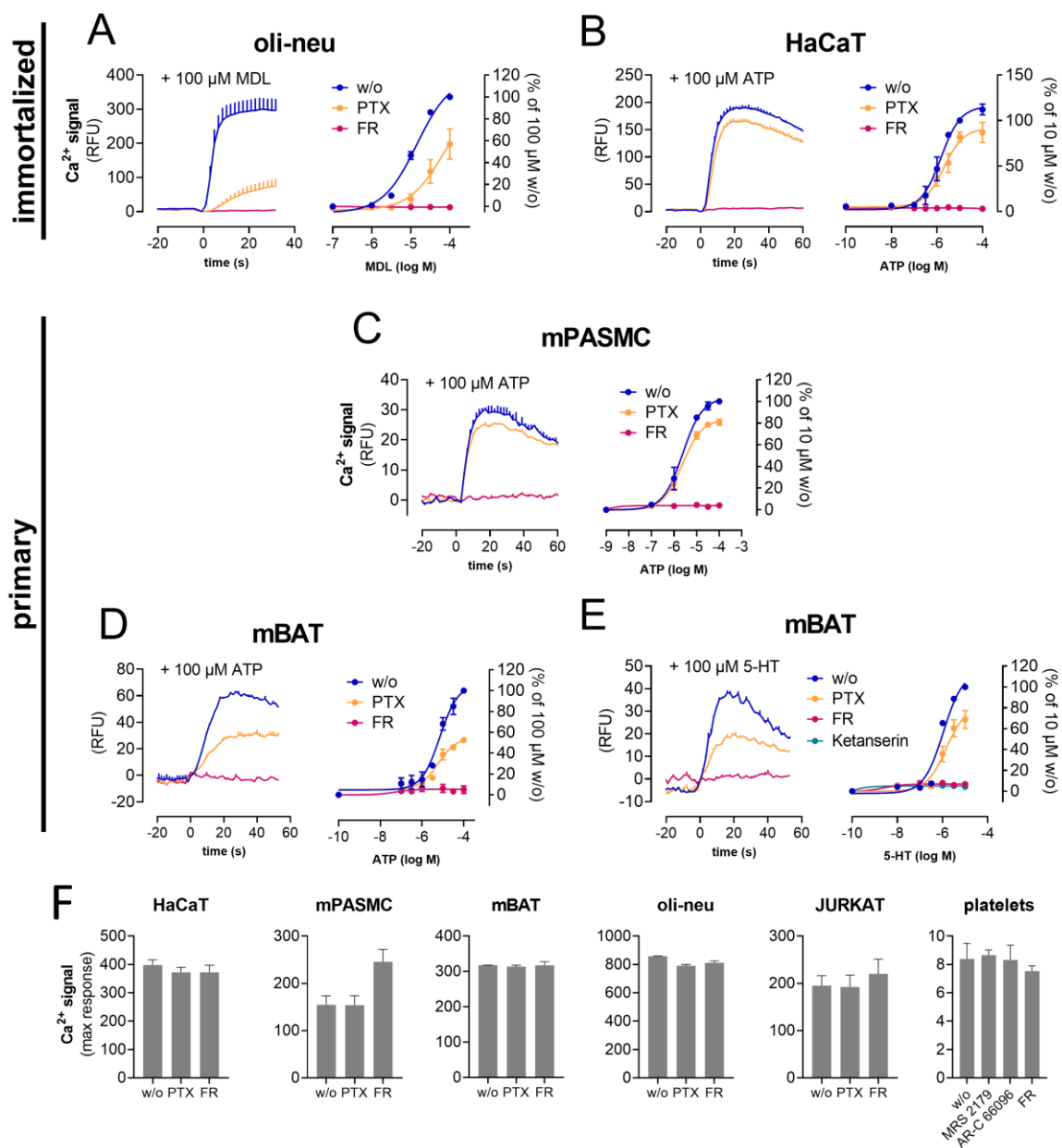


Figure 32: The Gq requirement for Gi-G $\beta\gamma$ -PLC $\beta$ -calcium is conserved across multiple cell types. (A-E) Mean + SEM of representative calcium kinetics (left panels), summarized as mean

± SEM of three biologically independent experiments (right panels). (A) In oli-neu cells, GPR17 stimulation with MDL29,951 induces calcium mobilization that is partially PTX-sensitive and completely abolished by FR. (B-D) In a human HaCaT cells (B), mouse pulmonary arterial smooth muscle cells (mPASMC, C) and mouse brown adipose tissue (D), ATP-mediated calcium release is partially PTX- yet completely FR sensitive. (E) 5-HT also induces partially PTX-sensitive calcium that is absent in FR-preincubated cells. (F) The viability control A23187, shown as mean + SEM of three biologically independent experiments, was intact across all cell types and treatment regimes.

### The Gq requirement for Gi-Gβγ-PLCβ-calcium is conserved across multiple cell types

So far, our investigations of Gq as a ‘master switch’ for Gi-calcium have been conducted in HEK cells. While HEK cells are a recombinant system that offers great advantages, such as easy culturing and transfection, and the availability of CRISPR/Cas9 generated KO cell lines, some doubt remains whether this cell line accurately represents the physiological situation. Thus, we were curious to see if other, more physiologically relevant cell lines would show the same Gq dependency for Gi-Gβγ-PLCβ-calcium. We selected a number of immortalized and primary cell lines from a wide range of physiological backgrounds to see if they share the Gq requirement for Gi-calcium. We started with GPCR stimuli that activate Gi and Gq simultaneously (Figure 32), testing if they would behave comparably to H1R and GPR17 in HEK cells. GPR17 is endogenously expressed in oli-neu cells (Simon et al., 2016), an immortalized neuronal cell line commonly used to investigate the behavior of oligodendrocytes. In this cell line, MDL29,951-stimulation elicited a partially PTX-sensitive calcium signal that was completely blocked in the presence of FR (Figure 32A), thus corroborating our HEK cell findings (Figure 6). Additionally, in the immortalized human keratinocyte cell line HaCaT, ATP triggered calcium via purinergic signaling, that was partially PTX-sensitive, but again fully blunted by FR (Figure 32B). A similar partially PTX-, but fully FR sensitive ATP-response was observed in primary mouse pulmonary arterial smooth muscle cells (mPASMC) (Figure 32C) and in primary brown preadipocytes isolated from mice (here mBAT, Figure 32D). The mBAT cells also responded with partially PTX-, fully FR-sensitive calcium release to serotonin (5-HT), which acted via endogenously expressed 5-HT<sub>2</sub> receptors, as it was fully blocked by 5-HT<sub>2</sub> antagonist ketanserin (Figure 32E). The viability control was intact across all cell lines and inhibitor treatment regimens (Figure 32F). In summary, all cell lines displayed Gi-calcium that was completely dependent on Gq. Indeed, Gq seems to be a ‘master switch’ for Gi-Gβγ-PLCβ-calcium in a variety of cell types and

## Results

organs, ranging from neuronal cells, to the immune system, to skin cells, metabolic tissue, and the cardiovascular system.

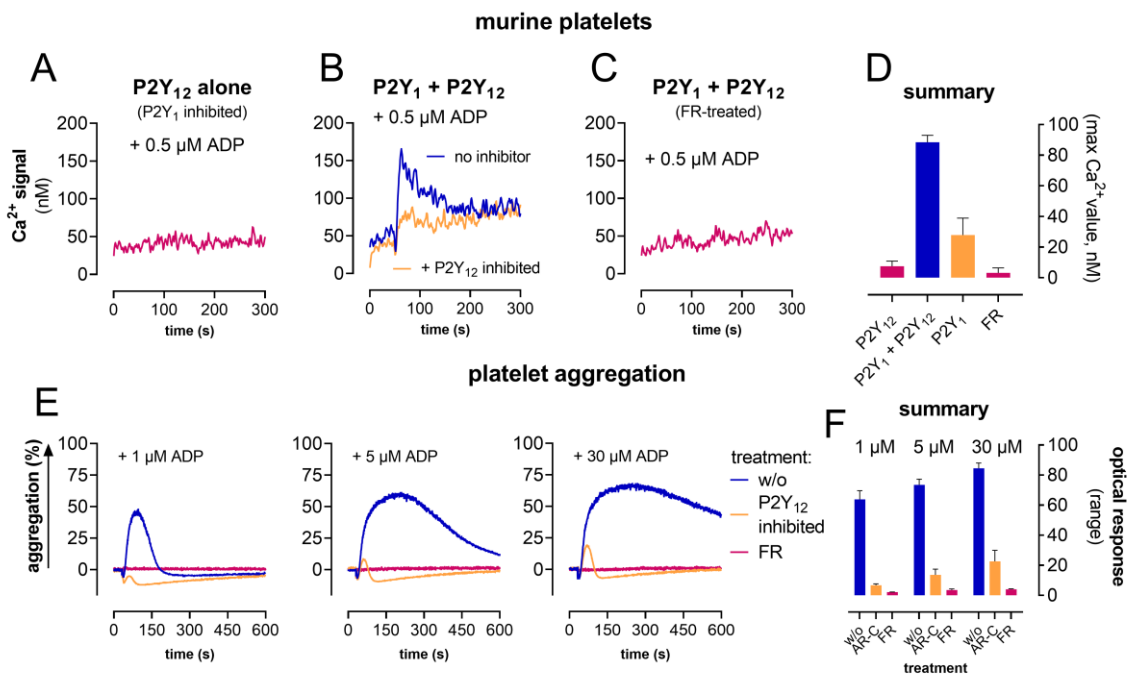


**Figure 33: platelet calcium and aggregation by Gi-coupled receptors requires Gq input.**

(A) In murine platelets, P2Y<sub>1</sub> and P2Y<sub>12</sub> agonist ADP was used in the presence of MRS 2179 to stimulate only Gi-coupled P2Y<sub>12</sub>. The representative kinetic shows no detectable calcium mobilization upon P2Y<sub>12</sub> stimulation. (B) When Gq-coupled P2Y<sub>1</sub> is not inhibited, ADP mediates calcium release that is partially blocked in the presence of P2Y<sub>12</sub> inhibitor AR-C. (C) In the presence of FR, no P2Y<sub>1</sub> + P2Y<sub>12</sub> dependent calcium is detectable. (D) Three biologically independent calcium mobilization experiments were summarized as mean + SEM. (E) Representative platelet aggregation measurements, summarized in (F), show no platelet aggregation via Gi-coupled P2Y<sub>12</sub> in the presence of FR, and only a slight shape-change via Gq-coupled P2Y<sub>1</sub> alone for all three employed ADP concentrations. When activated together, P2Y<sub>1</sub> and P2Y<sub>12</sub> induce robust platelet aggregation. All representative kinetics are shown as mean + SEM, summarized as mean + SEM of at least three biologically independent experiments.

### Platelet calcium and aggregation by Gi-coupled receptors requires Gq input

Next, we asked whether in a physiologically relevant system, specifically Gi-coupled GPCRs would require prestimulation of Gq-GPCRs to mobilize Gi-calcium. To test this hypothesis, we took advantage of primary murine platelets, the second-most abundant cell type in blood. Calcium mobilization is a crucial factor that regulates hemostasis and thrombosis (Mammadova-Bach et al., 2019). In this cell type, ADP mediates its biological effects via Gi-coupled P2Y<sub>12</sub> and Gq-coupled P2Y<sub>1</sub> receptors,

respectively (Gachet, 2012; Mangin et al., 2004; Hechler et al., 1998; Offermanns et al., 1997; Offermanns, 2006). To investigate the calcium mobilization via Gi-coupled P2Y<sub>12</sub> in isolation, we specifically blocked signaling via Gq-coupled P2Y<sub>1</sub> signaling with MRS 2179. As expected, ADP stimulation of Gi-coupled P2Y<sub>12</sub> did not elicit detectable calcium signals when platelets were pre-treated with the P2Y<sub>1</sub> inhibitor (Figure 33A). However, when Gq-coupled P2Y<sub>1</sub> was co-activated, we observed robust P2Y<sub>12</sub>-dependent calcium mobilization that was sensitive to inhibition via the P2Y<sub>12</sub>-specific inhibitor AR-C 66096 (Figure 33B). Entirely consistent with all earlier data, Gq inhibitor FR abolished the intracellular calcium rises including the Gi-component (Figure 33C, D).

Taken together, our results match with a myriad of previously published findings in a wide spectrum of cellular contexts (Gerwins & Fredholm, 1992; Okajima & Kondo, 1992; Dickenson & Hill, 1994; Buckley et al., 2001; Yeo et al., 2001; Werry et al., 2003b; Offermanns et al., 1997; Gao & Jacobson, 2016; Rives et al., 2009), and thus allows us to propose that the Gq requirement for Gi-βγ-calcium may likely be a unifying mechanism that governs the paradigmatic Gi-GPCR calcium pathway in living cells.

*Excursion 6.1: the role of G16 in the immune system*

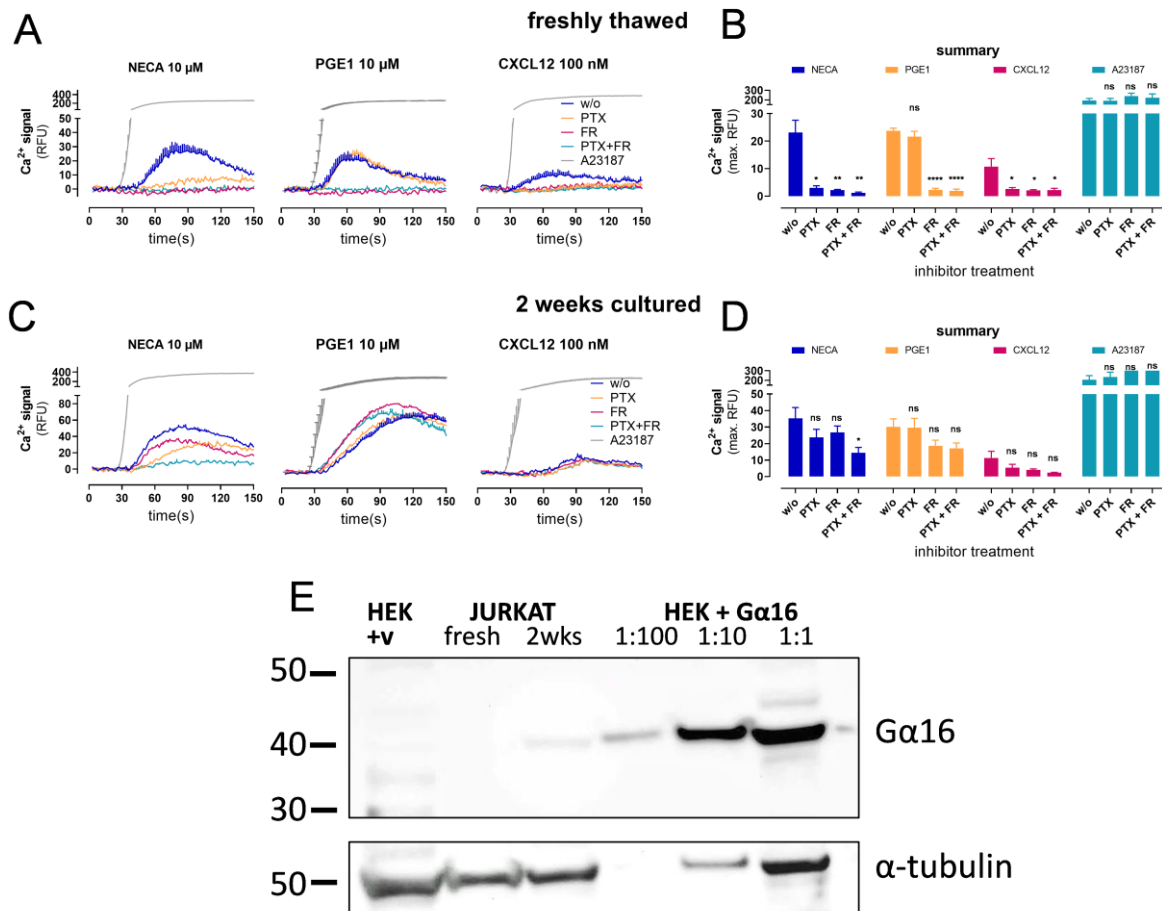


**Figure 34: G16 expression in JURKAT cells allows Gi-calcium.** (A) representative calcium kinetics of freshly thawed JURKAT cells show PTX-sensitive calcium mobilization in response to NECA and CXCL12 and Gi-independent calcium responses to PGE1. In all cases, the calcium mobilization is completely abolished by FR-treatment, and not inhibited further by a combination of PTX and FR. The summary of three independent experiments (B) shows a significant inhibition of NECA- and CXCL12-dependent calcium mobilization by PTX and FR treatment, and of PGE1-dependent calcium mobilization by FR, but no significant effect of either inhibitor on the viability control. (C, D) In JURKAT cells that have been cultured for at least two weeks, representative kinetics (C) and the summary of three independent experiments (D) show a loss sensitivity of the calcium responses to both PTX and FR. All data are displayed as mean + SEM. (B, D) A two-tailed student t-test was used to compare calcium values in the presence of inhibitor to those in the absence of inhibitor. P values were determined and P<0.05 depicted as (\*) if, P<0.01 as (\*\*), P<0.001 as (\*\*\*), and P<0.0001 as (\*\*\*\*). (E) A representative western blot comparing lysates from the cells used in (A, B) and (C, D) shows upregulation of Gα16 in cells that have been cultured longer. Lysates from HEK cells transfected with Gα16 were included as a positive control.



While investigating the Gq ‘master switch’ across multiple organs, we made a curious discovery. In JURKAT cells, an immortalized T-cell line chosen to represent immune-type cells, Gi-coupled A1 receptors stimulated with NECA, and CXCR4, mobilized calcium without prior Gq-stimulation (Figure 34A, B). These calcium responses were absent in PTX-treated cells, confirming their Gi-origin, and also completely blunted by FR, indicating Gq-dependency even though no additional Gq stimulus had been conducted. Even more remarkably, after a few weeks of cell culture, PTX- and FR-sensitivity was almost completely lost, with only the combination of both inhibitors visibly blunting the supposed “Gi-calcium” signal (Figure 34C, D). As we struggled to find an explanation that would reconcile these observations with our model of Gi-calcium (Figure 31), we specified two questions: In JURKAT cells, (i) why do Gi-coupled receptors mobilize calcium without an additional Gq stimulus, and (ii) why does the apparent Gi- and Gq-contribution decrease after prolonged cell culture? Regarding (i), since the Gi-calcium was still blocked by FR and thus clearly dependent on Gq, we reasoned that the required Gq activation was occurring without additional stimulation of Gq-GPCR. Since basal Gq-activity does not restore Gi-calcium very well (Figure 17), we hypothesized that A1 and CXCR4 must provide their own acute Gq-stimulation. Upon closer examination of the calcium data generated in freshly thawed cells, we noticed a slight remaining response to NECA in the presence of PTX that might represent this Gq-activation (Figure 34A). Out of the four Gq family members, these Gi-GPCRs most likely activate G16, a promiscuous G-protein that interacts with a wide variety of GPCRs (Offermanns & Simon, 1995). Indeed, immune cells are known to express G $\alpha$ 16 (Amatruda et al., 1991), and there are many speculations about its roles (Davignon et al., 2000; Su et al., 2009; Giannone et al., 2010). Thus, to check for G $\alpha$ 16 expression, we collected lysates from fresh and cultured JURKAT cells and performed a western blot. While G $\alpha$ 16 expression was undetectable in the fresh JURKAT cells, the cultured JURKAT cells showed a clear up-regulation of G $\alpha$ 16 (Figure 34E). This increased expression of a Gq family member is perfectly in line with decrease of the Gi-component (ii). Additionally, a loss of FR-inhibition (ii) is also expected, since G16 has very low sensitivity to FR. We tentatively concluded that, in cells that express G $\alpha$ 16, Gi-coupled receptors ‘bypass’ the need for a second receptor by generating their own Gq activation. This might be especially relevant in immune cells, which can express G $\alpha$ 16, and provides a great basis for future investigations.

# Discussion

## Gi-calcium requires Gq

For over 30 years, Gi-G $\beta\gamma$ -PLC $\beta$ -calcium has been considered an independent signaling paradigm (Sternweis & Smrcka, 1992; Smrcka & Sternweis, 1993; Cowen et al., 1990; Okajima & Ui, 1984; Goldman et al., 1985). However, despite the apparent clarity of the widely accepted mechanism behind this calcium mobilization, Gi-calcium has proven inexplicably variable and difficult to generate for a long time. Our investigation provides a mechanistic basis that explains this variability by demonstrating that the Gi-calcium signaling paradigm is entirely dependent on Gq activation. On a molecular level, Gq is required because, although Gi-G $\beta\gamma$  binds to PLC $\beta$ , this alone does not trigger an acute increase in substrate conversion. We find that this is because the auto-inhibition of PLC $\beta$  is not sufficiently released by G $\beta\gamma$ . Thus, PLC $\beta$  can be primed for G $\beta\gamma$  activation by G $\alpha_q$ -GTP, which relieves the auto-inhibition upon binding the enzyme (Lyon et al., 2011; Lyon et al., 2014; Charpentier et al., 2014). This investigation demonstrates that the required release of PLC $\beta$  auto-inhibition can be achieved by all four Gq subfamily members, namely G $\alpha_q$ , G $\alpha_{11}$ , G $\alpha_{14}$  and G $\alpha_{16}$ , or alternatively by the expression of PLC $\beta$  isoforms of impaired auto-inhibition. The Gq requirement for Gi-G $\beta\gamma$ -PLC $\beta$ -calcium exists for a variety of receptors in a variety of cellular backgrounds and affects at least one calcium-dependent physiological outcome, namely the aggregation of platelets in response to ADP.

## Literature discrepancy?

At first glance, it might seem that the Gq requirement for Gi-G $\beta\gamma$ -PLC $\beta$ -calcium described in this study is at odds with the general consensus in the literature, which portrays Gi-G $\beta\gamma$ -PLC $\beta$ -calcium as a stand-alone, fully competent signaling pathway (Kadamur & Ross, 2013; Smrcka, 2008). However, a dependency of Gi-G $\beta\gamma$ -PLC $\beta$ -calcium on Gq-coupled GPCRs has been shown by multiple findings across the past decades. Several older as well as recent studies demonstrated Gi-GPCR calcium that only occurs following stimulation of a Gq-GPCR (Okajima & Kondo, 1992; Okajima et al., 1993; Werry et al., 2003a, 2003b; Werry et al., 2002; Gerwins & Fredholm, 1992; Dickenson & Hill, 1994; Chan et al., 2000). Another study has demonstrated a lack of chemokine receptor calcium in Gq-deficient cell types (Shi et al., 2007). There are also a number of findings showing that Gi-G $\beta\gamma$  only activates PLC $\beta$ -‘cleaved C-tail’ variants

(Werry et al., 2003b). At the time, this was interpreted to indicate that the C-terminus of PLC $\beta$  covered the G $\beta\gamma$  binding site, and therefore, removal by cleavage or Gq-binding was required for Gi-G $\beta\gamma$ -calcium. However, it is now clear that these ‘cleaved c-tail’-PLC $\beta$  variants lack the auto-inhibitory HTH domain (Charpentier et al., 2014), making these findings entirely in line with the molecular model proposed by this study. With so many studies indicating Gq-dependency, the question arises why Gi-G $\beta\gamma$ -PLC $\beta$ -calcium has been viewed as ‘stand-alone’ until today.

Historically, our understanding of the ‘stand-alone’ Gi-G $\beta\gamma$ -PLC $\beta$ -calcium paradigm stems from two key observations that have been confirmed by many independent investigations (Smrcka, 2008): 1) calcium measurements in living cells that are blocked in the presence of the Gi-inhibitor PTX (Cowen et al., 1990; Okajima & Ui, 1984; Goldman et al., 1985), and 2) experiments conducted with purified proteins that show activation of PLC $\beta$  enzymes by G $\beta\gamma$ , but not G $\alpha_i$  (Boyer et al., 1992; Smrcka & Sternweis, 1993). Taken together, these findings demonstrate that Gi-coupled GPCRs mobilize calcium and that this occurs via Gi-G $\beta\gamma$ -dependent stimulation of PLC $\beta$ . Furthermore, because G $\beta\gamma$ -dependent PLC $\beta$  activation has been demonstrated by using purified proteins, i.e. in absence of G $\alpha_q$ , it has been concluded that this G-calcium pathway is a fully competent and independent pathway. However, while studies in the reconstituted system provide an elegant way to investigate the behavior of proteins in isolation, they do not always accurately predict the signaling outcome in living cells. In this case, activation of PLC $\beta$  with purified G $\beta\gamma$  has usually been measured as PLC $\beta$  substrate accumulation. In our study, we also detected an increase in IP $_1$  accumulation upon overexpression of G $\beta\gamma$  with PLC $\beta$  in absence of Gq, but this is insufficient to trigger the acute increase in IP $_3$  that is required for calcium mobilization. This finding is entirely in line with the well-known data in reconstituted systems, but also changes the predicted outcome in living cells.

Until recently, it has been difficult to investigate Gi-G $\beta\gamma$ -PLC $\beta$  activation and the subsequent calcium mobilization in living cells in isolation of Gq. The insight gained in this study has depended on the availability of the highly selective Gq inhibitors FR (Schrage et al., 2015) and its closely related derivative YM254890, as well as G $\alpha$ -KO cells, generated with CRISPR/Cas9 technology that lack G $\alpha_q$  and G $\alpha_{12/13}$  (Grundmann et al., 2018). The mechanism we have identified with the help of this newly available, cutting edge technology, that Gi-G $\beta\gamma$ -PLC $\beta$ -calcium requires Gq,

should not be understood as a contradiction, but rather an expansion of the long-known Gi-calcium paradigm.

### Gi-calcium might be more relevant than previously thought

Eukaryotic cells can express a wide range of calcium-sensitive proteins (Clapham, 2007), which is why a large variety of physiological functions are affected by calcium mobilization, i.e. the increase of cytosolic calcium concentrations. Thus, understanding the signaling routes that trigger calcium mobilization is of high interest to the scientific community. This study provides a crucial contribution to these efforts, because the expanded mechanistic model of the paradigmatic Gi-calcium pathway proposed in this study changes our perception of how Gi-GPCRs mobilize calcium. Up until this point, Gi-calcium has been considered especially relevant for chemokine receptors in immune cells. However, our results indicate that Gi calcium, or Gi-PLC $\beta$  signaling in general, might play a much larger physiological role than currently known. Together with many other findings (Okajima & Kondo, 1992; Okajima et al., 1993; Werry et al., 2003a, 2003b; Werry et al., 2002; Gerwins & Fredholm, 1992; Dickenson & Hill, 1994; Chan et al., 2000), we show that Gi-coupled GPCRs do not necessarily mobilize detectable calcium when stimulated in-vitro. Rather, an additional prior or concomitant Gq stimulus is required to allow detectable Gi-dependent calcium mobilization, thereby “unmasking” the Gi-GPCR’s capacity to trigger considerable calcium responses. Many investigations that aim to characterize the role of (Gi-)GPCRs use isolated cells, where the physiological environment, including potential external Gq-stimuli, is replaced by an inert buffer solution. It is plausible to assume that such studies have therefore frequently overlooked the capacity of Gi-GPCRs to mobilize calcium, despite its potentially high physiological relevance. With the knowledge of the Gq requirement for Gi-calcium that our mechanistic model provides, it will be easier to discover and understand calcium-dependent physiological roles of Gi-coupled receptors in a variety of cellular contexts in the future.

### G $\beta\gamma$ -calcium from other GPCRs?

Gi-GPCRs mobilize calcium because they release G $\beta\gamma$  which can activate PLC $\beta$ . However, the heterotrimeric G-proteins of other families also release G $\beta\gamma$  upon GPCR-activation, which raises the rather pressing question of why these are not considered to trigger PLC $\beta$ -calcium as well. Because of the high number of possible G $\beta\gamma$  subunit combinations that arises from the five G $\beta$ - and twelve G $\gamma$  subunits described to date

(Smrcka, 2008; McCudden et al., 2005; Khan et al., 2013), it is tempting to assume that the other G-protein families simply bind different G $\beta\gamma$  subunits and therefore activate different G $\beta\gamma$ -effectors. However, to date, there is not much evidence to suggest that each G $\alpha$  subunit preferentially binds a different set of G $\beta\gamma$  isoforms (McCudden et al., 2005; Smrcka, 2008; Dupré et al., 2009; Tennakoon et al., 2021; Masuho et al., 2021). Our data clearly shows that G $\beta 1\gamma 2$  subunits released from heterotrimeric Gq-proteins also bind to and potentially activate PLC $\beta 3$  upon stimulation of the Gq-coupled M3 receptor. This calls into question the hypothesis that only Gi-heterotrimers bind G $\beta\gamma$  subunit combinations that can activate the PLC $\beta$ -calcium-pathway. Of course, it is important to consider that all signaling components, including G $\alpha q$ , G $\beta 1$ , and G $\gamma 2$ , were overexpressed in the context of this experiment, making it difficult to draw conclusions on whether an interaction of Gq-G $\beta\gamma$  and PLC $\beta$  would occur at endogenous expression levels. In fact, several studies argue that because of the comparatively low potency of G $\beta\gamma$  at PLC $\beta$ , only G $\alpha i$  isoforms are endogenously expressed at sufficient levels to mobilize the high quantities of G $\beta\gamma$  required for PLC $\beta$  activation (Kadamur & Ross, 2013; Smrcka, 2008). However, without quantitative data on G $\alpha$  expression in every single eukaryotic cell, this remains speculation.

As mentioned above, a crucial factor in the discovery of Gi-calcium has been the long-available specific Gi-inhibitor PTX. It could be argued that with no other family-specific G-protein inhibitors available, discovering Gs-G $\beta\gamma$ - or G12/13-G $\beta\gamma$ -PLC $\beta$ -calcium in a physiologically relevant context would have been much more difficult to begin with. Thus, the well-accepted idea that Gi-GPCRs are the most relevant initiators of G $\beta\gamma$ -PLC $\beta$ -activation, or even G $\beta\gamma$ -signaling in general, might be at least in part based on a bias resulting from inhibitor availability. Another important factor in this context is the difficulty of generating G $\beta\gamma$ -PLC $\beta$ -calcium in isolated cells without applying Gq-stimulation that this study underlines. Finally, Gs, G12/13, and Gq are known to trigger calcium via G $\beta\gamma$ -independent mechanisms, which is why a potential G $\beta\gamma$ -PLC $\beta$ -dependent calcium response initiated by either of these G protein families might falsely be attributed to the previously described pathways, instead of being more closely investigated. In light of these points, reconsidering the notion of Gi-independent G $\beta\gamma$  signaling seems imperative. Interestingly, a number of thorough mechanistic investigations provide evidence that Gs-GPCRs mobilize calcium in a Gq-dependent, cAMP-independent manner (Stallaert et al., 2017), as well as following Gq

## Discussion

prestimulation (Werry et al., 2002). Now that it is clear that Gq activation is required to establish G $\beta\gamma$ -calcium, it will be interesting to reinvestigate the possibility that Gs- or G12/13-coupled GPCRs signal via this pathway as well. However, while these are intriguing speculations, there is only clear evidence for Gi-G $\beta\gamma$ -calcium at this point.

### Gi-calcium and G16

Conversely, because Gq allows Gi-GPCRs to mobilize calcium, a pressing question for future investigations will be where the Gq stimulus comes from and under which conditions it occurs in each physiological or disease-context. We have shown that the expression and up-regulation of G16 in JURKAT cells can meet the Gq requirement. Because G16 is promiscuous, i.e. can be activated by a wide range of GPCRs, including those that normally couple specifically to Gi but not Gq (Offermanns & Simon, 1995), this would help Gi-GPCRs provide their own Gq activation and allow them to mobilize Gi-dependent calcium without Gq prestimulation. This could be the reason why there are many accounts of Gi-calcium in immune cells, and why this pathway has thus been associated with this physiological system. Additionally, it is tempting to hypothesize that allowing Gi-coupled GPCRs such as chemokine receptors to trigger Gi-calcium without additional Gq-input could potentially be one physiological role of G16. This would be an interesting basis for future investigations, as the role of G16 for the immune system is not yet entirely clear. One investigation using G $\alpha 15^{-/-}$  mice has shown impaired cellular responses of immune cells, but no immunological phenotype (Davignon et al., 2000). Based on the results of our study, one might speculate that the isolated murine immune cells in this study require G16 for a full response, while in living mice, Gq-stimuli from surrounding cells and organs can compensate for the lack of G16 by providing prestimulation. While more investigations are necessary to draw any conclusion on the role of G16, its relevance for Gi-calcium could potentially be an interesting new starting point.

### Gq activation changes the signaling outcome of Gi-GPCRs

Other origins of Gq stimulation to allow Gi-calcium in a physiological context could be systems of inflammation (Sun & Ye, 2012). Surrounded by a variety of inflammatory mediators such as ATP or prostaglandins, the cellular response to Gi-stimuli might change from cAMP- to Gi-calcium-dependent signaling. Other sources of constitutive Gq activation could be viral infection or oncogenic mutations. The HCMV, a virus that has a prevalence of over 50% within the German population (Lachmann et al., 2018), encodes four GPCRs, at least two of which are constitutively active and Gq-coupled

(Vischer et al., 2006). Expression of the human chemokine receptor CCR1 has been shown to induce NF- $\kappa$ B activation only in cells expressing the constitutively active, Gq coupled human cytomegalovirus (HCMV)-encoded GPCR US28 (Bakker et al., 2004). Because NF- $\kappa$ B activation is PKC- and thus calcium-dependent, this finding provides an example of how constitutive Gq-activation of viral origin can change the signaling outcome of Gi-coupled receptors. Constitutive Gq activation is also a hallmark of some types of cancers. For instance, over 90% of patients with uveal melanoma, the most common cancer of the adult eye, carry a mutation in their genes expressing either Gq or G11 that leads to constitutive activity of the respective Gq family subunit (Kostenis et al., 2020, and references therein). We have shown that cells carrying this mutation can mobilize calcium in response to Gi without requiring Gq prestimulation. Thus, in these types of cancer, the outcome of Gi-signaling might be changed.

These are but a few speculations around how Gq control of Gi-calcium comes into play in a physiological or pathophysiological setting. They illustrate how the mechanistic model provided by this study will help identify the physiological role of Gi-GPCRs, support the interpretation of crosstalk events between Gi- and Gq-signaling, and facilitate the prediction of Gi-GPCR signaling outcomes.

### Gq inhibitors might appear to be unspecific.

One publication that provided a crucial basis for this study was the recent investigation of FR's specificity by Gao and Jacobsen (Gao & Jacobson, 2016). In their study, the aim of which was to test specificity of FR for G $\alpha$  vs. G $\beta\gamma$  signaling, they selected Gi-G $\beta\gamma$ -PLC $\beta$ -dependent IP $_1$  accumulation and calcium mobilization as their main readout for G $\beta\gamma$  activation. Their observation that FR fully abolished Gi-G $\beta\gamma$ -dependent PLC $\beta$  activation and calcium, but not G $\alpha_i$ -dependent cAMP depression, understandably led the authors to conclude that FR might be a G $\beta\gamma$  inhibitor. In our study, we clearly show that this is not the case, because a) FR does not inhibit, and in some cases even enhances, Gi-G $\beta\gamma$ -GIRK activation, and b) Gi-G $\beta\gamma$ -PLC $\beta$ -calcium is also absent in HEK- $\Delta$ Gq/11 cells, where no FR was applied, because this pathway is Gq-dependent. Thus, while the Gq inhibitor FR appeared to be unspecific in their study, in reality it abolishes Gi-calcium because the Gi-G $\beta\gamma$ - and Gq-calcium pathway are interdependent.

For a similar reason, a recent study of the Gq inhibitor YM-254890 (Peng et al., 2021), which is closely related to FR, has concluded that it additionally inhibits Gs. In this case, the authors measured Gs-dependent cAMP accumulation and observed a

## Discussion

considerable inhibition in the presence of YM-254890. Again, this is entirely in line with our data, which shows a reduction in GPR17-dependent cAMP accumulation in the presence of FR. However, again, this is not because the inhibitors are off-target, but rather because Gs-mediated cAMP accumulation occurs via calcium- and PKC-sensitive adenylyl cyclases (Halls & Cooper, 2011). There are many more examples of how multiple pathways contribute toward the same signaling outcome (Sunahara et al., 1996; Halls & Cooper, 2011; Gupte et al., 2017; Luttrell et al., 1999; Grundmann et al., 2018; Oligny-Longpré et al., 2012; Chang & Karin, 2001) and oftentimes, it is a matter of perspective which component ‘drives’ the signal: does Gi-Gβγ-PLCβ-calcium depend on Gq, or does Gi-Gβγ boost Gq-calcium? Regardless, the two above-mentioned cases underline the importance of understanding crosstalk mechanisms, such as the one described in this study, in order to guide data interpretation and hypothesis-based research.

## Implications for drug development

The hierarchical control of Gq over this Gi-pathway indicates that any drug that activates or inhibits Gq signaling could potentially affect the function of Gi-GPCRs as well. This is highly relevant information, because around 30% of FDA-approved drugs target GPCRs directly (Hauser et al., 2017), many of which specifically activate or inhibit Gq-GPCRs. Additionally, the Gq inhibitor FR, which blocks all Gq signaling downstream of GPCRs, is emerging as a potential basis for a therapeutic tool (Klepac et al., 2016; Matthey et al., 2017; Annala et al., 2019; Kostenis et al., 2020). The inhibitor has shown promising results in studies on adipose tissue (Klepac et al., 2016), asthma (Matthey et al., 2017) and cancer (Kostenis et al., 2020) among others. The knowledge provided in this study will help understand and predict potential, formerly ‘unexpected’ (side) effects of such drugs on Gi-calcium signaling, and thus be of great use in the development of new treatment options.

## Conclusion

In conclusion, the molecular mechanism of Gq-dependent Gi-GPCR calcium uncovered in this study i) provides the missing piece to explain why Gi-calcium can be highly variable and difficult to generate, ii) thereby reconciles a diverse range of complementary and even seemingly contradictory findings from the past three decades, iii) provides an interesting basis for future investigations in several physiological fields, and iv) is of high relevance for GPCR-centered drug research and development.



# Summary

The mobilization of calcium is an essential regulator relevant to all facets of eukaryotic life. Because of the wide range of cellular processes that calcium mobilization regulates, the question of how it is initiated in living cells has been of intense interest to the scientific community for many years. One long known, well-described signaling cascade that induces calcium mobilization is the Gi-GPCR-calcium paradigm. This paradigmatic signaling mechanism has been discovered over 30 years ago and describes how, upon activation of Gi-coupled GPCRs, G $\beta\gamma$  subunits released from heterotrimeric Gi proteins can activate the isoforms 2 and 3 of the PLC $\beta$  family, which in turn convert the membrane lipid PIP<sub>2</sub> into DAG and IP<sub>3</sub>. This is followed by an activation of IP<sub>3</sub>R, which are calcium channels located on the ER membrane and release calcium from the ER into the cytosol upon opening. While this signaling paradigm might seemingly dictate that activation of Gi-GPCRs should lead to calcium mobilization in all cells that express sufficient levels of the necessary components, i.e. heterotrimeric Gi-proteins, G $\beta\gamma$ -sensitive PLC $\beta$  enzymes, and IP<sub>3</sub>R on the ER membrane, Gi-GPCR-calcium has been surprisingly variable and sometimes inexplicably difficult to reproduce.

This study was based on the hypothesis that this Gi-G $\beta\gamma$ -PLC $\beta$ -calcium mechanism, which is considered an independent 'stand-alone' signaling pathway, has been unexpectedly variable because it is dependent on an unidentified factor. Indeed, many independent lines of research over the years suggest that this pathway is strongly influenced by Gq-coupled GPCRs, which also activate PLC $\beta$  via the G $\alpha_q$  subunit and thus mobilize calcium in a similar manner. Therefore, this work characterizes the interdependency of the Gi-GPCR-calcium and Gq-GPCR-calcium pathway, with the goal to determine the mechanism that controls Gi-G $\beta\gamma$ -PLC $\beta$ -calcium.

We combine well-established tools including the Gi-inhibitor PTX with the recently characterized specific Gq inhibitor FR and a set of newly available CRISPR/Cas9-edited cell lines that do not express G $\alpha_q$  isoforms. By using these in combination with a selection of GPCRs that couple to either Gi, Gq, or both, we investigate each step of the Gi-G $\beta\gamma$ -PLC $\beta$ -calcium cascade for a potential dependency on the Gq-pathway. We find that indeed, the Gi-G $\beta\gamma$ -PLC $\beta$ -calcium pathway, but not G $\alpha_i$ - or Gi-G $\beta\gamma$ -signaling in general, is entirely dependent on Gq. Furthermore, we discover that it is the active

## Summary

Gαq subunit, rather than the downstream consequences of Gq activation, that is required for Gi-Gβγ-PLCβ-calcium. On a molecular level, this is because Gi-derived Gβγ can bind to PLCβ but does not induce acute activation of the PLCβ-mediated conversion of PIP<sub>2</sub> into IP<sub>3</sub>. This is because PLCβ enzymes are strictly auto-inhibited in the inactive state by a molecular domain called the XY-linker, which covers the catalytic site of the enzyme to prevent binding of PIP<sub>2</sub>. Binding of Gβγ to PLCβ does not release the auto-inhibition sufficiently to achieve the acute increase in IP<sub>3</sub> production required for calcium mobilization. However, if the auto-inhibition of PLCβ is artificially removed by deletion or mutational disturbance of the auto-inhibitory domains (PLCβ3<sup>ΔXY</sup> or PLCβ3<sup>F715A</sup>), or by binding of active Gαq to the enzyme, Gi-Gβγ can activate PLCβ to induce calcium mobilization. We also demonstrate that despite being insufficient to induce acute PLCβ activation, Gβγ can increase long-term basal PLCβ-dependent IP<sub>1</sub> accumulation upon overexpression of both in absence of Gq. This explains why 30 years ago, when this pathway was first discovered upon mixing purified Gβγ with PLCβ and measuring hydrolysis product in absence of Gq, it was deemed to be Gq-independent. Finally, we demonstrate that the dependency of Gi-Gβγ-PLCβ-calcium on active Gαq is conserved across a wide variety of cellular systems, and involved in calcium-dependent physiological processes such as the aggregation of platelets in response to GPCR-stimulation.

The molecular mechanism proposed by this study provides the missing piece to the well-established Gi-calcium paradigm by underlining that this signaling cascade only occurs in the presence of active Gq and why so. It thereby not only sheds light on the previously unexplained variability of Gi-GPCR-calcium but also expands our general understanding of how Gi-GPCRs and Gq-GPCRs signal in synergy in living cells. Because GPCRs are a high-interest pharmacological target, this provides a highly relevant basis for future investigations across a wide field of physiological research as well as drug development. Additionally, as calcium mobilization controls a myriad of processes across all domains of eukaryotic life, the insight our study provides around how it can be initiated will hopefully lay the foundation for understanding and eventually manipulating many (patho-) physiological processes in human health and disease.

# References

- Alzayady, K.J., Wang, L., Chandrasekhar, R., Wagner, L.E., van Petegem, F., and Yule, D.I. (2016). Defining the stoichiometry of inositol 1,4,5-trisphosphate binding required to initiate Ca<sup>2+</sup> release. *Science signaling* *9*, ra35.
- Amatruda, T.T., Steele, D.A., Slepak, V.Z., and Simon, M.I. (1991). G alpha 16, a G protein alpha subunit specifically expressed in hematopoietic cells. *Proceedings of the National Academy of Sciences of the United States of America* *88*, 5587–5591.
- Annala, S., Feng, X., Shridhar, N., Eryilmaz, F., Patt, J., Yang, J., Pfeil, E.M., Cervantes-Villagrana, R.D., Inoue, A., Häberlein, F., Slodczyk, T., Reher, R., Kehraus, S., Monteleone, S., Schrage, R., Heycke, N., Rick, U., Engel, S., Pfeifer, A., Kolb, P., König, G., Bünemann, M., Tüting, T., Vázquez-Prado, J., Gutkind, J.S., Gaffal, E., and Kostenis, E. (2019). Direct targeting of G $\alpha$ q and G $\alpha$ 11 oncoproteins in cancer cells. *Science signaling* *12*.
- Atwood, B.K., Lopez, J., Wager-Miller, J., Mackie, K., and Straiker, A. (2011). Expression of G protein-coupled receptors and related proteins in HEK293, AtT20, BV2, and N18 cell lines as revealed by microarray analysis. *BMC genomics* *12*, 14.
- Bae, Y.-S., Lee, T.G., Park, J.C., Hur, J.H., Kim, Y., Heo, K., Kwak, J.-Y., Suh, P.-G., and Ryu, S.H. (2003). Identification of a compound that directly stimulates phospholipase C activity. *Molecular pharmacology* *63*, 1043–1050.
- Bakker, R.A., Casarosa, P., Timmerman, H., Smit, M.J., and Leurs, R. (2004). Constitutively active Gq/11-coupled receptors enable signaling by co-expressed G(i/o)-coupled receptors. *The Journal of Biological Chemistry* *279*, 5152–5161.
- Bastian, B.C. (2014). The molecular pathology of melanoma: an integrated taxonomy of melanocytic neoplasia. *Annual review of pathology* *9*, 239–271.
- Berridge, M.J., Bootman, M.D., and Roderick, H.L. (2003). Calcium signalling: dynamics, homeostasis and remodelling. *Nature reviews. Molecular cell biology* *4*, 517–529.
- Binti Mohd Amir, N.A.S., Mackenzie, A.E., Jenkins, L., Boustani, K., Hillier, M.C., Tsuchiya, T., Milligan, G., and Pease, J.E. (2018). Evidence for the Existence of a CXCL17 Receptor Distinct from GPR35. *Journal of immunology (Baltimore, Md. 1950)* *201*, 714–724.
- Boyer, J.L., Waldo, G.L., and Harden, T.K. (1992). Beta gamma-subunit activation of G-protein-regulated phospholipase C. *The Journal of Biological Chemistry* *267*, 25451–25456.
- Buckley, K.A., Wagstaff, S.C., McKay, G., Gaw, A., Hipskind, R.A., Bilbe, G., Gallagher, J.A., and Bowler, W.B. (2001). Parathyroid hormone potentiates nucleotide-induced Ca<sup>2+</sup> release in rat osteoblasts independently of Gq activation or cyclic monophosphate accumulation. A mechanism for localizing systemic responses in bone. *The Journal of Biological Chemistry* *276*, 9565–9571.
- Burgoyne, R.D. (2007). Neuronal calcium sensor proteins: generating diversity in neuronal Ca<sup>2+</sup> signalling. *Nature reviews. Neuroscience* *8*, 182–193.

## References

- Burns, D.L. (1988). Subunit structure and enzymic activity of pertussis toxin. *Microbiological sciences* 5, 285–287.
- Carafoli, E. (2004). Special issue: calcium signaling and disease. *Biochemical and biophysical research communications* 322, 1097.
- Carvajal, R.D., Schwartz, G.K., Tezel, T., Marr, B., Francis, J.H., and Nathan, P.D. (2017). Metastatic disease from uveal melanoma: treatment options and future prospects. *The British journal of ophthalmology* 101, 38–44.
- Chan, J.S., Lee, J.W., Ho, M.K., and Wong, Y.H. (2000). Preactivation permits subsequent stimulation of phospholipase C by G(i)-coupled receptors. *Molecular pharmacology* 57, 700–708.
- Chang, L., and Karin, M. (2001). Mammalian MAP kinase signalling cascades. *Nature* 410, 37–40.
- Charpentier, T.H., Waldo, G.L., Barrett, M.O., Huang, W., Zhang, Q., Harden, T.K., and Sondek, J. (2014). Membrane-induced allosteric control of phospholipase C- $\beta$  isozymes. *The Journal of Biological Chemistry* 289, 29545–29557.
- Clapham, D.E. (2007). Calcium signaling. *Cell* 131, 1047–1058.
- Cockcroft, S. (2006). The latest phospholipase C, PLCeta, is implicated in neuronal function. *Trends in biochemical sciences* 31, 4–7.
- Connor, M., and Henderson, G. (1996). delta- and mu-opioid receptor mobilization of intracellular calcium in SH-SY5Y human neuroblastoma cells. *British Journal of Pharmacology* 117, 333–340.
- Coward, P., Chan, S.D., Wada, H.G., Humphries, G.M., and Conklin, B.R. (1999). Chimeric G proteins allow a high-throughput signaling assay of Gi-coupled receptors. *Analytical biochemistry* 270, 242–248.
- Cowen, D.S., Baker, B., and Dubyak, G.R. (1990). Pertussis toxin produces differential inhibitory effects on basal, P2-purinergic, and chemotactic peptide-stimulated inositol phospholipid breakdown in HL-60 cells and HL-60 cell membranes. *Journal of Biological Chemistry* 265, 16181–16189.
- Dallanoce, C., Conti, P., Amici, M. de, Micheli, C. de, Barocelli, E., Chiavarini, M., Ballabeni, V., Bertoni, S., and Impicciatore, M. (1999). Synthesis and functional characterization of novel derivatives related to oxotremorine and oxotremorine-M. *Bioorganic & medicinal chemistry* 7, 1539–1547.
- Davignon, I., Catalina, M.D., Smith, D., Montgomery, J., Swantek, J., Croy, J., Siegelman, M., and Wilkie, T.M. (2000). Normal Hematopoiesis and Inflammatory Responses Despite Discrete Signaling Defects in G $\alpha$ 15 Knockout Mice. *Molecular and cellular biology* 20, 797–804.
- Dickenson, J.M., and Hill, S.J. (1994). Interactions between adenosine A1- and histamine H1-receptors. *The International journal of biochemistry* 26, 959–969.
- Dixon, A.S., Schwinn, M.K., Hall, M.P., Zimmerman, K., Otto, P., Lubben, T.H., Butler, B.L., Binkowski, B.F., Machleidt, T., Kirkland, T.A., Wood, M.G., Eggers, C.T., Encell, L.P., and Wood, K.V. (2016). NanoLuc Complementation Reporter Optimized for

- Accurate Measurement of Protein Interactions in Cells. *ACS chemical biology* *11*, 400–408.
- Dupré, D.J., Robitaille, M., Rebois, R.V., and Hébert, T.E. (2009). The role of Gbetagamma subunits in the organization, assembly, and function of GPCR signaling complexes. *Annual review of pharmacology and toxicology* *49*, 31–56.
- Fan, G.H., Yang, W., Sai, J., and Richmond, A. (2001). Phosphorylation-independent association of CXCR2 with the protein phosphatase 2A core enzyme. *The Journal of Biological Chemistry* *276*, 16960–16968.
- Feske, S. (2007). Calcium signalling in lymphocyte activation and disease. *Nature reviews. Immunology* *7*, 690–702.
- Filtz, T.M., Cunningham, M.L., Stanig, K.J., Paterson, A., and Harden, T.K. (1999). Phosphorylation by protein kinase C decreases catalytic activity of avian phospholipase C-beta. *Biochemical Journal* *338*, 257–264.
- Gachet, C. (2012). P2Y(12) receptors in platelets and other hematopoietic and non-hematopoietic cells. *Purinergic Signalling* *8*, 609–619.
- Gao, Z.-G., and Jacobson, K.A. (2016). On the selectivity of the G $\alpha$ q inhibitor UBO-QIC: A comparison with the G $\alpha$ i inhibitor pertussis toxin. *Biochemical pharmacology* *107*, 59–66.
- Gerwins, P., and Fredholm, B.B. (1992). Stimulation of adenosine A1 receptors and bradykinin receptors, which act via different G proteins, synergistically raises inositol 1,4,5-trisphosphate and intracellular free calcium in DDT1 MF-2 smooth muscle cells. *Proceedings of the National Academy of Sciences of the United States of America* *89*, 7330–7334.
- Giannone, F., Malpeli, G., Lisi, V., Grasso, S., Shukla, P., Ramarli, D., Sartoris, S., Monsurró, V., Krampera, M., Amato, E., Tridente, G., Colombatti, M., Parenti, M., and Innamorati, G. (2010). The puzzling uniqueness of the heterotrimeric G15 protein and its potential beyond hematopoiesis. *Journal of molecular endocrinology* *44*, 259–269.
- Goldman, D.W., Chang, F.H., Gifford, L.A., Goetzl, E.J., and Bourne, H.R. (1985). Pertussis toxin inhibition of chemotactic factor-induced calcium mobilization and function in human polymorphonuclear leukocytes. *The Journal of experimental medicine* *162*, 145–156.
- Gresset, A., Hicks, S.N., Harden, T.K., and Sondek, J. (2010). Mechanism of phosphorylation-induced activation of phospholipase C-gamma isozymes. *The Journal of Biological Chemistry* *285*, 35836–35847.
- Grundmann, M., Merten, N., Malfacini, D., Inoue, A., Preis, P., Simon, K., Rüttiger, N., Ziegler, N., Benkel, T., Schmitt, N.K., Ishida, S., Müller, I., Reher, R., Kawakami, K., Inoue, A., Rick, U., Köhl, T., Imhof, D., Aoki, J., König, G.M., Hoffmann, C., Gomeza, J., Wess, J., and Kostenis, E. (2018). Lack of beta-arrestin signaling in the absence of active G proteins. *Nature communications* *9*, 341.

## References

- Grynkiewicz, G., Poenie, M., and Tsien, R.Y. (1985). A new generation of Ca<sup>2+</sup> indicators with greatly improved fluorescence properties. *The Journal of Biological Chemistry* *260*, 3440–3450.
- Gulyás, G., Tóth, J.T., Tóth, D.J., Kurucz, I., Hunyady, L., Balla, T., and Várnai, P. (2015). Measurement of Inositol 1,4,5-Trisphosphate in Living Cells Using an Improved Set of Resonance Energy Transfer-Based Biosensors. *PloS one* *10*.
- Gupte, T.M., Malik, R.U., Sommese, R.F., Ritt, M., and Sivaramakrishnan, S. (2017). Priming GPCR signaling through the synergistic effect of two G proteins. *Proceedings of the National Academy of Sciences of the United States of America* *114*, 3756–3761.
- Halls, M.L., and Cooper, D.M.F. (2011). Regulation by Ca<sup>2+</sup>-signaling pathways of adenylyl cyclases. *Cold Spring Harbor perspectives in biology* *3*, a004143.
- Hauser, A.S., Attwood, M.M., Rask-Andersen, M., Schiöth, H.B., and Gloriam, D.E. (2017). Trends in GPCR drug discovery: new agents, targets and indications. *Nature reviews. Drug discovery* *16*, 829–842.
- Hechler, B., Eckly, A., Ohlmann, P., Cazenave, J.P., and Gachet, C. (1998). The P2Y1 receptor, necessary but not sufficient to support full ADP-induced platelet aggregation, is not the target of the drug clopidogrel. *British journal of haematology* *103*, 858–866.
- Hicks, S.N., Jezyk, M.R., Gershburg, S., Seifert, J.P., Harden, T.K., and Sondek, J. (2008). General and versatile autoinhibition of PLC isozymes. *Molecular cell* *31*, 383–394.
- Hill-Eubanks, D.C., Werner, M.E., Heppner, T.J., and Nelson, M.T. (2011). Calcium signaling in smooth muscle. *Cold Spring Harbor perspectives in biology* *3*, a004549.
- Inoue, A., Raimondi, F., Kadji, F.M.N., Singh, G., Kishi, T., Uwamizu, A., Ono, Y., Shinjo, Y., Ishida, S., Arang, N., Kawakami, K., Gutkind, J.S., Aoki, J., and Russell, R.B. (2019). Illuminating G-Protein-Coupling Selectivity of GPCRs. *Cell* *177*, 1933-1947.e25.
- Kadamur, G., and Ross, E.M. (2013). Mammalian phospholipase C. *Annual review of physiology* *75*, 127–154.
- Katan, M., and Cockcroft, S. (2020). Phospholipase C families: Common themes and versatility in physiology and pathology. *Progress in lipid research* *80*, 101065.
- Khan, S.M., Sleno, R., Gora, S., Zylbergold, P., Laverdure, J.P., Labbé, J.C., Miller, G.J., and Hébert, T.E. (2013). The expanding roles of G  $\beta$   $\gamma$  subunits in G protein-coupled receptor signaling and drug action. *Pharmacological reviews* *65*.
- Klec, C., Ziomek, G., Pichler, M., Malli, R., and Graier, W.F. (2019). Calcium Signaling in  $\beta$ -cell Physiology and Pathology: A Revisit. *International journal of molecular sciences* *20*.
- Klepac, K., Kilić, A., Gnad, T., Brown, L.M., Herrmann, B., Wilderman, A., Balkow, A., Glöde, A., Simon, K., Lidell, M.E., Betz, M.J., Enerbäck, S., Wess, J., Freichel, M., Blüher, M., König, G., Kostenis, E., Insel, P.A., and Pfeifer, A. (2016). The Gq

signalling pathway inhibits brown and beige adipose tissue. *Nature communications* 7, 10895.

Kostenis, E., Pfeil, E.M., and Annala, S. (2020). Heterotrimeric Gq proteins as therapeutic targets? *The Journal of Biological Chemistry* 295, 5206–5215.

Krebs, K.M., Pfeil, E.M., Simon, K., Grundmann, M., Häberlein, F., Bautista-Aguilera, O.M., Gütschow, M., Weaver, C.D., Fleischmann, B.K., and Kostenis, E. (2018). Label-Free Whole Cell Biosensing for High-Throughput Discovery of Activators and Inhibitors Targeting G Protein-Activated Inwardly Rectifying Potassium Channels. *ACS Omega* 3, 14814–14823.

Lachmann, R., Loenenbach, A., Waterboer, T., Brenner, N., Pawlita, M., Michel, A., Thamm, M., Poethko-Müller, C., Wichmann, O., and Wiese-Posselt, M. (2018). Cytomegalovirus (CMV) seroprevalence in the adult population of Germany. *PloS one* 13.

Li, Z., Jiang, H., Xie, W., Zhang, Z., Smrcka, A.V., and Wu, D. (2000). Roles of PLC-beta2 and -beta3 and PI3Kgamma in chemoattractant-mediated signal transduction. *Science (New York, N.Y.)* 287, 1046–1049.

Luke, J.J., Triozzi, P.L., McKenna, K.C., van Meir, E.G., Gershenwald, J.E., Bastian, B.C., Gutkind, J.S., Bowcock, A.M., Streicher, H.Z., Patel, P.M., Sato, T., Sossman, J.A., Sznol, M., Welch, J., Thurin, M., Selig, S., Flaherty, K.T., and Carvajal, R.D. (2015). Biology of advanced uveal melanoma and next steps for clinical therapeutics. *Pigment cell & melanoma research* 28, 135–147.

Lüscher, C., and Slesinger, P.A. (2010). Emerging roles for G protein-gated inwardly rectifying potassium (GIRK) channels in health and disease. *Nature reviews. Neuroscience* 11, 301–315.

Luttrell, L.M., Ferguson, S.S., Daaka, Y., Miller, W.E., Maudsley, S., Della Rocca, G.J., Lin, F., Kawakatsu, H., Owada, K., Luttrell, D.K., Caron, M.G., and Lefkowitz, R.J. (1999). Beta-arrestin-dependent formation of beta2 adrenergic receptor-Src protein kinase complexes. *Science (New York, N.Y.)* 283, 655–661.

Lyon, A.M., Begley, J.A., Manett, T.D., and Tesmer, J.J.G. (2014). Molecular mechanisms of phospholipase C  $\beta$  3 autoinhibition. *Structure (London, England 1993)* 22, 1844–1854.

Lyon, A.M., Tesmer, V.M., Dhamsania, V.D., Thal, D.M., Gutierrez, J., Chowdhury, S., Suddala, K.C., Northup, J.K., and Tesmer, J.J.G. (2011). An Autoinhibitory Helix in the C-Terminal Region of Phospholipase C- $\beta$  Mediates G  $\alpha$  q Activation. *Nature structural & molecular biology* 18, 999–1005.

Mammadova-Bach, E., Nagy, M., Heemskerk, J.W.M., Nieswandt, B., and Braun, A. (2019). Store-operated calcium entry in thrombosis and thrombo-inflammation. *Cell calcium* 77, 39–48.

Mangin, P., Ohlmann, P., Eckly, A., Cazenave, J.-P., Lanza, F., and Gachet, C. (2004). The P2Y1 receptor plays an essential role in the platelet shape change induced by collagen when TxA2 formation is prevented. *Journal of thrombosis and haemostasis JTH* 2, 969–977.

## References

- Masuhō, I., Skamangas, N.K., Muntean, B.S., and Martemyanov, K.A. (2021). Diversity of the G $\beta\gamma$  complexes defines spatial and temporal bias of GPCR signaling. *Cell systems*.
- Matthey, M., Roberts, R., Seidinger, A., Simon, A., Schröder, R., Kuschak, M., Annala, S., König, G.M., Müller, C.E., Hall, I.P., Kostenis, E., Fleischmann, B.K., and Wenzel, D. (2017). Targeted inhibition of Gq signaling induces airway relaxation in mouse models of asthma. *Science translational medicine* *9*.
- McCudden, C.R., Hains, M.D., Kimple, R.J., Siderovski, D.P., and Willard, F.S. (2005). G-protein signaling: back to the future. *Cellular and molecular life sciences CMLS* *62*, 551–577.
- Megson, A.C., Dickenson, J.M., Townsend-Nicholson, A., and Hill, S.J. (1995). Synergy between the inositol phosphate responses to transfected human adenosine A1-receptors and constitutive P2-purinoceptors in CHO-K1 cells. *British Journal of Pharmacology* *115*, 1415–1424.
- Milligan, G., and Inoue, A. (2018). Genome Editing Provides New Insights into Receptor-Controlled Signalling Pathways. *Trends in pharmacological sciences* *39*, 481–493.
- Nasser, M.W., Raghuwanshi, S.K., Grant, D.J., Jala, V.R., Rajarathnam, K., and Richardson, R.M. (2009). Differential activation and regulation of CXCR1 and CXCR2 by CXCL8 monomer and dimer. *Journal of immunology (Baltimore, Md. 1950)* *183*, 3425–3432.
- Nesbitt, W.S., Giuliano, S., Kulkarni, S., Dopheide, S.M., Harper, I.S., and Jackson, S.P. (2003). Intercellular calcium communication regulates platelet aggregation and thrombus growth. *The Journal of cell biology* *160*, 1151–1161.
- Offermanns, S. (2006). Activation of platelet function through G protein-coupled receptors. *Circulation research* *99*, 1293–1304.
- Offermanns, S., and Simon, M.I. (1995). G alpha 15 and G alpha 16 couple a wide variety of receptors to phospholipase C. *The Journal of Biological Chemistry* *270*, 15175–15180.
- Offermanns, S., Toombs, C.F., Hu, Y.H., and Simon, M.I. (1997). Defective platelet activation in G alpha(q)-deficient mice. *Nature* *389*, 183–186.
- Okajima, F., and Kondo, Y. (1992). Synergism in cytosolic Ca<sup>2+</sup> mobilization between bradykinin and agonists for pertussis toxin-sensitive G-protein-coupled receptors in NG 108-15 cells. *FEBS letters* *301*, 223–226.
- Okajima, F., Tomura, H., and Kondo, Y. (1993). Enkephalin activates the phospholipase C/Ca<sup>2+</sup> system through cross-talk between opioid receptors and P2-purinergic or bradykinin receptors in NG 108-15 cells. A permissive role for pertussis toxin-sensitive G-proteins. *Biochemical Journal* *290*, 241–247.
- Okajima, F., and Ui, M. (1984). ADP-ribosylation of the specific membrane protein by islet-activating protein, pertussis toxin, associated with inhibition of a chemotactic peptide-induced arachidonate release in neutrophils. A possible role of the toxin



substrate in Ca<sup>2+</sup>-mobilizing biosignaling. *Journal of Biological Chemistry* 259, 13863–13871.

Oldham, W.M., and Hamm, H.E. (2008). Heterotrimeric G protein activation by G-protein-coupled receptors. *Nature reviews. Molecular cell biology* 9, 60–71.

Oligny-Longpré, G., Corbani, M., Zhou, J., Hogue, M., Guillon, G., and Bouvier, M. (2012). Engagement of  $\beta$ -arrestin by transactivated insulin-like growth factor receptor is needed for V2 vasopressin receptor-stimulated ERK1/2 activation. *Proceedings of the National Academy of Sciences of the United States of America* 109, E1028-37.

Peng, Q., Alqahtani, S., Nasrullah, M.Z.A., and Shen, J. (2021). Functional evidence for biased inhibition of G protein signaling by YM-254890 in human coronary artery endothelial cells. *European journal of pharmacology* 891, 173706.

Pfeil, E.M., Brands, J., Merten, N., Vögtle, T., Vescovo, M., Rick, U., Im Albrecht, Heycke, N., Kawakami, K., Ono, Y., Ngako, K.F.M., Hiratsuka, S., Aoki, J., Häberlein, F., Matthey, M., Garg, J., Hennen, S., Jobin, M.L., Seier, K., Calebiro, D., Pfeifer, A., Heinemann, A., Wenzel, D., König, G.M., Nieswandt, B., Fleischmann, B.K., Inoue, A., Simon, K., and Kostenis, E. (2020). Heterotrimeric G Protein Subunit G $\alpha$ q Is a Master Switch for G $\beta$   $\gamma$ -Mediated Calcium Mobilization by Gi-Coupled GPCRs. *Molecular cell* 80.

Philip, F., Kadamur, G., Silos, R.G., Woodson, J., and Ross, E.M. (2010). Synergistic activation of phospholipase C-beta3 by G $\alpha$ (q) and Gbetagamma describes a simple two-state coincidence detector. *Current biology CB* 20, 1327–1335.

Premack, B.A., and Schall, T.J. (1996). Chemokine receptors: gateways to inflammation and infection. *Nature medicine* 2, 1174–1178.

Prole, D.L., and Taylor, C.W. (2019). Structure and Function of IP3 Receptors. *Cold Spring Harbor perspectives in biology* 11.

Putney, J.W. (2005). Capacitative calcium entry: sensing the calcium stores. *The Journal of cell biology* 169, 381–382.

Ravindranathan, A., Joslyn, G., Robertson, M., Schuckit, M.A., Whistler, J.L., and White, R.L. (2009). Functional characterization of human variants of the mu-opioid receptor gene. *Proceedings of the National Academy of Sciences of the United States of America* 106, 10811–10816.

Rebres, R.A., Roach, T.I.A., Fraser, I.D.C., Philip, F., Moon, C., Lin, K.-M., Liu, J., Santat, L., Cheadle, L., Ross, E.M., Simon, M.I., and Seaman, W.E. (2011). Synergistic Ca<sup>2+</sup> responses by G $\alpha$ i- and G $\alpha$ q-coupled G-protein-coupled receptors require a single PLC $\beta$  isoform that is sensitive to both G $\beta$  $\gamma$  and G $\alpha$ q. *The Journal of Biological Chemistry* 286, 942–951.

Rives, M.-L., Vol, C., Fukazawa, Y., Tinel, N., Trinquet, E., Ayoub, M.A., Shigemoto, R., Pin, J.-P., and Prézeau, L. (2009). Crosstalk between GABAB and mGlu1a receptors reveals new insight into GPCR signal integration. *The EMBO journal* 28, 2195–2208.

## References

- Rosenbaum, D.M., Rasmussen, S.G.F., and Kobilka, B.K. (2009). The structure and function of G-protein-coupled receptors. *Nature* 459, 356–363.
- Schmid, C.L., Streicher, J.M., Groer, C.E., Munro, T.A., Zhou, L., and Bohn, L.M. (2013). Functional selectivity of 6'-guanidinonaltrindole (6'-GNTI) at  $\kappa$ -opioid receptors in striatal neurons. *The Journal of Biological Chemistry* 288, 22387–22398.
- Schrage, R., Schmitz, A.-L., Gaffal, E., Annala, S., Kehraus, S., Wenzel, D., Büllsbach, K.M., Bald, T., Inoue, A., Shinjo, Y., Galandrin, S., Shridhar, N., Hesse, M., Grundmann, M., Merten, N., Charpentier, T.H., Martz, M., Butcher, A.J., Slodczyk, T., Armando, S., Effern, M., Namkung, Y., Jenkins, L., Horn, V., Stößel, A., Dargatz, H., Tietze, D., Imhof, D., Galés, C., Drewke, C., Müller, C.E., Hölzel, M., Milligan, G., Tobin, A.B., Gomeza, J., Dohlman, H.G., Sondek, J., Harden, T.K., Bouvier, M., Laporte, S.A., Aoki, J., Fleischmann, B.K., Mohr, K., König, G.M., Tüting, T., and Kostenis, E. (2015). The experimental power of FR900359 to study Gq-regulated biological processes. *Nature communications* 6, 10156.
- Schröder, R., Janssen, N., Schmidt, J., Kebig, A., Merten, N., Hennen, S., Müller, A., Blättermann, S., Mohr-Andrä, M., Zahn, S., Wenzel, J., Smith, N.J., Gomeza, J., Drewke, C., Milligan, G., Mohr, K., and Kostenis, E. (2010). Deconvolution of complex G protein-coupled receptor signaling in live cells using dynamic mass redistribution measurements. *Nature biotechnology* 28, 943–949.
- Schröder, R., Merten, N., Mathiesen, J.M., Martini, L., Kruljac-Letunic, A., Krop, F., Blaukat, A., Fang, Y., Tran, E., Ulven, T., Drewke, C., Whistler, J., Pardo, L., Gomeza, J., and Kostenis, E. (2009). The C-terminal tail of CRTH2 is a key molecular determinant that constrains Galphai and downstream signaling cascade activation. *The Journal of Biological Chemistry* 284, 1324–1336.
- Schröder, R., Schmidt, J., Blättermann, S., Peters, L., Janssen, N., Grundmann, M., Seemann, W., Kaufel, D., Merten, N., Drewke, C., Gomeza, J., Milligan, G., Mohr, K., and Kostenis, E. (2011). Applying label-free dynamic mass redistribution technology to frame signaling of G protein-coupled receptors noninvasively in living cells. *Nature protocols* 6, 1748–1760.
- Sedej, M., Schröder, R., Bell, K., Platzer, W., Vukoja, A., Kostenis, E., Heinemann, A., and Waldhoer, M. (2012). D-type prostanoid receptor enhances the signaling of chemoattractant receptor-homologous molecule expressed on T(H)2 cells. *The Journal of allergy and clinical immunology* 129, 492-500, 500.e1-9.
- Shi, G., Partida-Sánchez, S., Misra, R.S., Tighe, M., Borchers, M.T., Lee, J.J., Simon, M.I., and Lund, F.E. (2007). Identification of an alternative G $\alpha$ q-dependent chemokine receptor signal transduction pathway in dendritic cells and granulocytes. *The Journal of experimental medicine* 204, 2705–2718.
- Shihoya, W., Izume, T., Inoue, A., Yamashita, K., Kadji, F.M.N., Hirata, K., Aoki, J., Nishizawa, T., and Nureki, O. (2018). Crystal structures of human ETB receptor provide mechanistic insight into receptor activation and partial activation. *Nature communications* 9, 4711.
- Simon, K., Hennen, S., Merten, N., Blättermann, S., Gillard, M., Kostenis, E., and Gomeza, J. (2016). The Orphan G Protein-coupled Receptor GPR17 Negatively

- Regulates Oligodendrocyte Differentiation via  $G_{\alpha i/o}$  and Its Downstream Effector Molecules. *The Journal of Biological Chemistry* 291, 705–718.
- Singh, A.D., Turell, M.E., and Topham, A.K. (2011). Uveal melanoma: trends in incidence, treatment, and survival. *Ophthalmology* 118, 1881–1885.
- Sisley, K., Doherty, R., and Cross, N.A. (2011). What hope for the future? GNAQ and uveal melanoma. *The British journal of ophthalmology* 95, 620–623.
- Smrcka, A.V. (2008). G protein  $\beta \gamma$  subunits: central mediators of G protein-coupled receptor signaling. *Cellular and molecular life sciences CMLS* 65, 2191–2214.
- Smrcka, A.V., and Sternweis, P.C. (1993). Regulation of purified subtypes of phosphatidylinositol-specific phospholipase C beta by G protein alpha and beta gamma subunits. *The Journal of Biological Chemistry* 268, 9667–9674.
- Stallaert, W., van der Westhuizen, E.T., Schönege, A.-M., Plouffe, B., Hogue, M., Lukashova, V., Inoue, A., Ishida, S., Aoki, J., Le Gouill, C., and Bouvier, M. (2017). Purinergic Receptor Transactivation by the  $\beta 2$ -Adrenergic Receptor Increases Intracellular  $Ca^{2+}$  in Nonexcitable Cells. *Molecular pharmacology* 91, 533–544.
- Sternweis, P.C., and Smrcka, A.V. (1992). Regulation of phospholipase C by G proteins. *Trends in biochemical sciences* 17, 502–506.
- Strehler, E.E., and Treiman, M. (2004). Calcium pumps of plasma membrane and cell interior. *Current molecular medicine* 4, 323–335.
- Su, Y., Ho, M.K.C., and Wong, Y.H. (2009). A hematopoietic perspective on the promiscuity and specificity of Galpha16 signaling. *Neuro-Signals* 17, 71–81.
- Sun, L., and Ye, R.D. (2012). Role of G protein-coupled receptors in inflammation. *Acta pharmacologica Sinica* 33, 342–350.
- Sunahara, R.K., Dessauer, C.W., and Gilman, A.G. (1996). Complexity and diversity of mammalian adenylyl cyclases. *Annual review of pharmacology and toxicology* 36, 461–480.
- Suzuki, N., Hajicek, N., and Kozasa, T. (2009). Regulation and Physiological Functions of G12/13-Mediated Signaling Pathways. *Neuro-Signals* 17, 55–70.
- Syrovatkina, V., Alegre, K.O., Dey, R., and Huang, X.-Y. (2016). Regulation, Signaling, and Physiological Functions of G-Proteins. *Journal of molecular biology* 428, 3850–3868.
- Tennakoon, M., Senarath, K., Kankanamge, D., Ratnayake, K., Wijayarathna, D., Olupothage, K., Ubeyasinghe, S., Martins-Cannavino, K., Hébert, T.E., and Karunaratne, A. (2021). Subtype-dependent regulation of G  $\beta \gamma$  signalling. *Cellular signalling* 82, 109947.
- Uller, L., Mathiesen, J.M., Alenmyr, L., Korsgren, M., Ulven, T., Högborg, T., Andersson, G., Persson, C.G.A., and Kostenis, E. (2007). Antagonism of the prostaglandin D2 receptor CRTH2 attenuates asthma pathology in mouse eosinophilic airway inflammation. *Respiratory research* 8, 16.

## References

- van der Ploeg, I., Altiok, N., Kvanta, A., Nordstedt, C., and Fredholm, B.B. (1991). Role of a pertussis toxin sensitive G-protein in mediating the effects of phorbol esters on receptor activated cyclic AMP accumulation in Jurkat cells. *Naunyn-Schmiedeberg's archives of pharmacology* 344, 611–617.
- Vischer, H.F., Leurs, R., and Smit, M.J. (2006). HCMV-encoded G-protein-coupled receptors as constitutively active modulators of cellular signaling networks. *Trends in pharmacological sciences* 27, 56–63.
- Waldo, G.L., Ricks, T.K., Hicks, S.N., Cheever, M.L., Kawano, T., Tsuboi, K., Wang, X., Montell, C., Kozasa, T., Sondek, J., and Harden, T.K. (2010). Kinetic scaffolding mediated by a phospholipase C-beta and Gq signaling complex. *Science (New York, N.Y.)* 330, 974–980.
- Werry, T.D., Christie, M.I., Dainty, I.A., Wilkinson, G.F., and Willars, G.B. (2002). Ca<sup>2+</sup> signalling by recombinant human CXCR2 chemokine receptors is potentiated by P2Y nucleotide receptors in HEK cells. *British Journal of Pharmacology* 135, 1199–1208.
- Werry, T.D., Wilkinson, G.F., and Willars, G.B. (2003a). Cross talk between P2Y2 nucleotide receptors and CXC chemokine receptor 2 resulting in enhanced Ca<sup>2+</sup> signaling involves enhancement of phospholipase C activity and is enabled by incremental Ca<sup>2+</sup> release in human embryonic kidney cells. *The Journal of pharmacology and experimental therapeutics* 307, 661–669.
- Werry, T.D., Wilkinson, G.F., and Willars, G.B. (2003b). Mechanisms of cross-talk between G-protein-coupled receptors resulting in enhanced release of intracellular Ca<sup>2+</sup>. *The Biochemical journal* 374, 281–296.
- Wu, D.Q., Lee, C.H., Rhee, S.G., and Simon, M.I. (1992). Activation of phospholipase C by the alpha subunits of the Gq and G11 proteins in transfected Cos-7 cells. *The Journal of Biological Chemistry* 267, 1811–1817.
- Wydeven, N., Marron Fernandez de Velasco, E., Du, Y., Benneyworth, M.A., Hearing, M.C., Fischer, R.A., Thomas, M.J., Weaver, C.D., and Wickman, K. (2014). Mechanisms underlying the activation of G-protein-gated inwardly rectifying K<sup>+</sup> (GIRK) channels by the novel anxiolytic drug, ML297. *Proceedings of the National Academy of Sciences of the United States of America* 111, 10755–10760.
- Xu, A., Wang, Y., Xu, L.Y., and Gilmour, R.S. (2001). Protein kinase C alpha -mediated negative feedback regulation is responsible for the termination of insulin-like growth factor I-induced activation of nuclear phospholipase C beta1 in Swiss 3T3 cells. *The Journal of Biological Chemistry* 276, 14980–14986.
- Yeo, A., Samways, D.S., Fowler, C.E., Gunn-Moore, F., and Henderson, G. (2001). Coincident signalling between the Gi/Go-coupled delta-opioid receptor and the Gq-coupled m3 muscarinic receptor at the level of intracellular free calcium in SH-SY5Y cells. *Journal of neurochemistry* 76, 1688–1700.

# Abbreviations

5-HT	5-hydroxytryptamine, aka serotonin
ATP	adenosine-5'-triphosphate
cAMP	cyclic adenosine monophosphate
CCh	carbachol, aka. Carbamoylcholine
cDNA	complementary DNA
CRC	concentration response curve
CRISPR	Clustered Regularly Interspaced Short Palindromic Repeats
DAG	diacylglycerol
DMR	dynamic mass redistribution
DMSO	dimethylsulfoxide
DNA	desoxyribonucleic acid
E. coli	Escherichia coli
EC50	Concentration of half maximum effect
FACS	Fluorescence-activated single cell sorting
FBS	fetal bovine/calf serum
FSK	forskolin
FR	FR900359
GIRK	G protein-gated inwardly rectifying potassium (K <sup>+</sup> ) channel
GPCR	G protein-coupled receptor
HBSS	Hanks balanced salt solution
HEK	human embryonic kidney cells, HEK293 cells

## Abbreviations

HEPES	4-(2-hydroxyethyl)-1-piperazineethane- sulfonic acid
IP <sub>3</sub>	inositol-1,4,5-trisphosphate
NECA	5'-N-ethylcarboxamidoadenosine
PCR	Polymerase chain reaction
pEC <sub>50</sub>	-log(EC <sub>50</sub> )
PGD <sub>2</sub>	prostaglandin D <sub>2</sub>
PGE <sub>1</sub>	prostaglandin E <sub>1</sub>
PIP <sub>2</sub>	phosphoinositol-4,5-bisphosphate
PLC	phospholipase C
PTX	pertussis toxin
RE	restriction enzyme
RFU	relative fluorescence units
RNA	ribonucleic acid
UTP	uridine-5'-triphosphate

# List of Figures

Figure 1: Calcium mobilization from intracellular stores via IP <sub>3</sub> receptors. ....	10
Figure 2: The Phospholipase C family. ....	11
Figure 3: G protein activation via G protein-coupled receptors. ....	13
Figure 4: G protein families and their signaling pathways. ....	14
Figure 5: The structure of the PLCβ family. ....	17
Figure M1: Sanger Sequence of the PLCβ3 CRISPR target region of one sample clone. ....	35
Figure 6: Gi-calcium is completely blocked by Gq inhibitor FR. ....	42
Figure 7: FR-sensitive Gi-calcium is mobilized via PLCβ2 and PLCβ3. ....	43
Figure 8: Gq is required and sufficient to restore Gi-calcium in HEK-ΔGq/11 cells. ....	44
Figure 9: Gq overexpression shifts Gi/Gq balance of calcium signals towards Gq. ....	46
Figure 10: All Gαq family subunits restore Gi-calcium. ....	47
Figure 11: Specifically Gi-coupled DP2 requires additional Gq input to mobilize Gi-calcium. ....	48
Figure 12: Gi-calcium via CXCR2 and CXCR4 requires Gq input. ....	50
Figure 13: Both basal and acute Gq activation restore Gi-calcium, but acute Gq stimulation does so more reliably. ....	51
Figure 14: All model GPCRs are expressed and couple to Gi without Gq. ....	53
Figure 15: Gαi-mediated cAMP depression does not require Gq. ....	55
Figure 16: Gi-Gβγ-PLCβ signaling, but not Gi-Gβγ-GIRK activation, fully depends on Gq. ....	56
Figure 17: Gq hampers Gi-Gβγ-GIRK activation by depletion of GIRK co-factor PIP <sub>2</sub> . ....	58
Figure 18: Gi-Gβγ-PLCβ-calcium does not require Gq-PKC-activation. ....	59
Figure 19: An acute increase in intracellular calcium is not sufficient to allow Gi-calcium. ....	60

## List of Figures

Figure 20: Increased intracellular IP production does not restore Gi-G $\beta\gamma$ -PLC $\beta$ -calcium. ....	62
Figure 21: G $\alpha_q$ -PLC $\beta$ interaction, rather than Gq-G $\beta\gamma$ -signaling, is required for Gi-G $\beta\gamma$ -PLC $\beta$ -calcium. ....	63
Figure 22. NanoBiT sensor displays G $\beta\gamma$ -PLC $\beta$ binding. ....	65
Figure 23: Gq does not enhance G $\beta\gamma$ -PLC $\beta$ binding. ....	67
Figure 24: DP2 activates all G $\alpha_i$ subunits. ....	68
Figure 25: Gq-G $\beta\gamma$ binds to PLC $\beta_3$ upon stimulation of M3 receptors. ....	69
Figure 26: PLC $\beta_3$ constructs are not auto-inhibited and thus constitutively active. ....	69
Figure 27: Gi-G $\beta\gamma$ -PLC $\beta$ -calcium via crippled auto-inhibition PLC $\beta_3$ mutants does not require Gq. ....	71
Figure 28: When PLC $\beta_3$ auto-inhibition is disturbed by mutation, Gi-calcium no longer requires Gq input. ....	72
Figure 29: Without Gq, G $\beta\gamma$ slightly increases basal cellular PLC $\beta$ activity, but does not mediate Gi-GPCR induced activation. ....	72
Figure 30: Gi-G $\beta\gamma$ -PLC $\beta$ activation does not trigger real-time IP $_3$ increase without Gq. ....	74
Figure 31: Mechanistic model for Gi-G $\beta\gamma$ -PLC $\beta$ -calcium in living cells. ....	75
Figure 32: The Gq requirement for Gi-G $\beta\gamma$ -PLC $\beta$ -calcium is conserved across multiple cell types. ....	76
Figure 33: platelet calcium and aggregation by Gi-coupled receptors requires Gq input. ....	78
Figure 34: G16 expression in JURKAT cells allows Gi-calcium. ....	80



# List of Tables

Table 1: Chemicals and reagents .....	21
Table 2: Media bases .....	22
Table 3: Media supplements.....	23
Table 4: Antibodies .....	23
Table 5: Plasmids .....	24
Table 6: Bacterial strains .....	26
Table 7: Cell lines .....	26
Table 8: Organisms .....	26
Table 9: Commercial Assay Kits.....	27
Table 10: HEK standard media.....	28
Table 11: HEK-GPCR cell line media .....	28
Table 12: HEK-DP2-GIRK cell line media.....	29
Table 13: Oli-Neu cell media .....	29
Table 14: JURKAT media.....	30
Table 15: mPASC media .....	30
Table 16: PLC $\beta$ 1-4 CRISPR/Cas9 target regions.....	33
Table 17: CRISPR screening PCR mix (per 1 well).....	34
Table 18: CRISPR screening PCR conditions .....	34
Table 19: CRISPR screening RE mix.....	34
Table 20: Genetic sequence of target regions in functional PLC $\beta$ 1-4 knockout HEK cell line .....	36



# Publications

## Publications in peer-reviewed journals

1. Patt, J., Alenfelder, J., **Pfeil, E.M.**, Voss, J.H., Merten, N., Eryilmaz, F., Heycke, N., Rick, U., Inoue, A., Kehraus, S., Deupi, X., Müller, C.E., König, G.M., Crüsemann, M., and Kostenis, E. An experimental strategy to probe Gq contribution to signal transduction in living cells. **The Journal of Biological Chemistry** 2021, p. 100472. DOI: 10.1016/j.jbc.2021.100472.
2. **Pfeil, E. M.**; Brands, J.; Merten, N.; Vögtle, T.; Vescovo, M.; Rick, U.; Albrecht, I.-M.; Heycke, N.; Kawakami, K.; Ono, Y.; Ngako Kadji, F. M.; Hiratsuka, S.; Aoki, J.; Häberlein, F.; Matthey, M.; Garg, J.; Hennen, S.; Jobin, M.-L.; Seier, K.; Calebiro, D.; Pfeifer, A.; Heinemann, A.; Wenzel, D.; König, G. M.; Nieswandt, B.; Fleischmann, B. K.; Inoue, A.; Simon, K.; Kostenis, E. Heterotrimeric G Protein Subunit Gαq Is a Master Switch for Gβγ-Mediated Calcium Mobilization by Gi-Coupled GPCRs. **Molecular cell** 2020. DOI: 10.1016/j.molcel.2020.10.027.
3. Kostenis, E.; **Pfeil, E. M.**; Annala, S. Heterotrimeric Gq proteins as therapeutic targets? **The Journal of Biological Chemistry** 2020, 295 (16), 5206–5215. DOI: 10.1074/jbc.REV119.007061.
4. Holze, J.\*; Bermudez, M.\*; **Pfeil, E. M.**; Kauk, M.; Bödefeld, T.; Irmén, M.; Matera, C.; Dallanocce, C.; Amici, M. de; Holzgrabe, U.; König, G. M.; Tränkle, C.; Wolber, G.; Schrage, R.; Mohr, K.; Hoffmann, C.; Kostenis, E.; Bock, A. Ligand-Specific Allosteric Coupling Controls G-Protein-Coupled Receptor Signaling. **ACS pharmacology & translational science** 2020, 3 (5), 859–867. DOI: 10.1021/acspsci.0c00069.  
\*these authors contributed equally to this work
5. Annala, S.; Feng, X.; Shridhar, N.; Eryilmaz, F.; Patt, J.; Yang, J.; **Pfeil, E. M.**; Cervantes-Villagrana, R. D.; Inoue, A.; Häberlein, F.; Slodczyk, T.; Reher, R.; Kehraus, S.; Monteleone, S.; Schrage, R.; Heycke, N.; Rick, U.; Engel, S.; Pfeifer, A.; Kolb, P.; König, G.; Bünemann, M.; Tüting, T.; Vázquez-Prado, J.; Gutkind, J. S.; Gaffal, E.; Kostenis, E. Direct targeting of Gαq and Gα11 oncoproteins in cancer cells. **Science signaling** 2019, 12 (573). DOI: 10.1126/scisignal.aau5948.
6. Krebs, K. M.\*; **Pfeil, E. M.\***; Simon, K.; Grundmann, M.; Häberlein, F.; Bautista-Aguilera, O. M.; Gütschow, M.; Weaver, C. D.; Fleischmann, B. K.; Kostenis, E. Label-Free Whole Cell Biosensing for High-Throughput Discovery of Activators and Inhibitors Targeting G Protein-Activated Inwardly Rectifying Potassium Channels. **ACS Omega** 2018, 3 (11), 14814–14823. DOI: 10.1021/acsomega.8b02254.  
\*these authors contributed equally to this work



# Talks and posters

- 10/19      **Poster:** Eva M. Pfeil, Katharina Simon, Gabriele M. König, Bernd K. Fleischmann, Asuka Inoue, Evi Kostenis, *Gi-dependent calcium mobilization requires Gq*. Novo Nordisk Fonden Symposium GPCR, Copenhagen, Denmark
- 01/19      **Talk:** *Gi-Gβγ activation of PLCβ requires Gq*. Tohoku University, Sendai, Japan
- 08/19      **Poster:** Eva M. Pfeil, Katharina Simon, Gabriele M. König, Bernd K. Fleischmann, Asuka Inoue, Evi Kostenis, *Chemokine receptors require Gq to mobilize Gi-dependent calcium*. RTG1783 International Symposium, Bonn, Germany
- 10/18      **Talk:** *Gβγ-PLCβ signaling requires Gq*. RTG1873 annual retreat, Bonn, Germany
- 07/18      **Poster:** Katharina Simon, Eva M. Pfeil, Nicole Merten, Davide Malfacini, Raffael Reher, Gabriele König, Asuka Inoue, Jesus Gomeza, Evi Kostenis; *Elucidating G protein-independent signaling functions of GPR17*. ECC GLISTEN Symposium, Berlin, Germany
- 09/17      **Talk:** *On the mechanism of interaction of Gq with Gbg-mediated signaling outcomes*. RTG1873 annual retreat, Bonn
- 05/17      **Poster:** Eva M. Pfeil; *On the interaction of Gq proteins with Gi-βγ mediated signaling events*. RTG1873 funding review, Bonn, Germany



# Acknowledgements

An erster Stelle möchte ich mich hiermit bei Prof. Evi Kostenis bedanken, die mir ermöglicht hat, diese Arbeit in ihrem Arbeitskreis anzufertigen. Während der letzten vier Jahre konnte ich unter Deiner Aufsicht nicht nur meine praktischen Forschungsfähigkeiten erweitern, sondern habe auch meine Begeisterung für die Wissenschaft entdeckt und gelernt, mit Ehrgeiz, Zielstrebigkeit und Eigeninitiative zu arbeiten. Bei dem Projekt, was Du mir anvertraut hast, habe ich gelernt, mit systematischer Kreativität auf das ‚große Ganze‘ hinzuarbeiten, und doch dabei nicht die Liebe zum Detail zu vernachlässigen. Auch danke ich Dir für die vielen Gespräche, in denen wir gegenseitig unsere Gedanken und Überlegungen zum Projekt austauschen konnten und Du stets Deinen Erfahrungsschatz über wissenschaftliche und nicht-wissenschaftliche Dinge mit mir geteilt hast. Ich bin froh, unter Deiner Betreuung gewachsen zu sein.

Des Weiteren bedanke ich mich natürlich bei meinem Zweitbetreuer Prof. Fleischmann, der seine wertvolle Expertise und seinen physiologischen Blickwinkel mit uns geteilt hat um das Projekt und mich zu unterstützen.

Zusätzlich danke ich Katharina Simon, die mich die ersten zwei Jahre meiner Doktorarbeit betreut hat und mir stets Fragen zur Seite stand.

Außerdem bedanke ich mich natürlich bei all denen, die das Projekt im Labor oder Konzeptionell unterstützt haben. Vielen Dank an die Mitglieder der Kostenis Arbeitsgruppe, ganz besonders unseren beiden Stars Uli und Nina, sowie Julian Brands und Nicole Merten, die das Projekt in der Endphase besonders tatkräftig unterstützt haben. Bei Prof. Wenzel sowie den Mitarbeitern der Fleischmann und Wenzel Arbeitsgruppen, beim GRK1873 unter der Leitung von Herrn Prof. Pfeifer sowie allen Student:innen und Professor:innen für die hilfreichen Hinweise bei regelmäßigen Meetings, und bei unseren externen Kollaborationspartnern.

I am deeply grateful to Aska-san (Asuka Inoue) and the members of his “GPCR team” for welcoming me at their lab in Sendai, teaching me about their cool CRISPR/Cas9, TGF $\alpha$ -shedding and nanoBiT methods, as well as so much more about science, and for trusting me and taking care of me during my stay in Japan. Aska-san, thank you especially for allowing me to work under your supervision, organizing to use every available method at your lab to support this research project, as well as taking the time to make sure I was comfortable, doing well and having a good time during my stay. Kadji-san, thank you so much for demonstrating your remarkable experimental skills so that I could learn from you, and sharing advice and stories with me during our times in the assay/storage room. Kawakami-san, you are one of the kindest, most hardworking people I have had the pleasure of meeting. I appreciate you taking the time to help me with my endless questions on ‘what to do next?’, ‘where to find stuff?’, ‘how to use this?’, and ‘why isn’t this working?’ Ono-san, your optimism and humor made my time at the lab so much more fun! Thank you for helping me out with my experiments and allowing me to mess up your super-well-organized lab bench

## Acknowledgements

whenever I needed to! Sato-san, you were wonderful! I enjoyed doing molecular biology with an expert like you, so thank you so much for your help and kindness. And of course, thank you to Junken Aoki for having me at his research lab, and to all the other lab members that helped me with my experiments and made we feel welcome, I am grateful to all of you!

I would also like to thank Maddalena Vescovo, who supported this project as a master student for six months. I had a great time with you and especially appreciated your self-reliant style of work and relaxed humor. Thank you for all the wonderful data you generated to support this project.

Mein besonderer Dank gilt meinen Büro-Kolleg:innen Funda Eryilmaz (mit ‚th‘), Nicole Merten und Julian Patt. Danke für Eure wissenschaftliche, konzeptionelle, emotionale und moralische Unterstützung! Ohne Euch an meiner Seite, die gemeinsamen Höhen und Tiefen, die dummen Witze und die weinroten Therapiestunden hätte ich vermutlich auf halber Strecke einfach den Verstand verloren. Funda, Dir danke ich zusätzlich ganz besonders dafür, dass wir innerhalb und außerhalb des Labors zusammengehalten haben und für all die Weisheiten, die aus dem gemeinsamen Reflektieren aller Aspekte unseres Lebens entstanden sind. Ihr alle drei wart die besten Bürokollegen, und ich danke Euch für die tolle Zeit.

Natürlich möchte ich noch all meinen anderen Kolleg:innen danken. Danke für Eure Unterstützung im Labor, die lieben Gespräche und die freundliche und kollegiale Atmosphäre die letzten vier Jahre!

Zum Abschluss bedanke ich mich hiermit bei all den Menschen, die mich außerhalb des Labors unterstützt haben. Vor allem natürlich bei meinen Eltern, die mir alles Notwendige mitgegeben haben, damit ich meinen eigenen Weg einschlagen kann, und die immer bereit sind, wenn ich Unterstützung brauche. Danke auch an meinen Bruder Felix und seiner Partnerin Kathrin für all die strategischen Hinweise und Erfahrungswerte zu allen Situationen der Arbeitswelt und des Lebens.

Und ‚last but not least‘ danke ich von ganzem Herzen meinem Partner Marcel und meinen Freundinnen Caro, Nina, Annika, Anna, Anna, Sukanya und Funda. Danke, dass Ihr immer für mich da seid, und dass wir den ‚Wahnsinn des Alltags‘ und die großen und kleinen Herausforderungen des Lebens gemeinsam angehen. Diese Arbeit widme ich Euch!